

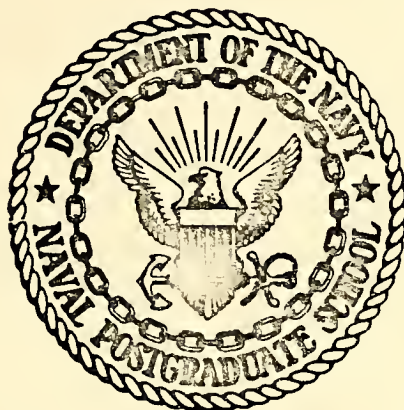
MANEUVERING CHARACTERISTICS OF AUTOMATICALLY  
CONTROLLED SHIPS WITH DIRECTIONALLY UNSTABLE  
HULLS

Andreas G. Hozos

Library  
Naval Postgraduate School  
Monterey, California 93940

# NAVAL POSTGRADUATE SCHOOL

## Monterey, California



# THESIS

MANEUVERING CHARACTERISTICS OF AUTOMATICALLY  
CONTROLLED SHIPS WITH DIRECTIONALLY UNSTABLE  
HULLS

by

Andreas G. Hozos

December 1974

Thesis Advisor:

G. J. Thaler

Approved for public release; distribution unlimited.

T164057



UNCLASSIFIED

SECURITY CLASSIFICATION OF THIS PAGE (When Data Entered)

REPORT DOCUMENTATION PAGE		READ INSTRUCTIONS BEFORE COMPLETING FORM
1. REPORT NUMBER	2. GOVT ACCESSION NO.	3. RECIPIENT'S CATALOG NUMBER
4. TITLE (and Subtitle) Maneuvering Characteristics of Automatically Controlled Ships with Directionally Unstable Hulls		5. TYPE OF REPORT & PERIOD COVERED Master's Thesis; December 1974
7. AUTHOR(s) Andreas G. Hozos		6. PERFORMING ORG. REPORT NUMBER
9. PERFORMING ORGANIZATION NAME AND ADDRESS Naval Postgraduate School Monterey, California 93940		8. CONTRACT OR GRANT NUMBER(s)
11. CONTROLLING OFFICE NAME AND ADDRESS Naval Postgraduate School Monterey, California 93940		10. PROGRAM ELEMENT, PROJECT, TASK AREA & WORK UNIT NUMBERS
14. MONITORING AGENCY NAME & ADDRESS (if different from Controlling Office) Naval Postgraduate School Monterey, California 93940		12. REPORT DATE December 1974
		13. NUMBER OF PAGES 144
		15. SECURITY CLASS. (of this report) Unclassified
		15a. DECLASSIFICATION/DOWNGRADING SCHEDULE
16. DISTRIBUTION STATEMENT (of this Report)  Approved for public release; distribution unlimited.		
17. DISTRIBUTION STATEMENT (of the abstract entered in Block 20, if different from Report)		
18. SUPPLEMENTARY NOTES		
19. KEY WORDS (Continue on reverse side if necessary and identify by block number) Ship Maneuvers Dynamically Unstable Ships Dead Zone Automatic Control Maneuverability		
20. ABSTRACT (Continue on reverse side if necessary and identify by block number) The stabilization of a dynamically unstable ship and the maneuvering characteristics of the combination unstable - stabilized ship were studied using the linear and non linear equations of motion of a ship. The Digital Simulation Language (DSL/360) was used to simulate the dynamics of the systems.		



UNCLASSIFIED

SECURITY CLASSIFICATION OF THIS PAGE(When Data Entered)

UNCLASSIFIED

SECURITY CLASSIFICATION OF THIS PAGE(When Data Entered)





Maneuvering Characteristics of Automatically Controlled  
Ships with Directionally Unstable Hulls

by

Andreas G. Hozos  
Lieutenant Commander, Hellenic Navy  
Hellenic Naval Academy, 1962  
B.S., Naval Postgraduate School, 1974

Submitted in partial fulfillment of the  
requirements for the degree of

MASTER OF SCIENCE IN ELECTRICAL ENGINEERING

from the

NAVAL POSTGRADUATE SCHOOL  
December 1974



## ABSTRACT

The stabilization of a dynamically unstable ship and the maneuvering characteristics of the combination unstable - stabilized ship were studied using the linear and non linear equations of motion of a ship. The Digital Simulation Language (DSL/360) was used to simulate the dynamics of the systems.



## TABLE OF CONTENTS

I.	INTRODUCTION-----	13
II.	EQUATIONS OF SHIP MOTION-----	14
III.	DYNAMIC STABILITY OF THE SHIP-----	18
	A. LINEAR EQUATIONS OF MOTION-----	18
	B. DYNAMIC STABILITY WITH FIXED CONTROL-----	21
	C. NON LINEAR EQUATIONS OF MOTION-----	22
IV.	STABILIZATION OF THE DYNAMICALLY UNSTABLE SHIP WITH RUDDER CONTROL. SIMULATION-----	28
	A. MOTION ON A STRAIGHT LINE. LINEAR MODELS----	29
	B. SIMULATION OF THE LINEAR MODELS-----	31
	1. "Helmsman" Operation-----	35
	2. Turning Maneuvers-----	42
	C. GENERAL MOTION. NON LINEAR MODELS-----	42
	D. SIMULATION OF THE NONLINEAR MODELS-----	46
	1. ZIG-ZAG Maneuvers-----	46
	2. "360° Turn" Test-----	47
V.	SHIP RESPONSES WHEN A SINUSOIDAL WAVE IS PRESENT-	59
	A. MODELS FOR THE SINUSOIDAL EXCITATION-----	59
	B. SIMULATION-----	62
	1. Models A and Stabilized C without Dead-Zone-----	63
	2. Models A and Stabilized C with Dead-Zone-	63
	C. SUPPRESSION OF THE RUDDER OSCILLATIONS-----	75
	D. INTRODUCTION OF FILTERS IN THE STABILIZING LOOP-----	77
	E. USE OF DEAD ZONE-----	96
VI.	CONCLUSIONS-----	109



VII. RECOMMENDATIONS----- 110

APPENDIX A----- 111

APPENDIX B----- 113

APPENDIX C----- 115

APPENDIX D----- 120

APPENDIX E----- 122

COMPUTER PROGRAM----- 124

LIST OF REFERENCES----- 143

INITIAL DISTRIBUTION LIST----- 144





## LIST OF DRAWINGS

1.	Coordinate System Fixed to the Ship-----	15
2.	Orientation of Fixed and Moving Axes-----	27
3.	Block Diagrams of Models A, C and Stabilized C----	30
4.	Block Diagram for Simulation of Models A, C-----	33
5.	Block Diagram for Simulation of the Stabilized Model C-----	34
6.	Block Diagram for Simulation of Models A and C with the Unity Feedback Loop Connected-----	36
7.	Block Diagram for Simulation of the Stabilized Model C with the Unity Feedback Loop Connected and the Pole Introduced-----	37
8.	Rudder's Characteristic-----	38
9.	Rudder Deflections vs. Time in the "Helmsman Operation" Test-----	39
10.	Ship Headings ( $\psi$ ) vs. Time in the "Helmsman Operation" Test-----	40
11.	Ship Trajectories in the "Helmsman Operation" Test-----	41
12.	Rudder Deflections vs. Time in the "Turning Maneuvers" Test-----	43
13.	Ship Headings ( $\psi$ ) vs. Time in the "Turning Maneuvers" Test-----	44
14.	Ship Trajectories in the "Turning Maneuvers" Test-	45
15.	Rudder Deflections and Ship Headings ( $\psi$ ) vs. Time in the "Zig-Zag Maneuvers" Test (Models A and C)--	48
16.	Input Commands and Ship Headings ( $\psi$ ) vs. Time in the "Zig-Zag Maneuvers" Test (Models A and C Stabilized)-----	49
17.	Rudder Deflections and Ship Headings ( $\psi$ ) vs. Time in the "Zig-Zag Maneuvers" Test (Model C Stabilized)-----	50
18.	Yawing Rate and Sway Velocity vs. Time in the "Zig-Zag Maneuvers" Test (Models A and C)-----	51



19.	Yawing Rate and Sway Velocity vs. Time in the "Zig-Zag Maneuvers" Test (Models A and C Stabilized)-----	52
20.	Ship Trajectories in the "Zig-Zag Maneuvers" Test (Models A and C)-----	53
21.	Ship Trajectories in the "Zig-Zag Maneuvers" Test (Models A and C Stabilized)-----	54
22.	Input Command and Ship Headings ( $\psi$ ) vs. Time in the "360° Turn" Test-----	56
23.	Ship Trajectories in the "360° Turn" Test-----	57
24.	Block Diagram Representation of the Two Models A and C in the Presence of Waves-----	60
25.	Block Diagram Representation of the Two Models A and C (Figure 24 Transformed)-----	61
26.	Block Diagram Representation of Models A and C with the Unity Feedback Loop-----	61
27.	Block Diagram for Simulation of Models A and C in the Presence of Waves-----	64
28.	Block Diagram for Simulation of the Stabilized Model C in the Presence of Waves-----	65
29.	Error Signals vs. Time in the Presence of Sinusoidal Waves-----	66
30.	Ship Trajectories in the Presence of Sinusoidal Waves-----	67
31.	Rudder Deflections vs. Time of the Stabilized Model C in the Presence of Sinusoidal Waves-----	68
32.	Figure of Merit vs. Time-----	69
33.	Error Signals vs. Time in the Presence of Sinusoidal Waves (Model A with Dead Zone)-----	70
34.	Error Signals vs. Time in the Presence of Sinusoidal Waves (Stabilized Model C with Dead Zone)--	71
35.	Ship Trajectories in the Presence of Sinusoidal Waves (Models A and C Stabilized with Dead Zone)--	72
36.	Rudder Deflections vs. Time in the Presence of Sinusoidal Waves (Model C Stabilized with Dead Zone)-----	73



37.	Figure of Merit for Models A and C Stabilized with Dead Zone-----	74
38.	Root Locus for Model C with a Pole Introduced in the Stabilizing Feedback Loop-----	76
39.	Error Signals vs. Time in the Presence of Sinusoidal Waves (Models A and C Stabilized Loop)-----	78
40.	Ship Trajectories in the Presence of Sinusoidal Waves (Models A and C Stabilized with a Pole in the Stabilizing Loop)-----	79
41.	Rudder Deflections vs. Time of the Stabilized Model C in the Presence of Sinusoidal Waves, with a Pole in the Stabilizing Loop-----	80
42.	Figure of Merit for Models A and C Stabilized (with a Pole in the Stabilizing Loop) in the Presence of Sinusoidal Waves-----	81
43.	Error Signals vs. Time in the Presence of Sinusoidal Waves (Models A and C Stabilized with only Velocity Feedback)-----	82
44.	Ship Trajectories in the Presence of Sinusoidal Waves (Models A and C Stabilized with only Velocity Feedback)-----	83
45.	Rudder Deflections vs. Time in the Presence of Sinusoidal Waves (Model C Stabilized with only Velocity Feedback)-----	84
46.	Figure of Merit (Models A and C Stabilized with only Velocity Feedback)-----	85
47.	Block Diagram of the Stabilizing Loop-----	86
48.	Gain and Phase vs. Frequency Curves for the Filters of the Stabilizing Loop-----	88
49.	Root Locus for the Stabilized Model C with the Filters in the Stabilizing Loop-----	89
50.	Rudder Deflections vs. Time in the Presence of Sinusoidal Waves (Model C Stabilized with the Filters in the Stabilizing Loop) with $w = 12.41$ ----	90
51.	Ship Trajectories in the Presence of Sinusoidal Waves (Models A and C Stabilized with the Filters in the Stabilizing Loop) with $w = 12.41$ ----	91
52.	Figure of Merit. (Models A and C Stabilized with the Filters in the Stabilizing Loop in the Presence of Sinusoidal Waves with $w = 12.41$ )-----	92



53.	Rudder Deflections vs. Time in the Presence of Sinusoidal Waves (Model C Stabilized with the Filters in the Stabilizing Loop) with $w = 20$ -----	93
54.	Ship Trajectories in the Presence of Sinusoidal Waves (Models A and C Stabilized with the Filters in the Stabilizing Loop) with $w = 20$ -----	94
55.	Figure of Merit. (Models A and C Stabilized with the Filters in the Stabilizing Loop in the Presence of Sinusoidal Waves with $w = 20$ )-----	95
56.	Rudder Deflections vs. Time in the Presence of Sinusoidal Waves (Model C Stabilized with the Filters and the Dead Zone)-----	97
57.	Ship Trajectories in the Presence of Sinusoidal Waves (Models A and C Stabilized with the Filters and the Dead Zone)-----	98
58.	Figure of Merit. (Models A and C Stabilized with the Filters and the Dead Zone in the Presence of Sinusoidal Waves)-----	99
59.	Block Diagram of the Stabilized Model C. (Final Version)-----	100
60.	Input Commands and Ship Headings ( $\psi$ ) vs. Time in the "Zig-Zag Maneuvers" Test. (Models A and C Stabilized, without the Dead Zone)-----	101
61.	Input Commands and Ship Headings ( $\psi$ ) vs. Time in the "Zig-Zag Maneuvers" Test. (Models A and C Stabilized, with the Dead Zone)-----	102
62.	Rudder Deflections and Ship Headings ( $\psi$ ) vs. Time in the "Zig-Zag Maneuvers" Test. (Model C Stabilized, without the Dead Zone)-----	103
63.	Rudder Deflections and Ship Headings ( $\psi$ ) vs. Time in the "Zig-Zag Maneuvers" Test. (Model C Stabilized, with the Dead Zone)-----	104
64.	Yawing Rate and Sway Velocity vs. Time in the "Zig-Zag Maneuvers" Test. (Models A and C Stabilized, without the Dead Zone)-----	105
65.	Yawing Rate and Sway Velocity vs. Time in the "Zig-Zag Maneuvers" Test. (Models A and C Stabilized, with the Dead Zone)-----	106
66.	Ship Trajectories in the "Zig-Zag Maneuvers Test (Models A and C Stabilized, without the Dead Zone)--	107





67.	Ship Trajectories in the "Zig-Zag Maneuvers"	
	Test. (Models A and C Stabilized, with the Dead	
	Zone) -----	108



## ACKNOWLEDGEMENT

This student wishes to express his sincere appreciation to Dr. George J. Thaler, Professor of Electrical Engineering, Naval Postgraduate School. It was through Dr. Thaler's guidance, persistence and understanding that this thesis was at all possible.



## I. INTRODUCTION

A ship is said to be dynamically stable on a straight course or in a turn of constant curvature if, when slightly disturbed from its steady motion, it will soon resume that same motion along a slightly shifted path without any correcting control being applied. A ship which is dynamically unstable in straight line motion cannot maintain straight line motion without any control action. However, with regard to maneuverability, a ship which is too stable will not turn as tightly as a less stable ship so that a highly stable ship may compromise maneuverability.

So a ship having at will the behavior of a dynamically stable or unstable ship is of potential importance.

In Reference 1 the stability and maneuverability of five different ships was studied. From those five ships (models), model A (stable ship) and model C (unstable ship) are selected for study in this thesis.

The stabilization of the unstable model C with the use of the rudder is considered. Then the behavior of the, so called, stabilized model C as compared with that of the stable model A under a variety of (same) conditions is studied in order to get its characteristics and see if and under what conditions that system is realizable.



## II. EQUATIONS OF SHIP MOTION

The motion of a ship is that of a rigid body with six degrees of freedom, subjected to gravity, buoyancy and controlling forces. With axes fixed to the ship and parallel to the principal axes of inertia the linear and angular momentum equations are:

$$\vec{F} = \frac{d}{dt} (m\vec{U}) = m\dot{\vec{U}} + \vec{\Omega} \times (m\vec{U}) \quad (1)$$

$$\vec{M} = \frac{d}{dt} (\overrightarrow{\text{Angular momentum}}) = \overrightarrow{(\text{Ang. Mom})} + \vec{\Omega} \times (\overrightarrow{\text{Angular Momentum}}) \quad (2)$$

where

$m$  = mass of ship

$\vec{U} = u\vec{i} + v\vec{j} + w\vec{k}$  = linear velocity vector with components along  $x$ ,  $y$ , and  $z$  axes respectively

$u$  = rate of surging

$v$  = rate of swaying

$w$  = rate of heaving

$\vec{\Omega} = p\vec{i} + q\vec{j} + r\vec{k}$  = vector angular velocity with components about  $x$ ,  $y$ , and  $z$  axes respectively (3)

$p$  = rate of roll =  $\dot{\phi}$

$q$  = rate of yaw =  $\dot{\theta}$

$r$  = rate of pitch =  $\dot{\psi}$

$\vec{F} = X\vec{i} + Y\vec{j} + Z\vec{k}$  = vector force acting on the ship (4)

$X$  = hydrodynamic force along  $x$ -axis

$Y$  = hydrodynamic force along  $y$ -axis





$Z$  = hydrodynamic force along  $z$ -axis

$\vec{M} = K\vec{i} + M\vec{j} + N\vec{k}$  = vector moment acting on the ship (5)

$K$  = rolling moment about  $x$ -axis

$M$  = pitching moment about  $y$ -axis

$N$  = yawing moment about  $z$ -axis

(Angular Momentum) =  $I_x p\vec{i} + I_y q\vec{j} + I_z r\vec{k}$  (6)

$I_x, I_y, I_z$  = mass moment of inertia about  $x, y,$  and  $z$  axes respectively.

The coordinate system where the above quantities are referred is shown in Figure 1.

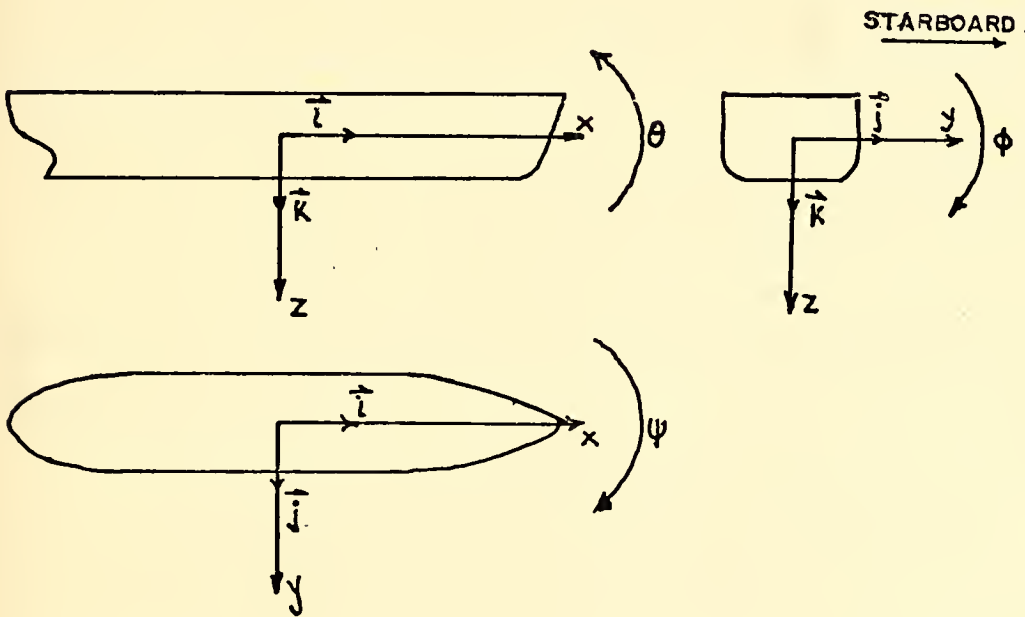


Figure 1. Coordinate System Fixed to the Ship.

Inserting equations (3), (4), (5), and (6) into equations (1) and (2) the six equations of motion are obtained as follows:



$$\begin{aligned} X &= m[\dot{u} + qw - rv - x_G(q^2 + r^2) + y_G(pq - \dot{r}) + z_G(pr + \dot{q})] \\ Y &= m[\dot{v} + ru - pw - y_G(r^2 + p^2) + z_G(qr - \dot{p}) + x_G(qp + \dot{r})] \end{aligned} \quad (7)$$

$$\begin{aligned} Z &= m[\dot{w} + pv - qu - z_G(p^2 + q^2) + x_G(rp - \dot{q}) + y_G(rq + \dot{p})] \\ K &= I_x \dot{p} + (I_z - I_y)qr + m[y_G(\dot{w} + pv - qu) - z_G(\dot{v} + ru - pw)] \\ M &= I_y \dot{q} + (I_x - I_z)rp + m[z_G(\dot{u} + qw - rv) - x_G(\dot{w} + pv - qu)] \\ N &= I_z \dot{r} + (I_y - I_x)pq + m[x_G(\dot{v} + ru - pw) - y_G(\dot{u} + qw - rv)] \end{aligned} \quad (8)$$

In Equations (7) and (8), the left hand sides represent the forces and moments acting on the ship while the right hand sides represent the dynamic responses. The forces and moments acting on the ship depend on the geometry of the hull, the motion and the fluid. Since the properties of ship and fluid are constant for a given ship in a given fluid without excitation forces, the forces or moments may be expressed as a function of the motion,

$$\vec{F} \text{ (or } \vec{M}) = f(x_0, y_0, z_0, \phi, \theta, \psi, u, v, w, p, q, r, \dot{u}, \dot{v}, \dot{w}, \dot{p}, \dot{q}, \dot{r}, \delta, \dot{\delta}, \ddot{\delta}, \text{etc}) \quad (9)$$

where  $x_0, y_0, z_0$  represent a system of reference axes fixed to the earth and

$x_0, y_0, z_0, \phi, \theta, \psi$  = orientation parameters

$u, v, w, p, q, r, \dot{u}, \dot{v}, \dot{w}, \dot{p}, \dot{q}, \dot{r}$  = motion parameters

$\delta, \dot{\delta}, \ddot{\delta}$  = control surface parameters

Considering motion in unrestricted calm water only three degrees of freedom are of concern: yaw, sway, and surge. So forces and moments are independent of the change in orientation with respect to the earth axes.

Furthermore since the forces and moments produced on the ship as a result of  $\dot{\delta}$  and  $\ddot{\delta}$  are normally negligible, and



because the motion is considered to take place on the horizontal plane for the surface ship in calm water, ( $p = q = w = 0$ ) equation (9) becomes:

$$\vec{F}(\text{or } \vec{M}) = f(u, v, r, \dot{u}, \dot{v}, \dot{r}, \delta). \quad (10)$$

Most ships have  $y_G = 0$ . Equations (7) and (8) may be written as:

$$\begin{aligned} X &= m(\dot{u} - rv - x_G r^2) \\ Y &= m(\dot{v} + ru + x_G \dot{r}) \\ N &= I_z \dot{r} + m[x_G(\dot{v} + ur)]. \end{aligned} \quad (11)$$

Combining equations (10) and (11) it is obtained:

$$\begin{aligned} X: \quad m(\dot{u} - rv - x_G r^2) &= f_X(u, v, r, \dot{u}, \dot{v}, \dot{r}, \delta) \\ Y: \quad m(\dot{v} + ru + x_G \dot{r}) &= f_Y(u, v, r, \dot{u}, \dot{v}, \dot{r}, \delta) \\ N: \quad I_z \dot{r} + mx_G(\dot{v} + ur) &= f_N(u, v, r, \dot{u}, \dot{v}, \dot{r}, \delta). \end{aligned} \quad (12)$$



### ① III. DYNAMIC STABILITY OF THE SHIP

Dynamic stability is directly related to the magnitude of yaw and sway deviations caused by small disturbances.

#### A. LINEAR EQUATIONS OF SHIP MOTION

In order to linearize the equations of motion about an initial equilibrium condition the Taylor expansion of the X, Y, and N functions is used. Components of the series expansion higher than the first order are discarded. This is consistent for the motion on a straight path, because motion stability determines whether a very small perturbation from an initial equilibrium position is going to increase with time or decay with time. And for very small perturbations the terms higher than the first order are negligible.

The following assumptions are made too:

$p = q = r = 0$

(1) The water is calm and so the motion is restricted to the horizontal plane only.

(2) Yaw and sway do not affect the forward speed appreciably, and small changes in forward speed do not affect yaw and sway motions so that the surge equation is decoupled.

(3) The ship has one rudder at the stern along the centerline and the effect of the propeller is disregarded.

(4) The forces and moments on hull and rudder are expressed by means of velocity and acceleration derivatives.

From equation (10) we have:

$$X = X_0 + X_u \Delta u + X_v \Delta v + X_r \Delta r + X_{\dot{u}} \Delta \dot{u} + X_{\dot{v}} \Delta \dot{v} + X_{\delta} \Delta \delta.$$





Since in initial equilibrium

$$v_0 = r_0 = \dot{u}_0 = \dot{v}_0 = \dot{r}_0 = \delta_0 = 0, \text{ then}$$

$$\Delta v = v - v_0 = v$$

$$\Delta r = r - r_0 = r$$

$$\Delta \dot{u} = \dot{u} - \dot{u}_0 = \dot{u}$$

$$\Delta \dot{v} = \dot{v} - \dot{v}_0 = \dot{v}$$

$$\Delta \dot{r} = \dot{r} - \dot{r}_0 = \dot{r}$$

$$\Delta \delta = \delta - \delta_0 = \delta.$$

Therefore

$$X = X_0 + X_u \Delta u + X_v v + X_r r + X_{\dot{u}} \dot{u} + X_{\dot{v}} \dot{v} + X_{\dot{r}} \dot{r} + X_{\delta} \delta \quad (13)$$

and likewise,

$$Y = Y_0 + Y_u \Delta u + Y_v v + Y_r r + Y_{\dot{u}} \dot{u} + Y_{\dot{v}} \dot{v} + Y_{\dot{r}} \dot{r} + Y_{\delta} \delta \quad (14)$$

$$N = N_0 + N_u \Delta u + N_v v + N_r r + N_{\dot{u}} \dot{u} + N_{\dot{v}} \dot{v} + N_{\dot{r}} \dot{r} + N_{\delta} \delta \quad (15)$$

where  $X_0$ ,  $Y_0$ , and  $N_0$  are the values of the initial equilibrium conditions.

In the initial equilibrium conditions of straight ahead motion at constant speed, there are no forces acting on the ship. Hence  $X_0 = Y_0 = N_0 = 0$ . Furthermore, since the ship is symmetric about the x-z plane:

$$Y_u = Y_{\dot{u}} = X_v = X_r = X_{\dot{r}} = N_u = N_{\dot{u}} = X_{\delta} = 0.$$

Therefore,

$$\begin{aligned} X &= X_u \Delta u + X_{\dot{u}} \dot{u} \\ Y &= Y_v v + Y_r r + Y_{\dot{v}} \dot{v} + Y_{\dot{r}} \dot{r} + Y_{\delta} \delta \\ N &= N_v v + N_r r + N_{\dot{v}} \dot{v} + N_{\dot{r}} \dot{r} + N_{\delta} \delta . \end{aligned} \quad (16)$$

In order to be consistent before we combine equations (11) and (16) we must linearize the right hand parts of



equations (11) too. So for the X equation we have,

$$\begin{aligned} X &= m[(\dot{u}_0 + \Delta\dot{u}) - (r_0 + \Delta r)(v_0 + \Delta v) - x_G(r_0 + \Delta r)^2] = \\ &= m(\Delta\dot{u} - \Delta r \Delta v - x_G \Delta \dot{r}), \end{aligned}$$

and dropping second order terms we have,

$$X = m\Delta\dot{u} = m\dot{u}. \quad (17)$$

Likewise

$$Y = m(\dot{v} + ru_0 + x_G \dot{r}) \quad (18)$$

$$N = I_z \dot{r} + mx_G(\dot{v} + ru_0). \quad (19)$$

Combining now equations (16), (17), (18), and (19) we have:

$$(X_u - m)\dot{u} + X_u \Delta u = 0 \quad (20)$$

$$(Y_v - m)\dot{v} + Y_v v + (Y_r - mx_G)\dot{r} + (Y_r - mu_0)r + Y_\delta \delta = 0 \quad (21)$$

$$(N_v - mx_G)\dot{v} + N_v v + (N_r - I_z)\dot{r} + (N_r - mx_G u_0)r + N_\delta \delta = 0. \quad (22)$$

For convenience equations (20), (21), and (22) are non-dimensionalized. Equations (20) and (21) have dimensions of Force, so we divide both sides by  $\frac{1}{2}\rho L H U^2$ . Equation (22) has dimensions of Moment, so we divide both sides by  $\frac{1}{2}\rho L^2 H U^2$ .

Above

$\rho$  = density of ship

$L$  = ship's length

$H$  = ship's draft

$U$  = ship's speed.

That gives

$$(X'_u - m')\dot{u}' + X'_u \Delta u = 0 \quad (23)$$

$$(Y'_v - m')\dot{v}' + Y'_v v' + (Y'_r - m'x'_G)\dot{r}' + (Y'_r - m'u'_0)r' + Y'_\delta \delta = 0 \quad (24)$$

$$(N'_v - m'x'_G)\dot{v}' + N'_v v' + (N'_r - I'_z)\dot{r}' + (N'_r - m'x'_G u'_0)r' + N'_\delta \delta = 0 \quad (25)$$

where:



$$m' = \frac{m}{\frac{1}{2}\rho L^2 H} \quad , \quad v' = \frac{v}{U} \quad , \quad \dot{v}' = \frac{\dot{v}}{U^2/L} \quad , \quad u'_0 = \frac{u}{V} \approx 1$$

$$I'_z = \frac{I_z}{\frac{1}{2}L^4 H} \quad , \quad r' = \frac{r}{U/L} \quad , \quad \dot{r}' = \frac{\dot{r}}{U^2/L^2} \quad , \quad x'_G = \frac{x_G}{L}$$

$$Y'_\delta = \frac{Y_\delta}{\frac{1}{2}LHU^2} \quad , \quad N'_\delta = \frac{N_\delta}{\frac{1}{2}\rho L^2 HU^2} \quad , \quad Y'_v = \frac{Y_v}{\frac{1}{2}\rho LHU} \quad , \quad Y'_r = \frac{Y_r}{\frac{1}{2}\rho L^2 HU}$$

$$N'_v = \frac{N_v}{\frac{1}{2}\rho L^2 HU} \quad , \quad N'_r = \frac{N_r}{\frac{1}{2}\rho L^3 HU} \quad , \quad Y'_v = \frac{Y_v}{\frac{1}{2}\rho L^2 H} \quad , \quad N'_v = \frac{N_v}{\frac{1}{2}\rho L^3 H}$$

$$N'_r = \frac{N_r}{\frac{1}{2}\rho L^3 H} \quad .$$

In equations (23), (24), and (25) the dimensionless time is defined as:

$$t' = \frac{U}{L} t.$$

#### B. DYNAMIC STABILITY WITH FIXED CONTROL

Solving the cross coupled differential equations (24) and (25) with the rudder fixed at  $\delta = 0$ , we obtain:

$$v'(t') = v_1 e^{\sigma_1 t'} + v_2 e^{\sigma_2 t'} \quad (26)$$

$$r'(t') = r_1 e^{\sigma_1 t'} + r_2 e^{\sigma_2 t'} \quad (27)$$

where  $v_1$ ,  $v_2$ ,  $r_1$ ,  $r_2$  are arbitrary constants depending on the initial conditions

$$\sigma_1 = \frac{-\frac{B}{A} + \sqrt{(\frac{B}{A})^2 - 4(\frac{C}{A})}}{2} \quad (28)$$

$$\sigma_2 = \frac{-\frac{B}{A} - \sqrt{(\frac{B}{A})^2 - 4(\frac{C}{A})}}{2} \quad (29)$$



$$A = (Y_V' - m') (N_R' - I_Z') - (Y_R' - m' x_G') (N_V' - m' x_G') \quad (30)$$

$$B = (Y_V' - m') (N_R' - m' x_G') - Y_V' (N_R' - I_Z') - \quad (31)$$

$$N_V' (Y_R' - m' x_G') - (Y_R' - m') (N_V' - m' x_G')$$

$$C = Y_V' (N_R' - m' x_G') - N_V' (Y_R' - m'). \quad (32)$$

From equations (26) and (27) we see that for  $\sigma_1 < 0$  (and because  $\sigma_1 \geq \sigma_2$ ):

$$\lim_{t' \rightarrow \infty} v'(t') = 0$$

and

$$\lim_{t' \rightarrow \infty} r'(t') = 0.$$

If  $\sigma_1 > 0$  then  $\lim_{t' \rightarrow \infty} v'(t') \neq 0$  and  $\lim_{t' \rightarrow \infty} r'(t') \neq 0$  which means that the ship is dynamically unstable in straight line motion. The root  $\sigma_1$  is called "the stability index."

In Appendix A the principal characteristics of a five foot Series 60 model of the Davidson Laboratory are listed.

In Reference 1 that model was modified to give five other models (A, B, C, D, E) the stable, marginally unstable, unstable, very unstable and extremely unstable.

Models A and C are selected for this thesis. The hydrodynamic derivatives for those two models and the roots of their characteristic equations are listed in Appendix A.

### C. NONLINEAR EQUATIONS OF MOTION

The linear equations developed in the previous section are not valid for large rudder angles. So in order to predict the performance of a dynamically unstable ship as well as to





get realistic predictions of maneuvers with large rudder angles, the nonlinear mathematical equations are needed.

The complete Taylor expansion of equation (12) with terms up to the third order is as follows for X with similar expressions for Y and N.

$$\begin{aligned}
 X = & X_0 + [X_u \Delta u + X_v v + X_r r + X_{\dot{u}} \dot{u} + X_{\dot{v}} \dot{v} + X_{\dot{r}} \dot{r} + X_{\delta} \delta] \\
 & + \frac{1}{2!} [X_{uu} \Delta u^2 + X_{vv} v^2 + \dots + X_{\delta\delta} \delta^2 + 2X_{uv} \Delta u v + 2X_{ur} \Delta u r \\
 & + \dots + 2X_{r\delta} \dot{r} \delta] + \frac{1}{3!} X_{uuu} \Delta u^3 + X_{vvv} v^3 + \dots + X_{\delta\delta\delta} \delta^3 \\
 & + 3X_{uuv} \Delta u^2 v + 3X_{uur} \Delta u^2 r + \dots + 3X_{r\delta\delta} \dot{r} \delta^2 + 6X_{uvr} \Delta u v r \\
 & + 6X_{uv\dot{u}} \Delta u v \dot{u} + \dots + 6X_{vr\delta} \dot{v} \dot{r} \delta
 \end{aligned} \tag{33}$$

where  $X_0$  is the force in the x-direction at the equilibrium position, i.e.,  $u_1 = U$ ,

$$X_{uu} = \frac{\partial^2 X}{\partial u^2}, \quad X_{\delta\delta} = \frac{\partial^2 X}{\partial \delta^2}, \quad X_{uv} = \frac{\partial^2 X}{\partial u \partial v}$$

$$X_{uuu} = \frac{\partial^3 X}{\partial u^3}, \quad X_{uur} = \frac{\partial^3 X}{\partial u^2 \partial r} \text{ etc.}$$

Terms higher than third order are not included in equation (33) because the accuracy is not significantly improved by their inclusion. Furthermore [Ref. 2]:

1. Cross coupling terms such as  $X_{vu} v \Delta u$ ,  $X_{ru} r \Delta u$ ,  $X_{\delta u} \delta \Delta u$  and so on, involving odd powers of  $v$ ,  $r$ ,  $\delta$ ,  $v$ ,  $r$  are negligible.

2. Cross coupling terms such as  $X_{vvu} v^2 \Delta u$ ,  $X_{rru} r^2 \Delta u$  and so on, involving even powers of  $v$ ,  $r$ ,  $\delta$ , are nonzero. However the values of the derivatives for the models used in this thesis are zero (Appendix B).



3. Even terms in  $v$ ,  $r$ ,  $\delta$ ,  $\dot{v}$ , and  $\dot{r}$  in the Y-force and N-moment equations are eliminated due to symmetry.

4. Cross coupling terms between acceleration and velocity are neglected.

5. Rudder force and moment derivatives of higher than first order, and effects of rudder angular rate are negligible.

Combining equation (11) with the Taylor expansions for  $X$ ,  $Y$ ,  $N$  and taking into account the above assumptions, we have:

$$(m - X_{\dot{u}}) \dot{u} = f_1(u, v, r, \delta) \quad (34)$$

$$(m - Y_{\dot{v}}) \dot{v} + (mx_G - Y_{\dot{r}}) \dot{r} = f_2(u, v, r, \delta) \quad (35)$$

$$(mx_G - N_{\dot{v}}) \dot{v} + (I_z - N_{\dot{r}}) \dot{r} = f_3(u, v, r, \delta) \quad (36)$$

where:

$$\begin{aligned} f_1(u, v, r, \delta) = & X_0 + X_u \Delta u + \frac{1}{2} X_{uu} \Delta u^2 + \frac{1}{6} X_{uuu} \Delta u^3 \\ & + \frac{1}{2} X_{vv} v^2 + \left( \frac{1}{2} X_{rr} + mx_G \right) r^2 + \frac{1}{2} X_{\delta\delta} \delta^2 \\ & + \frac{1}{2} X_{vvu} v^2 \Delta u + \frac{1}{2} X_{rru} r^2 \Delta u + \frac{1}{2} X_{\delta\delta u} \delta^2 \Delta u \\ & + (X_{vr} + m) vr + X_{v\delta} v\delta + X_{r\delta} r\delta + X_{vru} vr \Delta u \\ & + X_{v\delta u} v\delta \Delta u + X_{r\delta u} r\delta \Delta u \end{aligned} \quad (34a)$$

$$\begin{aligned} f_2(u, v, r, \delta) = & Y_0 + Y_u \Delta u + Y_{uu} \Delta u^2 + Y_v v + \frac{1}{6} Y_{vvv} v^3 \\ & + \frac{1}{2} Y_{vrr} vr^2 + \frac{1}{2} Y_{v\delta\delta} v\delta^2 + Y_{vu} v \Delta u \\ & + \frac{1}{2} Y_{vu u} v \Delta u^2 + Y_{\delta\delta} \delta + \frac{1}{6} Y_{\delta\delta\delta} \delta^3 \\ & + \frac{1}{2} Y_{\delta vv} \delta v^2 + \frac{1}{2} Y_{\delta rr} \delta r^2 + Y_{\delta u} \delta \Delta u \\ & + \frac{1}{2} Y_{\delta u u} \delta \Delta u^2 + Y_{vr\delta} vr\delta. \end{aligned} \quad (35a)$$



$$\begin{aligned}
f_3(u, v, r, \delta) = & N_0 + N_u \Delta u + N_{uu} \Delta u^2 + N_v v \\
& + \frac{1}{6} N_{vvv} v^3 + \frac{1}{2} N_{vrr} v r^2 + \frac{1}{2} N_{v\delta\delta} v \delta^2 \\
& + N_{vu} v \Delta u + \frac{1}{2} N_{vu u} v \Delta u^2 + (N_r - m x_G u) r \\
& + \frac{1}{6} N_{rrr} r^3 + \frac{1}{2} N_{rvv} r v^2 + \frac{1}{2} N_{r\delta\delta} r \delta^2 \\
& + N_{ru} r \Delta u + \frac{1}{2} N_{ru u} r \Delta u^2 + N_\delta \delta + \frac{1}{6} N_{\delta\delta\delta} \delta^3 \\
& + \frac{1}{2} N_{\delta u u} \delta \Delta u^2 + N_{vr\delta} v r \delta + \frac{1}{2} N_{\delta v v} \delta v^2 \\
& + \frac{1}{2} N_{\delta r r} \delta r^2 + N_{\delta u} \delta \Delta u.
\end{aligned} \tag{36a}$$

The above equations have been developed in dimensional form. The equations are equally valid in nondimensional form with the stipulation that the velocity used for the nondimensionalization should be the velocity at any time  $t$ , rather than the initial velocity. For further simplification the nondimensionalizing velocity in the nonlinear equations is taken as  $u(t)$  rather than  $U(t)$ .

The hydrodynamic derivatives of the second order for the nonlinear equations are listed in Appendix B.

Solving equations (34), (35), and (36) for the accelerations  $\dot{u}$ ,  $\dot{v}$ , and  $\dot{r}$  taking into account the nondimensionalization we obtain:

$$\dot{u}' = \frac{f_1(u', v', r', \delta)}{m' - X_{\dot{u}}'} \tag{37}$$

$$\dot{v}' = \frac{(I'_z - N'_{\dot{r}}) f_2(u', v', r', \delta) - (m' x'_G - Y'_{\dot{r}}) f_3(u', v', r', \delta)}{(m' - Y'_{\dot{v}}) (I'_z - N'_{\dot{r}}) - (m' x'_G - Y'_{\dot{r}}) (m' x' - Y'_{\dot{r}})} \tag{38}$$



$$\dot{\mathbf{r}}' = \frac{(m' - Y_V^I) f_3(u', v', r', \delta) - (m' x_G^I N_V^I) f_2(u', v', r', \delta)}{(m' - Y_V^I) (I_Z^I - N_{\dot{\mathbf{r}}}^I) - (m' x_G^I - N_V^I) (m' x_G^I - Y_{\dot{\mathbf{r}}}^I)} \quad (39)$$

Integrating the above equations we get:

$$u'(t') = \int_0^{t'} \dot{u}'(t') dt'$$

$$v'(t') = \int_0^{t'} \dot{v}'(t') dt'$$

$$r'(t') = \int_0^{t'} \dot{r}'(t') dt'$$

$$\Psi(t') = \int_0^{t'} r'(t') dt'.$$

So far the reference axes  $x$ ,  $y$ , and  $z$  are fixed to the moving ship. In order to determine the path of the ship it is necessary to take the reference axes  $x_0$  and  $y_0$  fixed to the earth as shown in Figure 2.

Referring ship's velocities  $(\dot{x}, \dot{y})$  to the new coordinates we have:

$$\dot{x}_0(t) = u(t) \cos \Psi(t) - v(t) \sin \Psi(t) \quad (40)$$

$$\dot{y}_0(t) = u(t) \sin \Psi(t) + v(t) \cos \Psi(t). \quad (41)$$

Integrating

$$x_0(t) = \int_0^t \dot{x}_0(t) dt \quad (42)$$





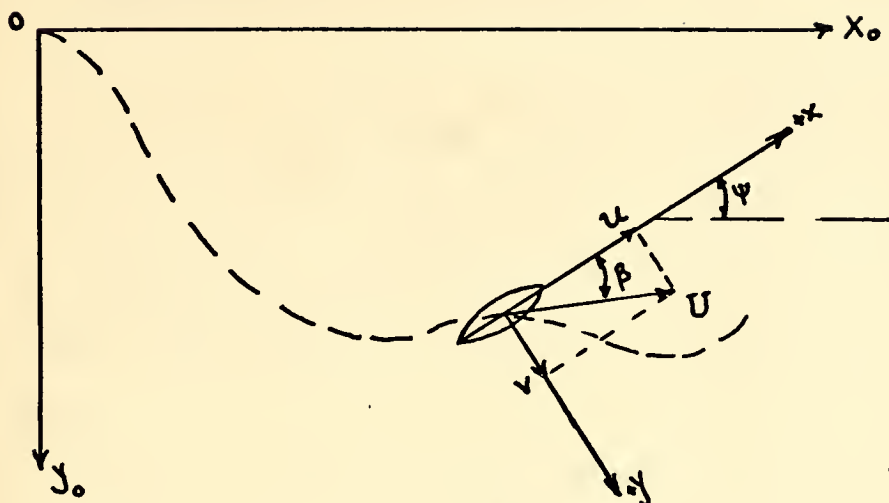


Figure 2. Orientation of Fixed and Moving Axes.

$$y_0(t) = \int_0^t \dot{y}_0(t) dt. \quad (43)$$

Nondimensionalizing equations (40), (41), (42), (43) using the definitions:

$$x' = \frac{x_0}{L}, \quad \dot{x}' = \frac{\dot{x}_0}{U}, \quad y' = \frac{y_0}{L}, \quad \dot{y}' = \frac{\dot{y}_0}{U} \text{ and } t' = t \frac{U}{L}$$

we get

$$\dot{x}'(t') = u'(t') \cos \Psi(t') - v'(t') \sin \Psi(t') \quad (40a)$$

$$\dot{y}'(t') = u'(t') \sin \Psi(t') + v'(t') \cos \Psi(t') \quad (41a)$$

$$x'(t') = \frac{x_0}{L} = \int \frac{\dot{x}_0}{L} dt = \int \frac{\dot{x}}{U} \frac{U}{L} dt = \int \dot{x}' dt' \quad (42a)$$

$$y'(t') = \int \dot{y}'(dt') \quad (43a)$$



#### IV. STABILIZATION OF THE DYNAMICALLY UNSTABLE SHIP WITH RUDDER CONTROL. SIMULATION.

In order to study the behavior of the two ships, both the linear and nonlinear equations, presented in chapter III, are used. For the case studied in this thesis the ship can be modeled as a transfer function which has as an input the rudder deflection and as an output the heading ( $\Psi$ ) of the ship.

The rudder can be used to stabilize the unstable ship. It can be deflected according to any measureable parameter - within the limits of the rudder system - which results in a signal capable of activating the rudder.

Ship's heading ( $\Psi$ ) and its first and second derivatives ( $r$  and  $\dot{r}$ ) are available in real life, even though considerable noise is present in measuring the second derivative ( $\dot{r}$ ). So any combination of those variables such as

$$s(t) = K\Psi(t)$$

$$s(t) = Kr(t)$$

$$s(t) = K_1\Psi(t) + K_2r(t)$$

$$s(t) = K_1r(t) + K_2\dot{r}(t)$$

and so on, can be used (at least theoretically) to construct the control signal necessary to activate the rudder and stabilize the dynamically unstable ship.

In order to have a reference and make comparisons and so investigate if the whole system is realizable, the dynamically



unstable ship is stabilized and its behavior forced to approach that of the stable ship.

The Digital Simulation Language (DSL/360) is used exclusively in the present study to simulate the three systems, stable, unstable and stabilized.

#### A. MOTION ON A STRAIGHT LINE. LINEAR MODELS

In the case of motion on a straight line, the two linear equations for Y-force and N-moment can be used to study and compare the behaviors of the stable and unstable ships, and can also be used to determine the necessary conditions for the stabilization of the dynamically unstable ship.

In order to make the behavior of the dynamically unstable ship approach that of the stable ship for the same excitations the roots of the characteristic equation of the unstable ship must be made to be the same as those of the stable ship.

Because the two cross-coupled differential equations (24) and (25), which for convenience are rewritten below

$$(Y'_V - m')\dot{v}' + Y'_V v' + (Y'_R - m'x'_G)\dot{r}' + (Y'_R - m'u'_O)r' + Y'_\delta \delta = 0 \quad (24)$$

$$(N'_V - m'x'_G)\dot{v}' + N'_V v' + (N'_R - I'_Z)\dot{r}' + (N'_R - m'x'_G u'_O)r' + N'_\delta \delta = 0 \quad (25)$$

include the first and second derivatives of  $\Psi(t)$  and not  $\Psi(t)$  itself, the heading  $\Psi(t)$  cannot be used in the control signal. This is because using  $\Psi(t)$  a third root  $\sigma_3$  is introduced in the characteristic equation of the stabilized system.

Also because we have to change the positions of two roots, two parameters are needed. So the signals which must be fed back to activate the rudder and accomplish the previously stated purposes are:



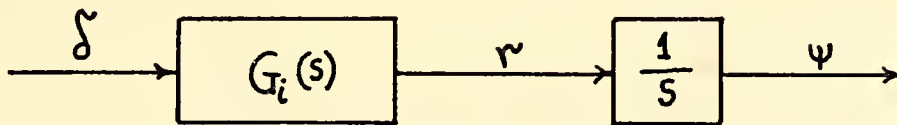
$$s(t) = K_1 r(t) + K_2 \dot{r}(t).$$

In Appendix C the procedures necessary for the computations of the numerical values for  $K_1$  and  $K_2$  are presented, and

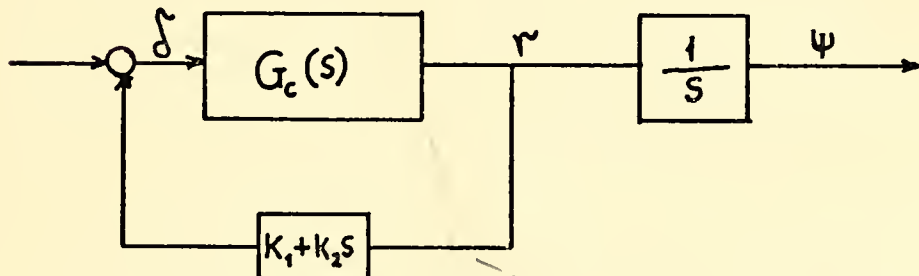
$$K_1 = -1.0232$$

$$K_2 = -0.207472.$$

In Figure 3 the block diagrams for the stable, unstable and stabilized models are shown.



(a)



(b)

Figure 3. Block Diagrams of Models A, C and Stabilized C.

From Figure 3(a) and Figure 3(b) it is clear that a distinction between rudder deflection and input command must be taken into account. That is the deflection of the rudder in the stable model is the input command to the system, while the deflection of the rudder in the stabilized model is the





result of the comparison of the input command and the fed back signal.

## B. SIMULATION OF THE LINEAR MODELS

In Appendix C the two differential equations (24) and (25) have been written in the form

$$A\dot{v} + Bv + C\dot{r} + Dr + Y\delta = 0 \quad (44)$$

$$E\dot{v} + Fv + G\dot{r} + Hr + N\delta = 0 \quad (45)$$

and the numerical values for the parameters are also listed. Then the transfer function for the three models, stable A, unstable C and stabilized C is found and is repeated here for convenience:

$$P(s) = \frac{r(s)}{y(s)} = \frac{(As+B)N - (Es+F)Y}{(Cs+D)(Es+F) - (As+B)(Gs+H)} \quad (46)$$

In Appendix D a method for computer simulation of a transfer function in the form of equation (46) is presented, which gives the first derivative ( $\dot{r}$ ) of the output needed for the stabilization of the unstable model, so allowing us to avoid the use of the DSL DERIV block.

The parameters used in Appendix D were computed for both models A and C and are listed below.

### (i) Model A

$$K_A = -1.2412$$

$$J_A = 1.449$$

$$I_A = 3.4363$$

$$N_A = 1.002$$



(ii) Model C

$$K_C = - 1.3051$$

$$J_C = 1.506$$

$$I_C = 2.624$$

$$N_C = - 0.73728$$

In Figure 4 the block diagram for models A and C is shown. In Figure 5 the block diagram for the stabilized model C is shown. In both block diagrams an integration of the output  $r(t)$  is included in order to obtain  $\Psi$ .

In the block diagram of Figure 5 there is a loop, indicated with the dotted lines, containing no storage elements. In other words there exists an algebraic loop (or implicit loop), and so simulation cannot be achieved unless a history block is introduced. So a pole ( $p/s+p$ ) with unity gain and  $p$  very large ( $p = 1000$ ) is introduced in the algebraic loop, in order to provide the history block (REALPL) without affecting the system dynamics. This is shown in Figure 7.

In order to use equations (40) and (41) to determine the path followed by the ships, the velocity  $v(t)$  is computed during the simulation from equation (44)

$$v(s) = - \frac{Cs+D}{As+B} r(s) - \frac{Y}{As+B} \delta(s).$$

An attempt to use equation (45) to compute  $v(t)$  led to failure of the simulation due to an OVERFLOW error. That was because the individual blocks are unstable as having poles in the right half plane; i.e. using equation (44)  $-p = B/A$  is positive, and using equation (45)  $p = F/E$  is negative.



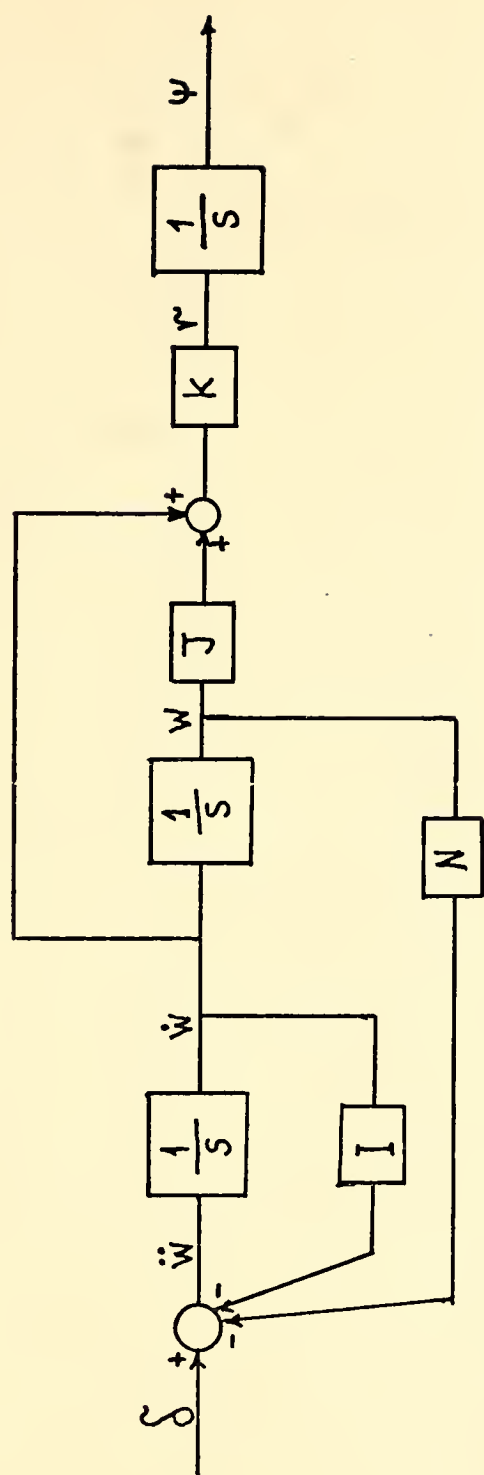


Figure 4. Block Diagram for Simulation of Models A and C.



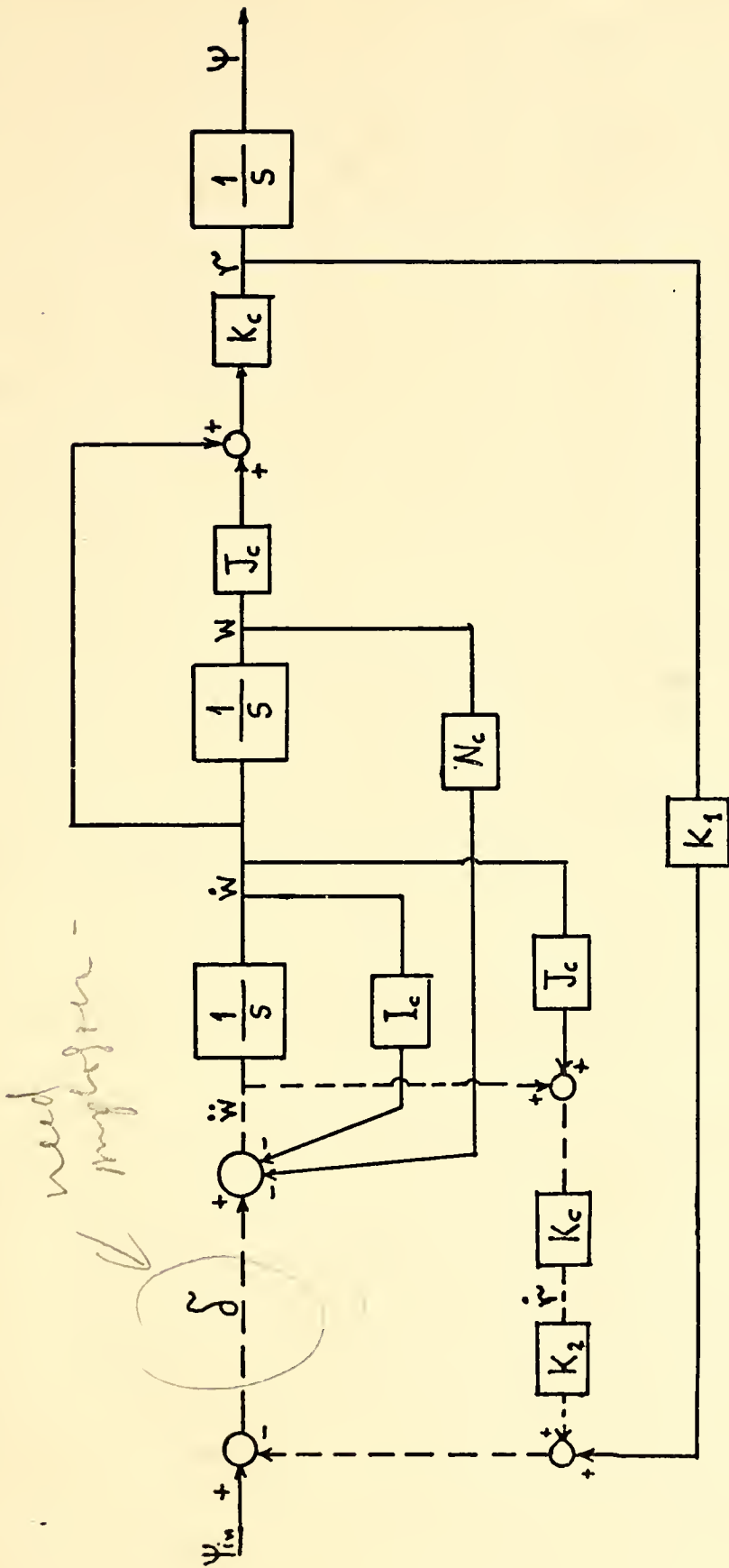


Figure 5. Block Diagram for Simulation of the Stabilized Model C.





In Figures 6 and 7 the block diagrams shown in Figures 4 and 5 are presented with a unity feedback path introduced. This feedback path provides a comparison of the ship's heading (angle  $\Psi$ ) with a course keeping input command, giving an error signal for the necessary corrections. In other words this feedback loop represents the "helmsman" who takes an order to keep a certain course. The signal feedback is added to the input (positive feedback) because according to the sign convention adopted for the development of the equations of motion a positive rudder deflection produces a negative angle  $\Psi$ .

The rudder is assumed, to have no time lag, to turn with a rate of two degrees per second, and to have a maximum deflection of thirty five degrees.

With  $L = 500$  and assuming  $U = 15 \times 1.6878$  the rate of deflection nondimensionalized becomes:

$$D_{\text{rate}} = \frac{2}{U/L} = 40.$$

In Figure 8 the characteristic of the rudder operation is shown.

Two kinds of tests were performed with the linear models as follows.

#### 1. "Helmsman" Operation

The simulation of the two models A and stabilized C with unity feedback is made with Computer Program No. 1 (Referred to Figure 6 and Figure 7). The same excitation at the same time is applied to both systems, which in this case is a step command, or in other words, an order to the "helmsman" to keep a certain course.



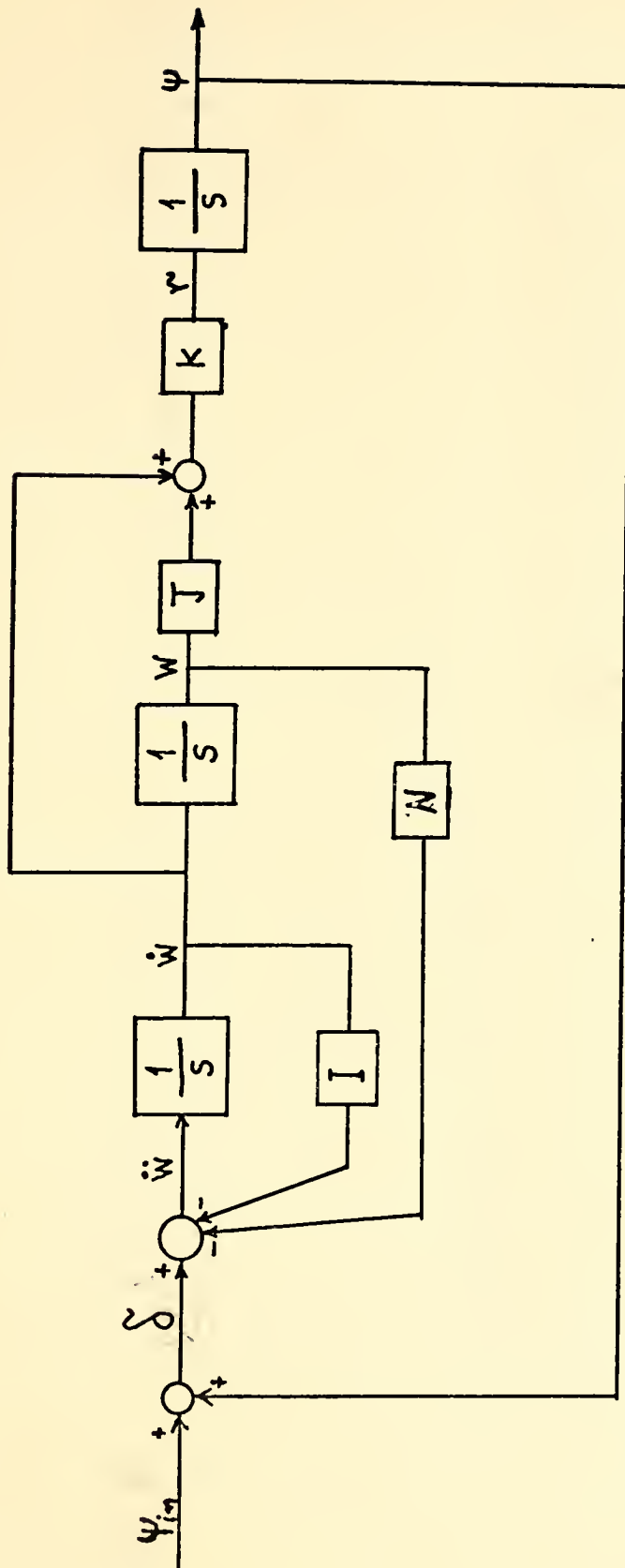


Figure 6. Block Diagram for Simulation of Models A and C with the Unity Feedback Loop Connected.







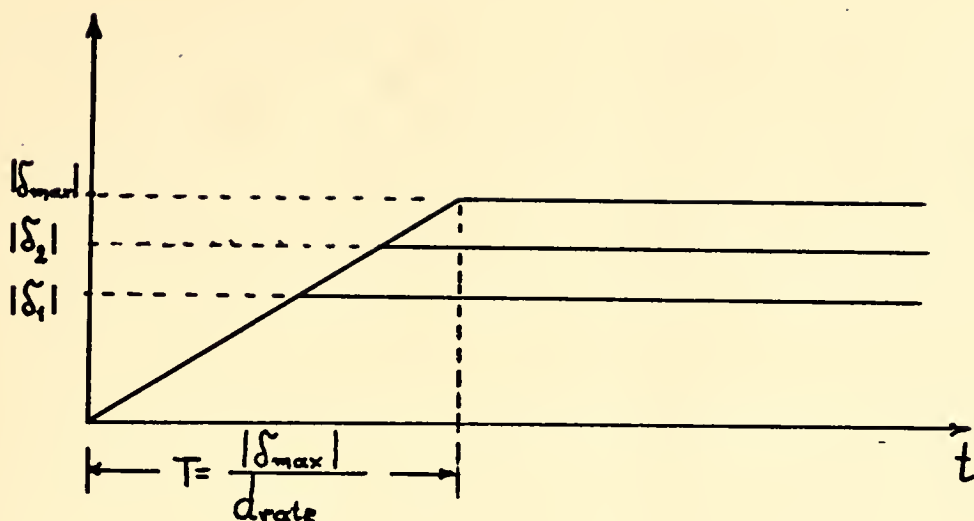


Figure 8. Rudder Characteristic.

In Figure 9 the graph represents the deflections of the two rudders vs. time. In Figure 10 the headings are shown and in Figure 11 the trajectories of both ships.

From those plotted results the following can be stated:

(a) The deflections of the rudder of the stabilized model C are within the limits between which the rudder of model A moves.

(b) The rates of change of the deflections,  $\delta(t)$  are almost the same.

(c) The heading angles ( $\Psi$ ) approach the given command in almost the same way and at the same time.

(d) The trajectories of both models are almost identical.





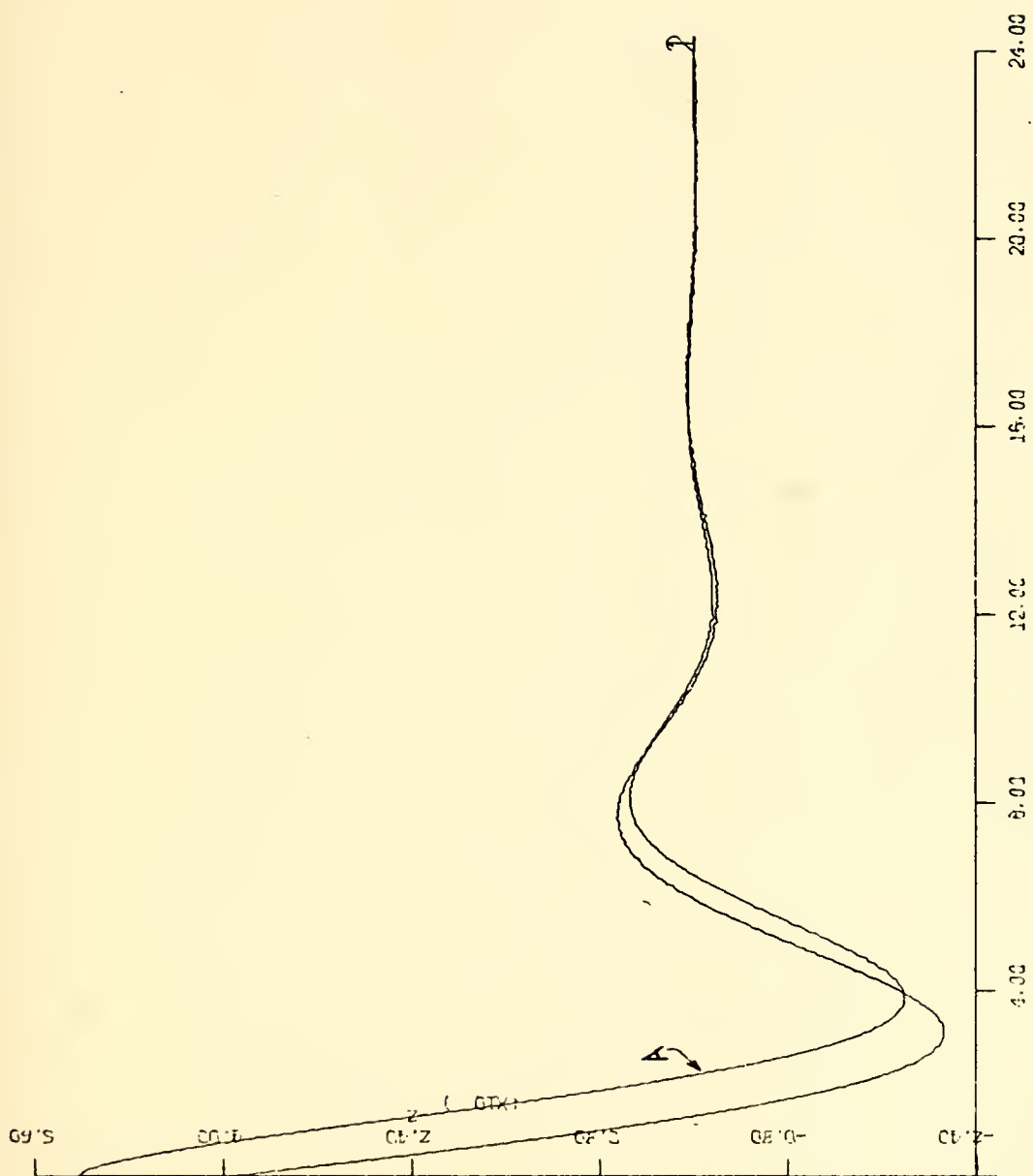


Fig. 9. Rudder deflections vs time in the "Helmsman" Operation test.



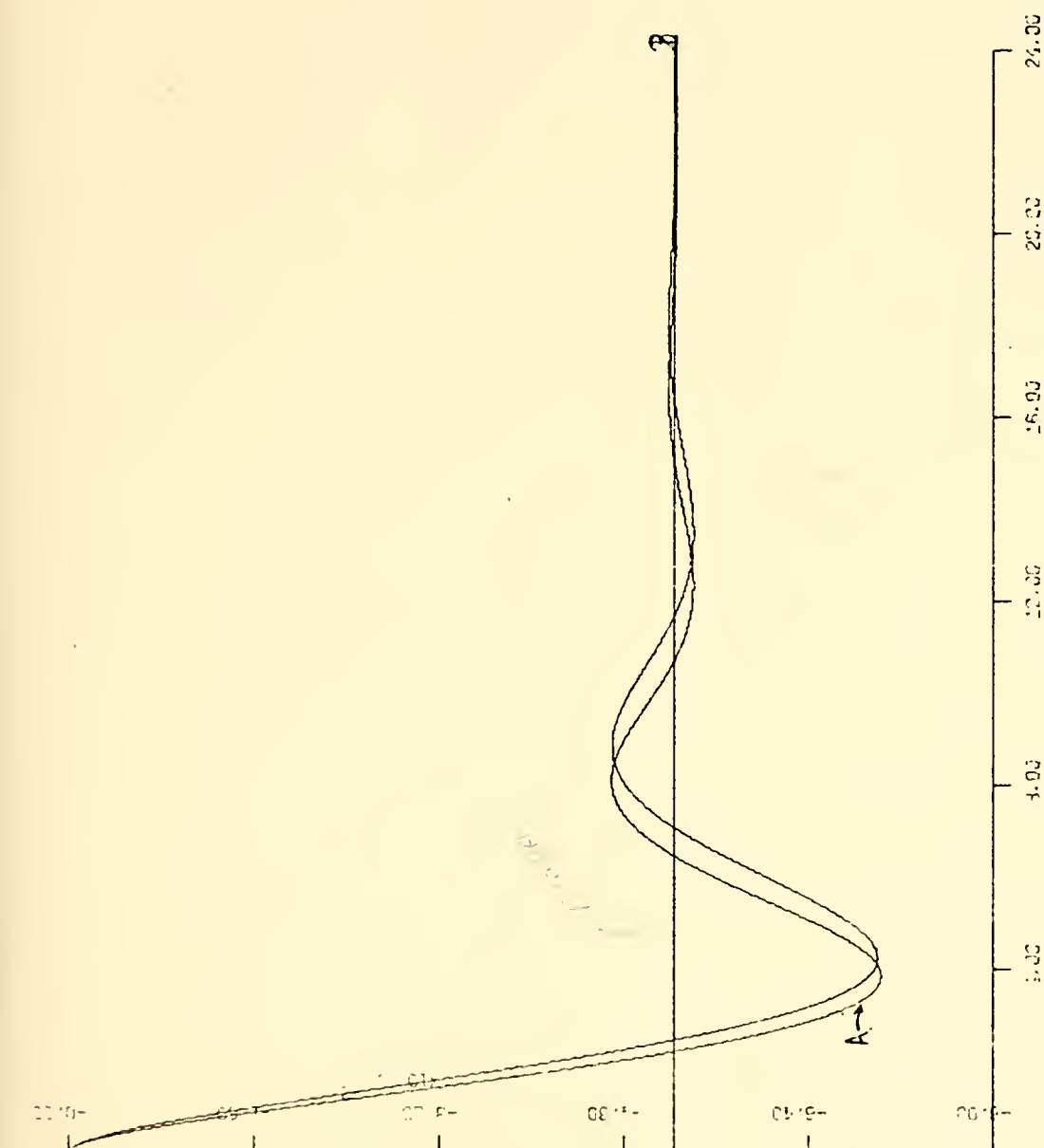


Fig. 10. Ship headings ( $\psi$ ) vs time in the "Helmsman" Operation test.



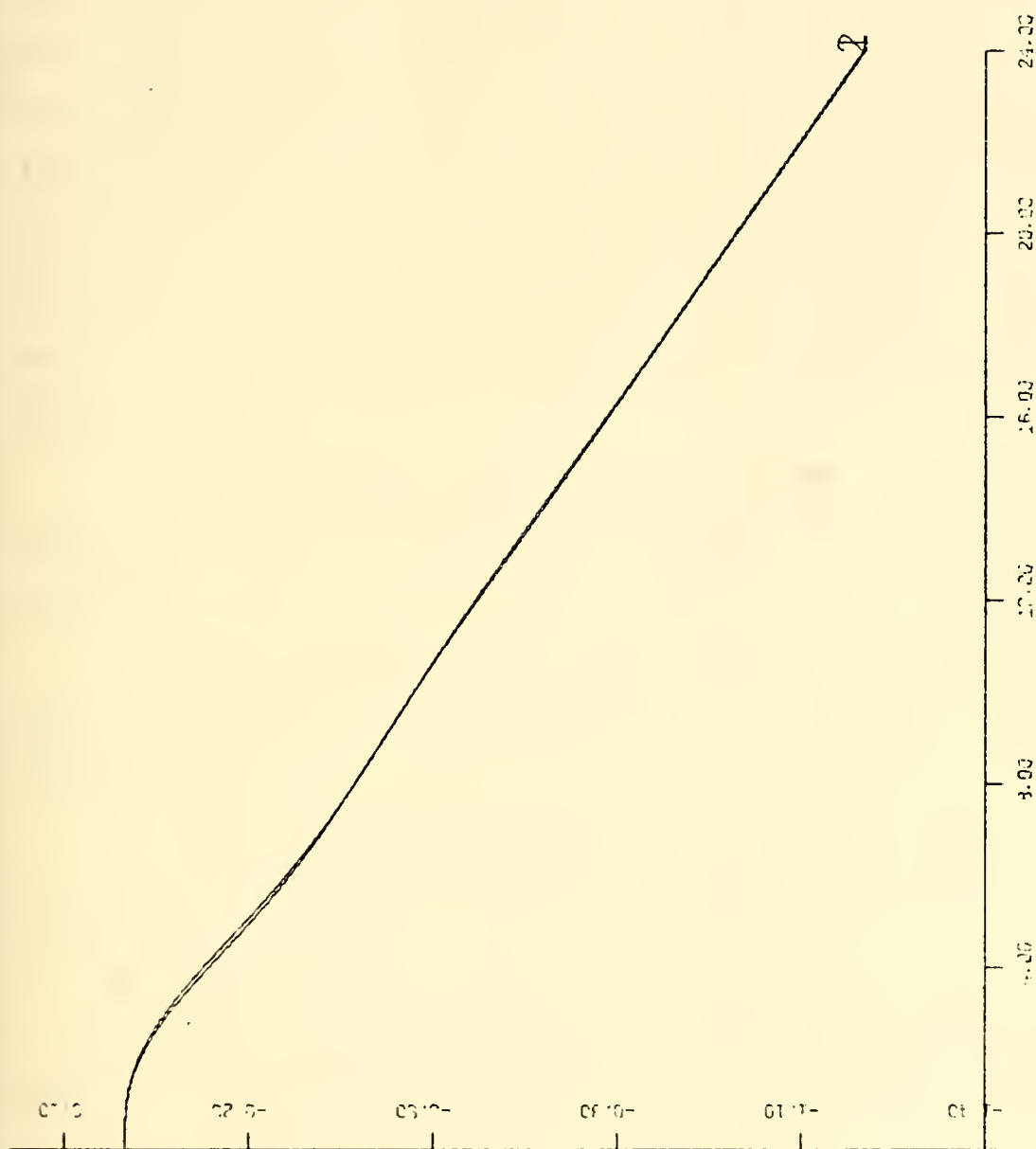


Fig. 11. Ship trajectories in the "Helmsman" Operation test.



## 2. Turning Maneuvers

Not

The models developed in this study from the linear equations of motion can only describe the motion of a ship on a straight line and/or after a small perturbation has been applied. Nevertheless with the Computer Program No. 2 (Referred to Figure 4 and Figure 5) the two models are simulated, with the unity feedback loop disconnected, for tight maneuvers in order to investigate if and how closely the behavior of the stabilized model C approaches that of the stable model A. Again the same input command is given at the same time which in this case is a combination of Ramp functions.

The results of the simulation are shown plotted in Figure 12, Figure 13, and Figure 14 and can be stated as follows:

(a) The deflection of the rudder of the stabilized model C exceeds the limit within which that of the stable model A varies.

(b) The rate of change of the rudder's deflection of the stabilized model C does not exceed the rate of change of the input command.

(c) The heading angle ( $\Psi$ ) and the trajectory of the stabilized model approach those of the stable model.

### C. GENERAL MOTION. NONLINEAR MODELS

Not

The motion of a ship under tight maneuvers is governed by the nonlinear equations of motion presented in section III which (equations) are also suitable for computer programming.





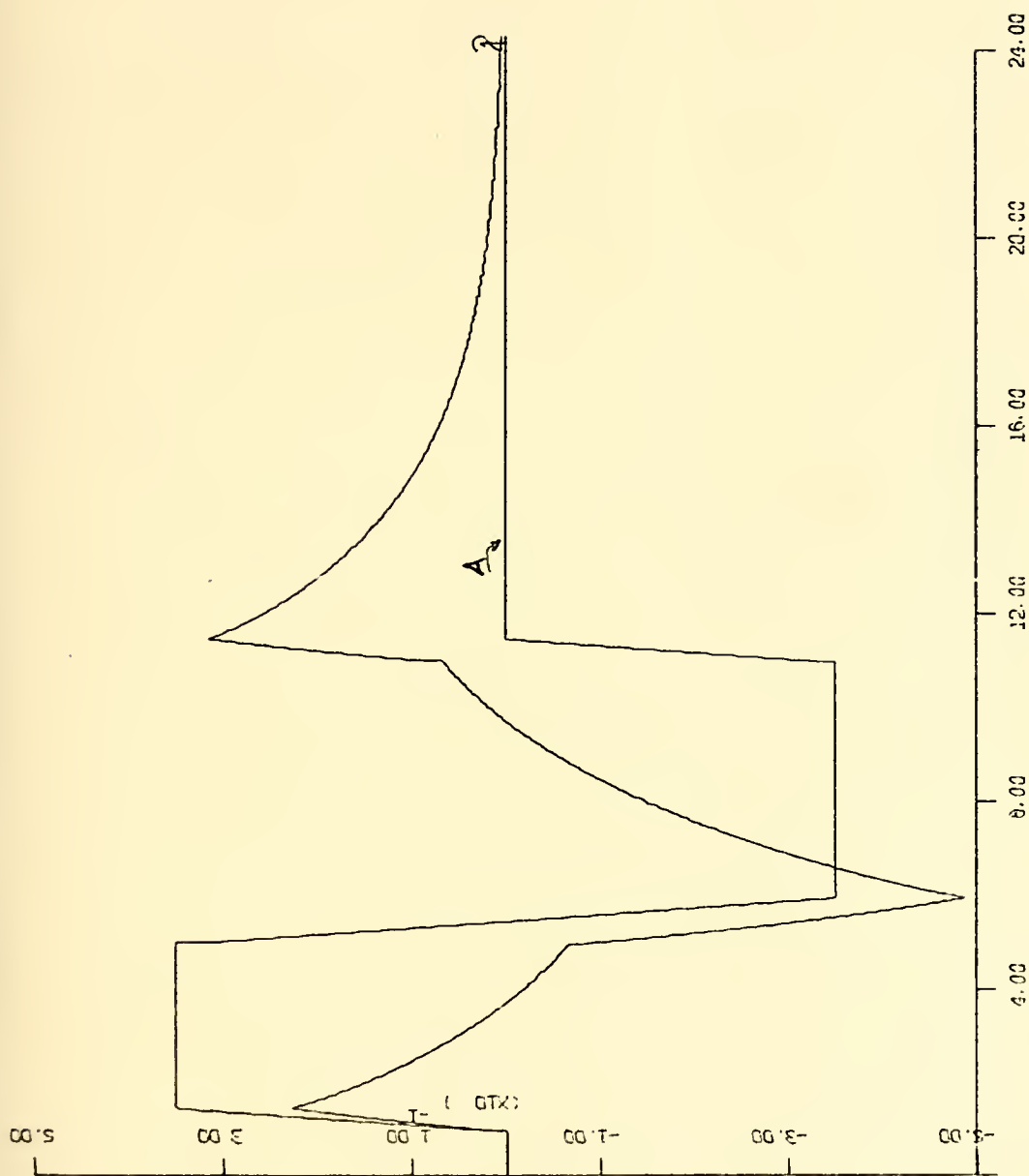


Fig. 12. Rudder deflections vs time in the "Turning Maneuvers" test.



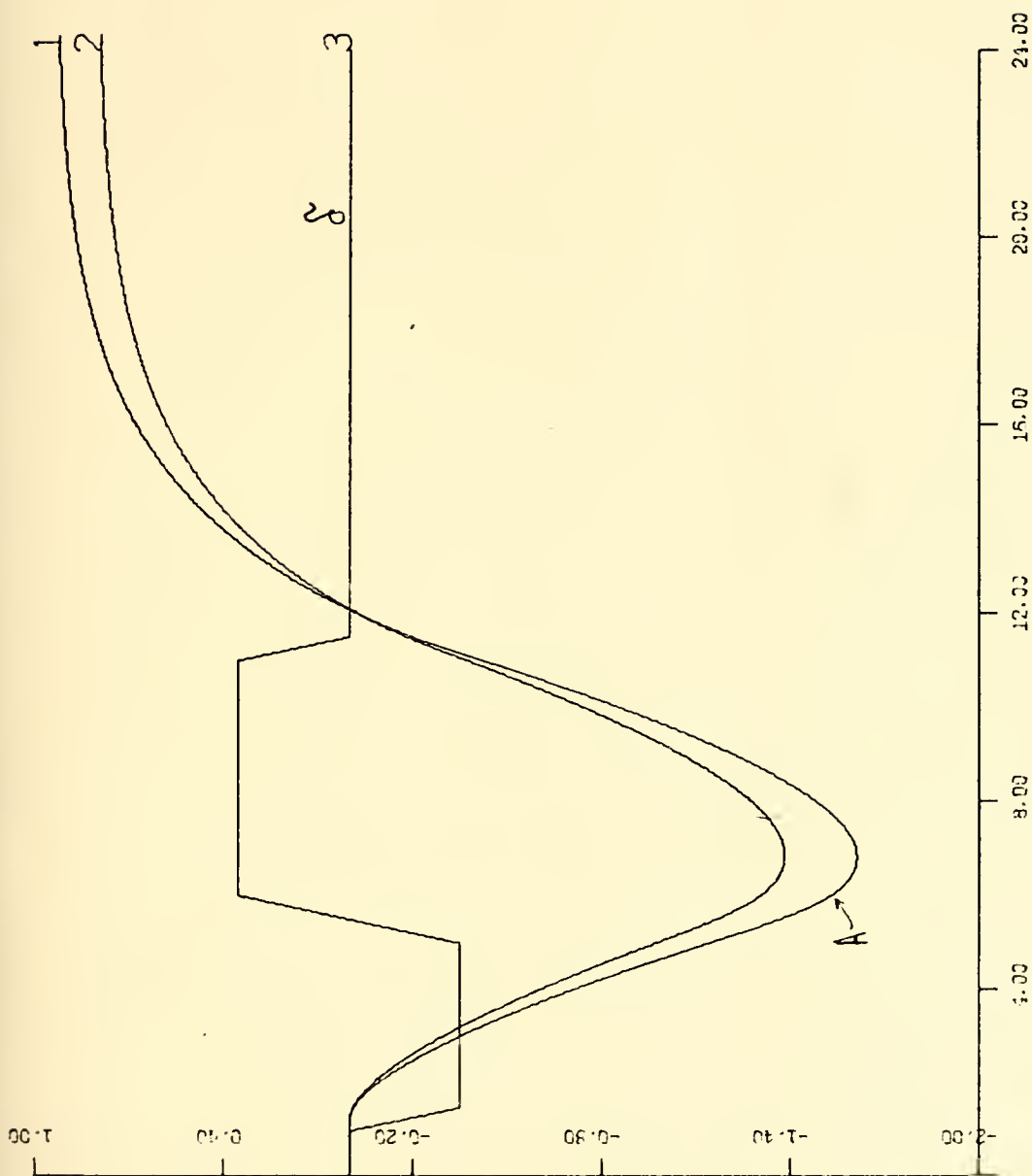


Fig. 13. Ship headings ( $\Psi$ ) vs time in the "Turning Maneuvers" test.



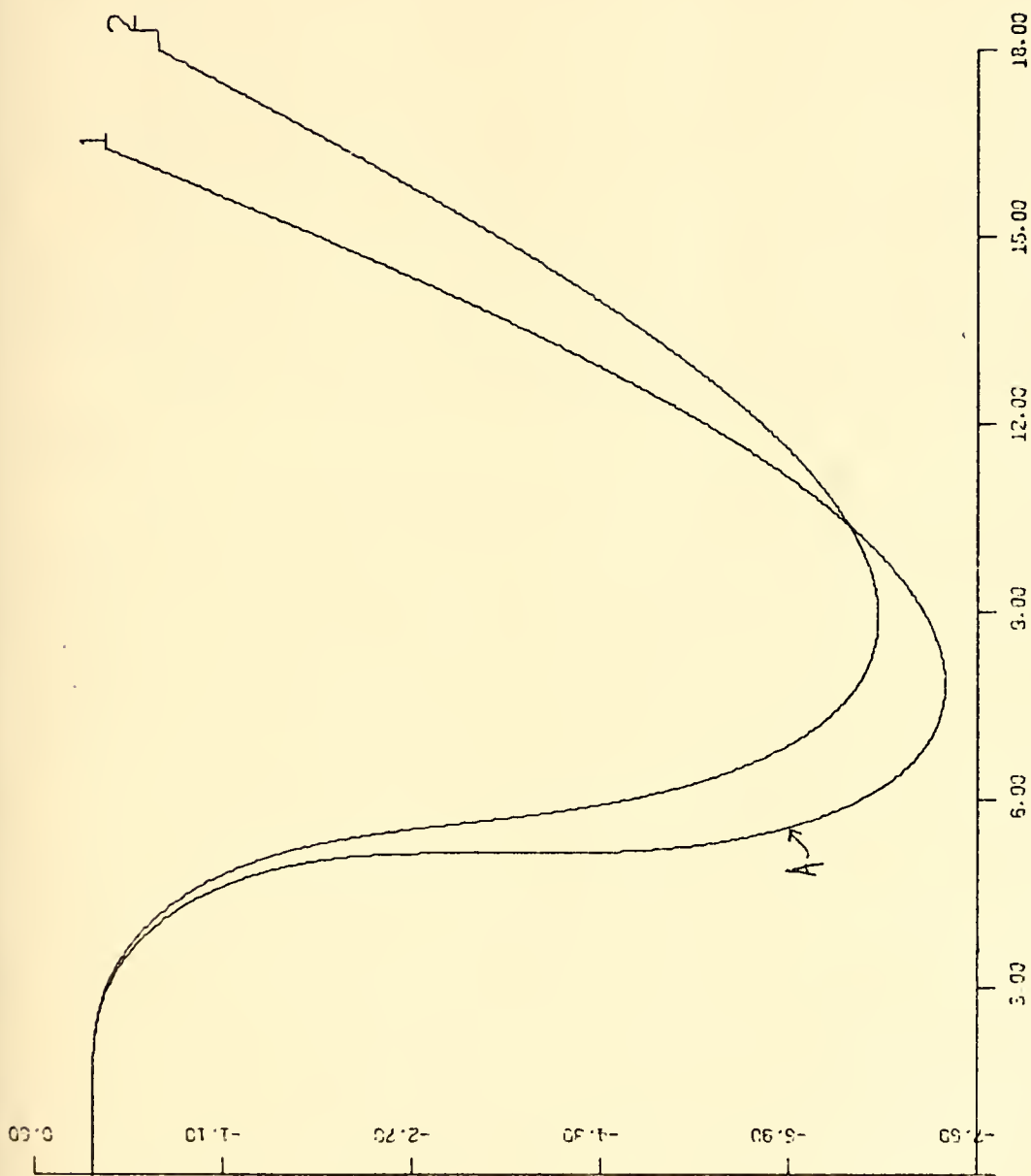


Fig. 14. Ship trajectories in the "Turning Maneuvers" test.



The parameters (hydrodynamic derivatives) for equations (38) and (39) are listed in Appendix B.

The signal  $s(t) = K_1 r(t) + K_2 \dot{r}(t)$  with  $K_1$  and  $K_2$  equal to those computed in Appendix C for the linear case, is used again to deflect the rudder and stabilize the dynamically unstable ship.

#### D. SIMULATION OF THE NONLINEAR MODELS *note*

Equations (35a), (36a), (38), (39), (39a), (40), (41), (42), and (43) are used directly for the simulation of the nonlinear models, stable A, unstable C, and stabilized C.

For the simulation the following assumptions have been made:

(1) A nondimensionalized velocity  $u'(t') = 1$  is used during the whole simulation interval. That means that in order to get the dimensionalized quantities from the computed nondimensionalized we have to use the  $u$ -velocity with which the ship is considered moving at that particular time.

(2) The  $Y$ -force and  $N$ -moment induced by the rotation of the single propeller of the ship at  $v = \delta = 0$ , identified as  $Y'_0$  and  $N'_0$ , are included.

(3) The rudder has no time lag, a two degrees per second rate of turn and a thirty five degrees maximum deflection.

Two kinds of tests were performed with the nonlinear models as follows.

##### 1. Zig-Zag Maneuvers

The way the Zig-Zag maneuvers are performed is described in Appendix E. This test is used to study the behavior of the stabilized model C as compared to the behavior of the





unstable model C and stable model A. With the use of Computer Programs No. 3 and No. 4, the three models were simulated for the Zig-Zag maneuver performance. The results of the simulation are shown in Figures 15, 16, 17, 18, 19, 20 and 21, and can be stated as follows:

(a) The maximum deflection of the rudder of the stabilized model C exceeds the maximum value of the input command.

(b) The rate of change of the rudder deflection of the stabilized model C does not exceed the rate of change of the input command, but the rudder stays in motion during the whole interval of the test performance.

(c) The heading angle ( $\Psi$ ), the velocities  $r$  and  $v$  and the trajectory of the stabilized model C differ from the respective quantities of the unstable model C and approach to those of stable model A.

## 2. "360° Turn" Test

With the use of Computer Program No. 5, the "360° turn" test was devised in an attempt to study the turning characteristics of the combination unstable - stabilized ship as compared to the turning characteristics of the stable ship. The following assumptions and steps were made and followed in devising this "360° turn" test:

(a) The simulation time units were taken to be the nondimensionalized time units.

(b) From  $t' = 0$  to  $t' = 1$  the two ships were moving with constant speed on a straight line. During that interval it was taken  $Y'_0 = N'_0 = 0$ .



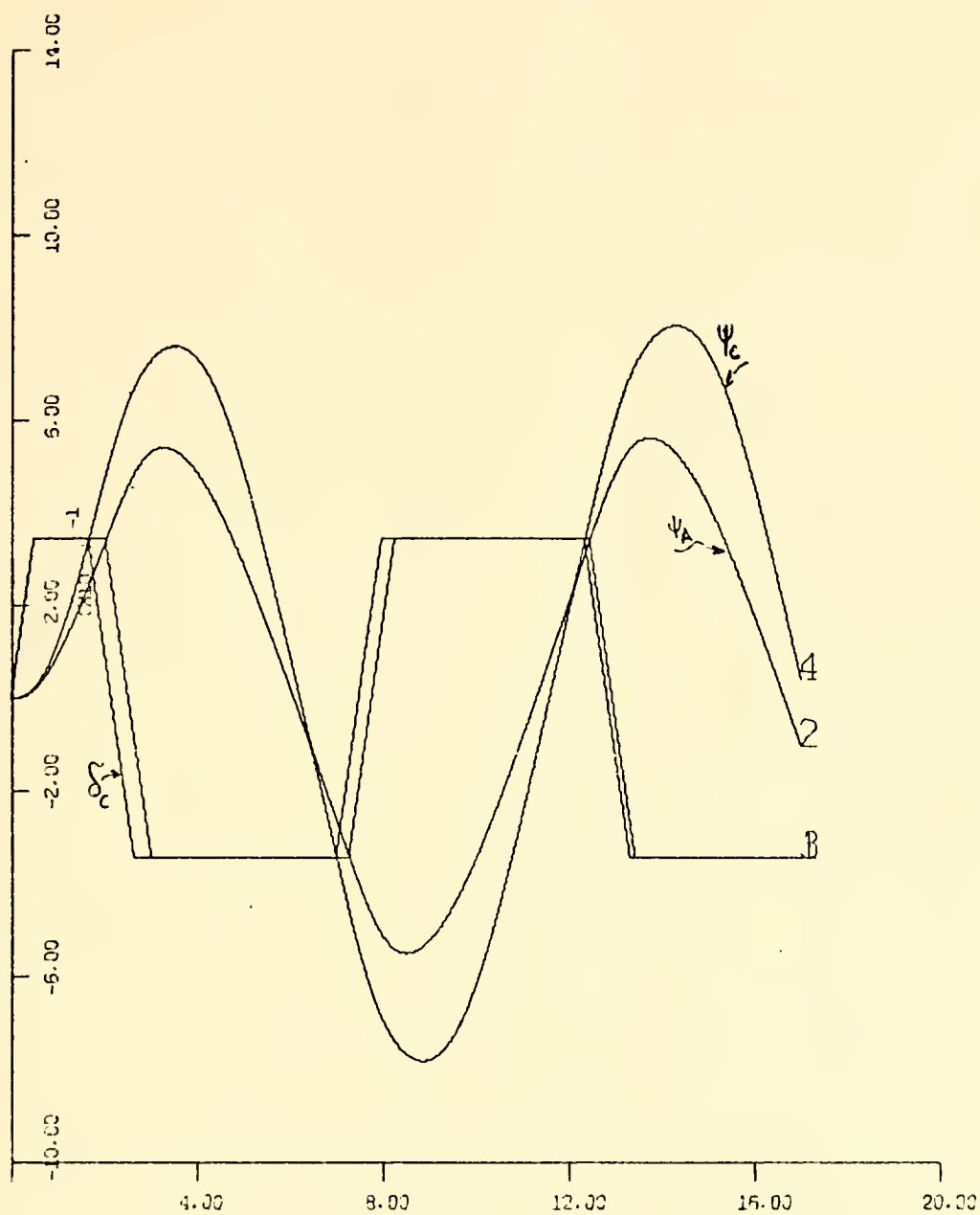


Fig. 15. Rudder deflections and ship headings ( $\Psi$ ) vs time in the "Zig-Zag Maneuvers" test. (Models A and C)



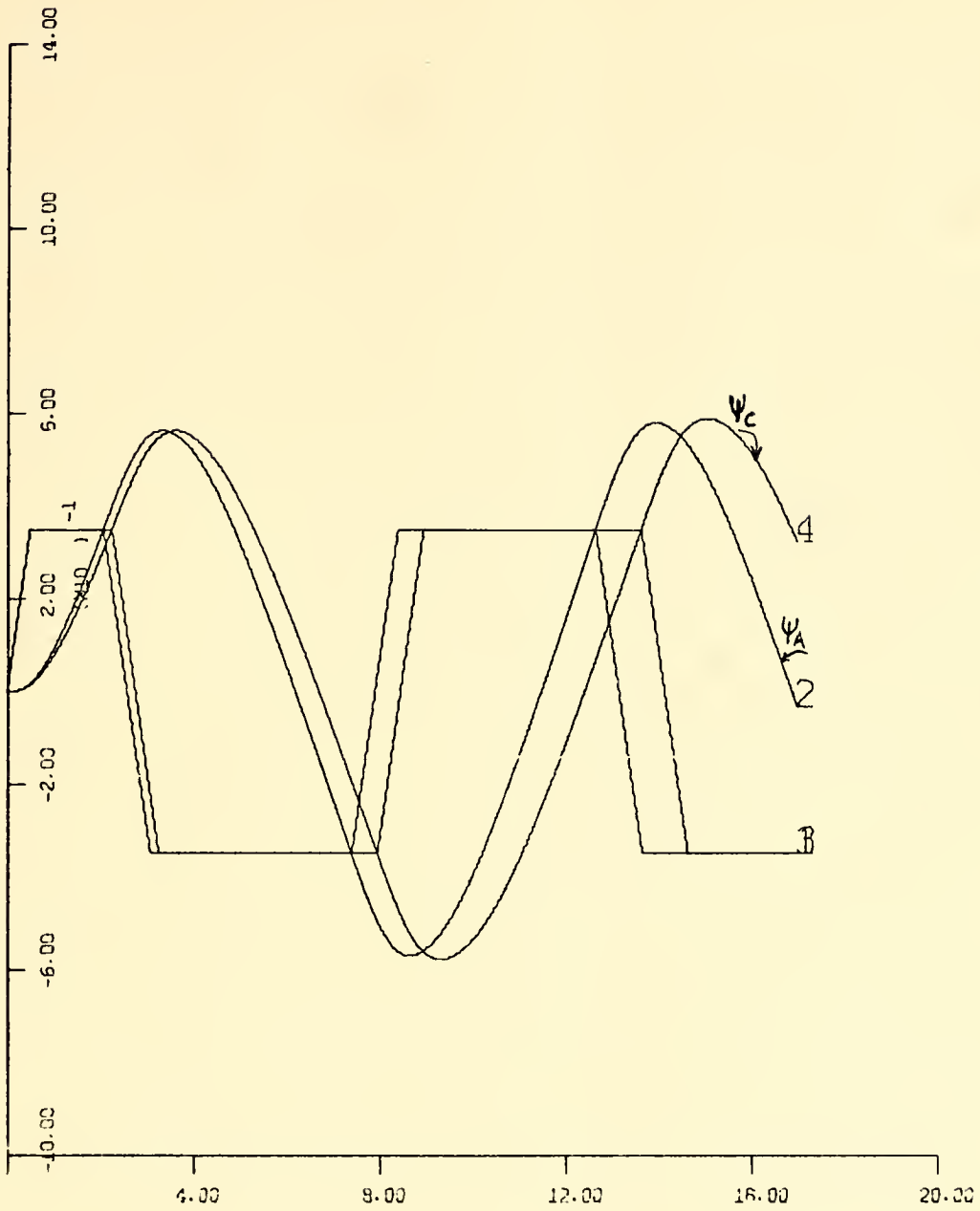


Fig. 16. Input commands and ship headings ( $\Psi$ ) vs time in the "Zig-Zag Maneuvers" test (Models A and C stabilized)



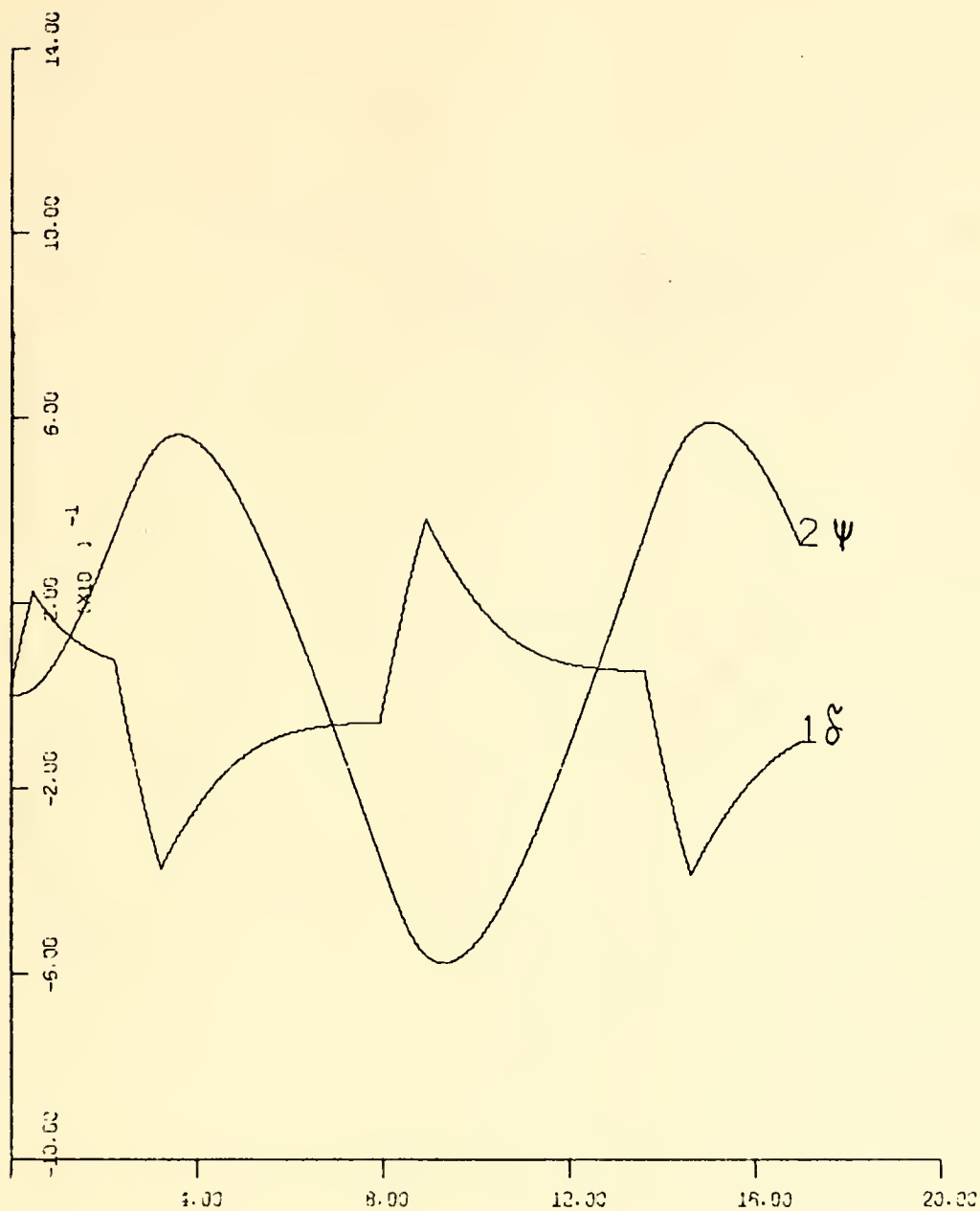


Fig. 17. Rudder deflections and ship headings ( $\Psi$ ) vs time in the "Zig-Zag Maneuvers" test (Model C stabilized)





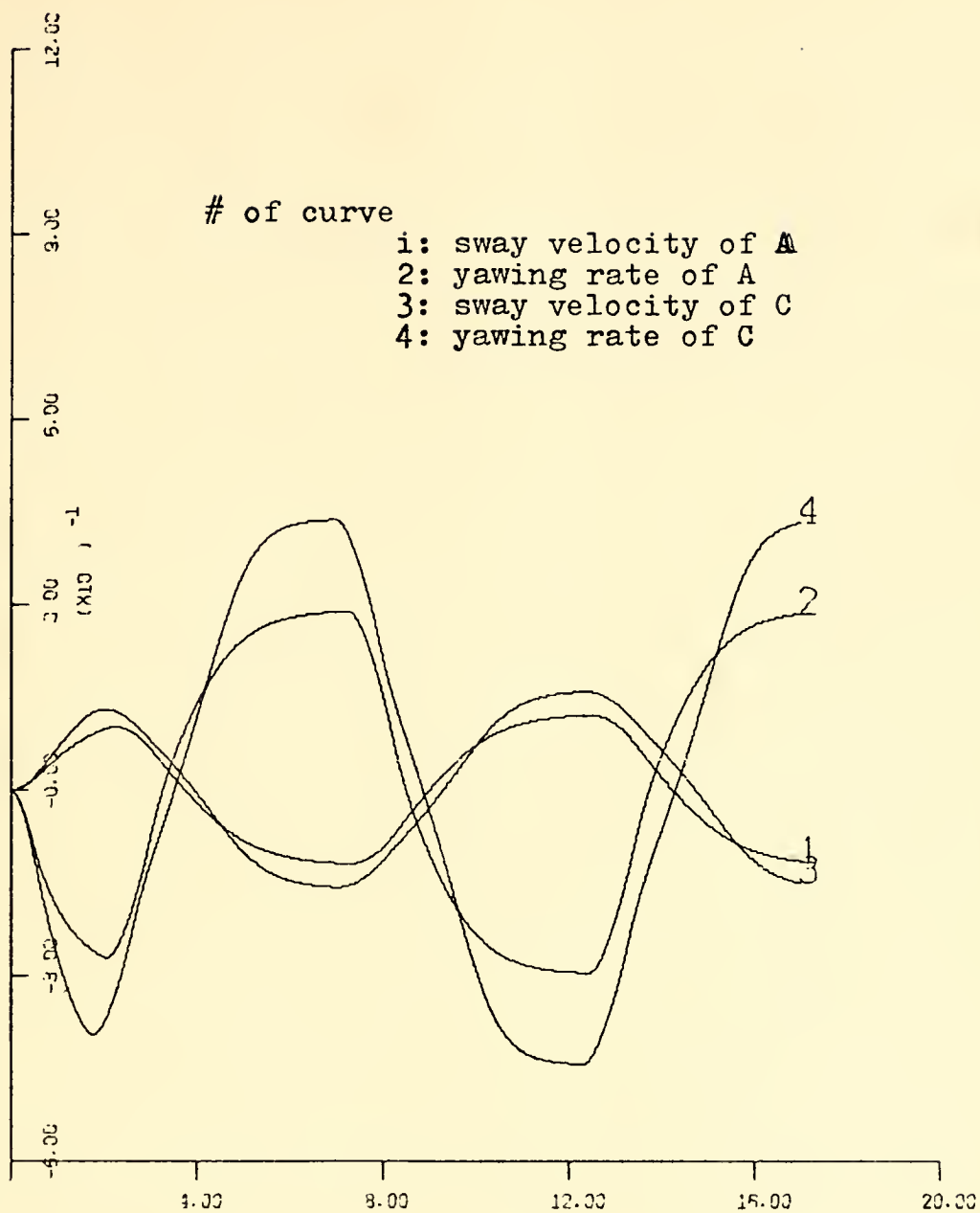


Fig. 18. Yawing rate and sway velocity vs time in the "Zig-Zag Maneuvers" test (Models A and C)



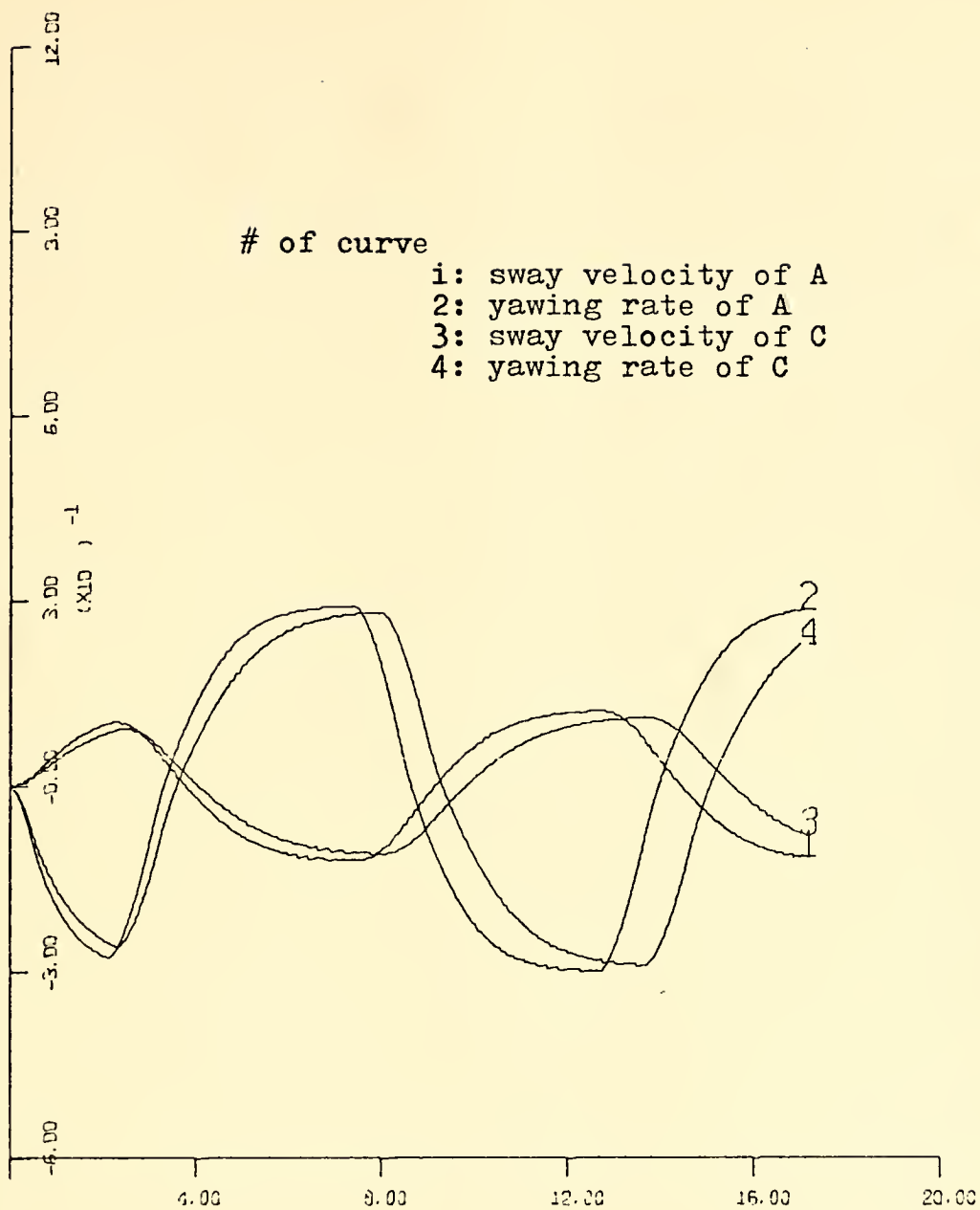


Fig. 19. Yawing rate and sway velocity vs time in the "Zig-Zag Maneuvers" test (Models A and C stabilized)



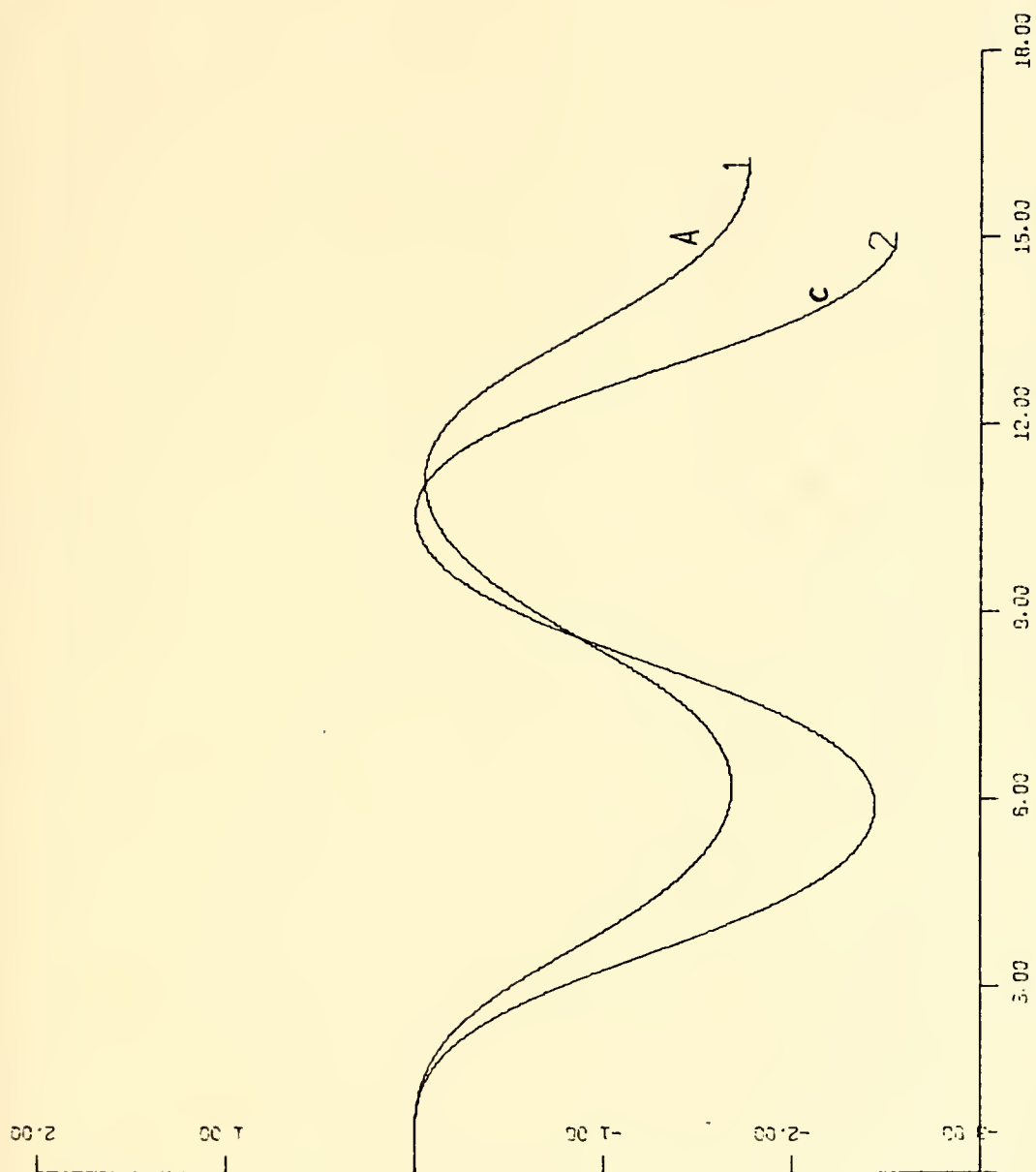


Fig. 20. Ship trajectories in the "Zig-Zag Maneuvers" test (Models A and C)



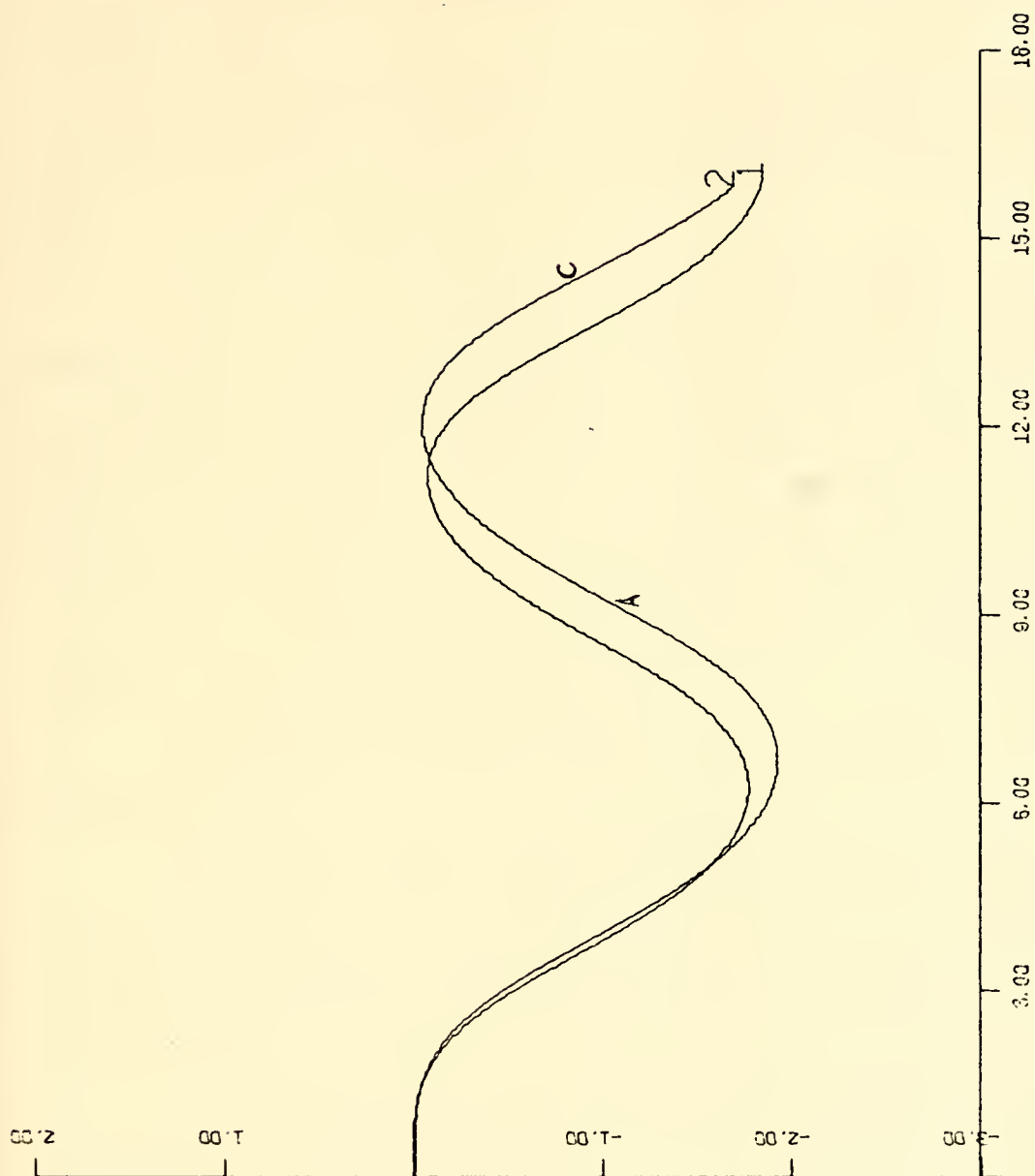


Fig. 21. Ship trajectories in the "Zig-Zag Maneuvers" test (Models A and C stabilized)





(c) At time  $t' = 1$  a command for a  $20^\circ$  rudder position was given to both ships. The rate of change of rudder deflection was taken to be  $40^\circ$  per nondimensionalized time unit. MO

(d)  $Y'_0$  and  $N'_0$  assumed their numerical values at the same time  $t' = 1$ .

(e) The stabilizing feedback loop for the ship C was held open from time  $t' = 1$  until almost the end of the turn.

(f) When  $\Psi = 344^\circ$  was reached each rudder was brought to  $\delta' = 0$  and the unity feedback loop ("helmsman") was connected and a course keeping command  $\Psi = 360^\circ$  was given. Furthermore at the same instant (when  $\Psi = 344^\circ$ ) the stabilizing feedback loop was energized in ship C.

(g) At the same instant the parameters  $Y'_0$  and  $N'_0$  were put again equal to zero.

The results of this simulation are shown in Figure 22 and Figure 23.

In order to get actual numerical values for the various parameters of the motion and be able to compare the behaviors of the two ships the following should be taken into account:

(a)  $U(t)$  is the speed of the ship, tangent to the instantaneous path and is given by:  $U(t) = \sqrt{v(t)^2 + u(t)^2}$ .

(b)  $U(t)$  before the beginning of the turn is equal to the speed after the completion of the turn (and when steady state conditions have been reached), both are equal to the  $u(t)$  velocity.



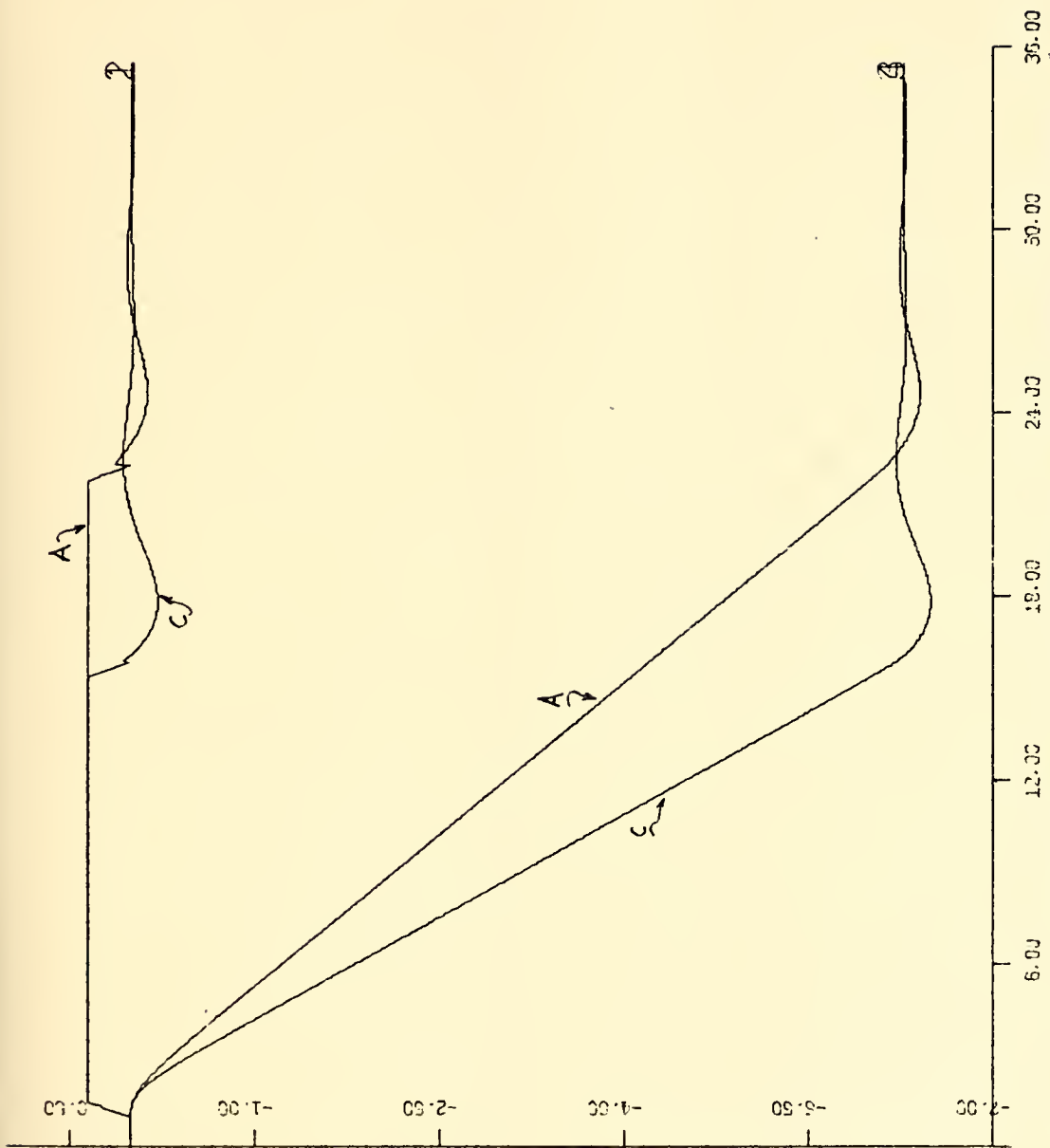


Fig. 22. Input command and ship headings ( $\psi$ ) vs time in the "360° turn" test.



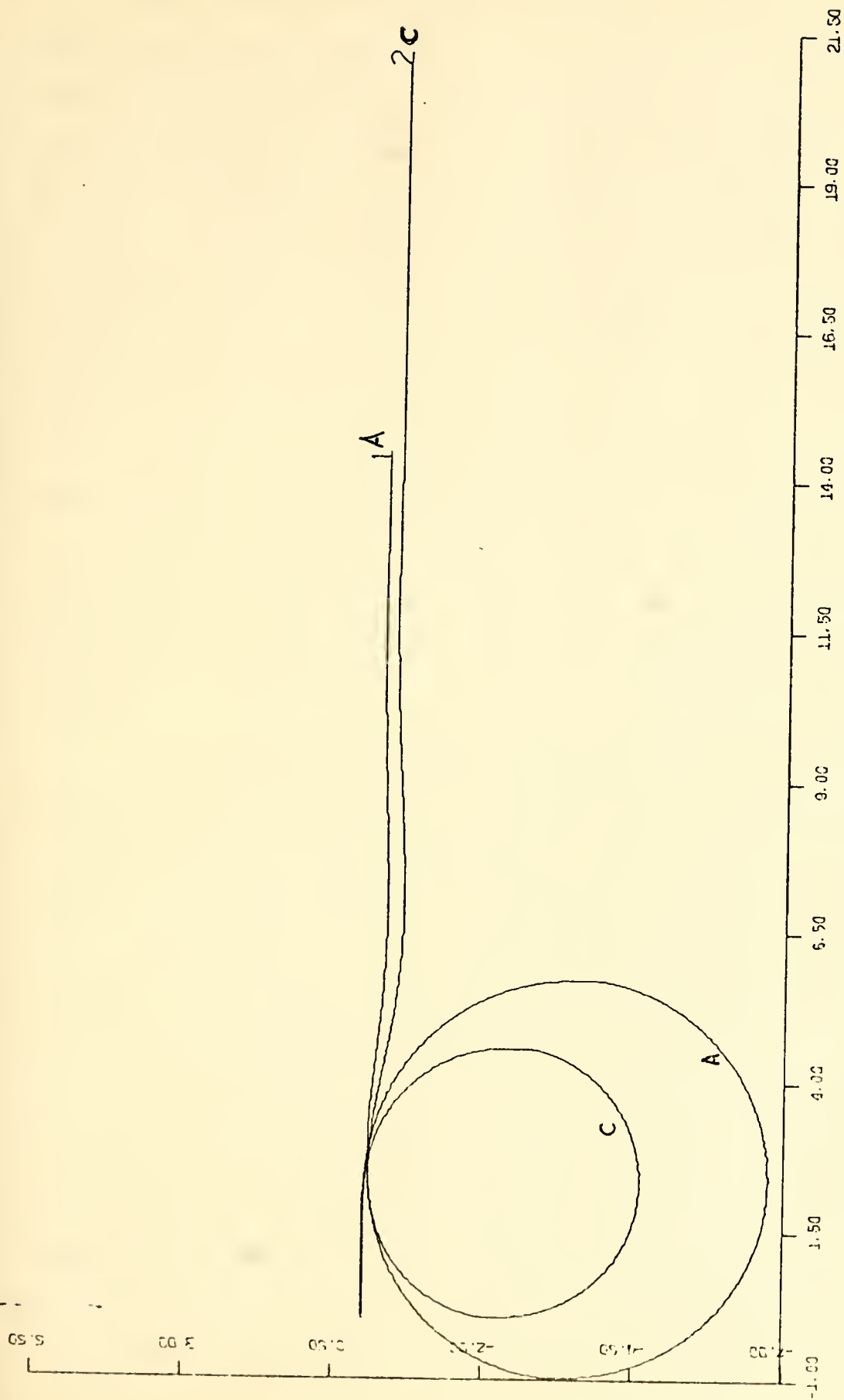


Fig. 23. Ship trajectories in the "360° turn test."



(c) The speed of the ship during the turn is different than that in case (b). This is due to the speed reduction during the turn. This speed reduction is inversely proportional to the turn diameter, that is the smaller the diameter of turn the higher the speed reduction. In spite of the increasingly severe speed loss associated with tighter turns, it has been shown (Ref. 2), that by decreasing the tactical diameter significant operational aspects of turning are improved.

(d) It is repeated here that the nondimensionalizing speed is taken to be the  $u(t)$  velocity.

(e) In Reference 2 (Page 482) information for the speed reduction of the model used in this study as a function of the turning diameter (expressed in ship's lengths) is given.

(f) The assumed  $40^\circ$  per nondimensionalized time unit does not correspond to the same rate of change of rudder deflection ( $2^\circ$  per second), for both models, due to the change in the nondimensionalizing velocity and the difference in speed between the two ships (different turn diameters). However, this is not significant because we are not concerned (at all) with the transient phase in this study.

From the graph shown in Figure 23 it is clear that the turning characteristics of model C are better than those of model A; that is, the turning diameter of model C is smaller than that of model A. Subsequently model C has covered more distance in the original course than model A has, in the same interval of time.





## V. SHIP RESPONSES WHEN A SINUSOIDAL WAVE IS PRESENT

OK

In chapter IV the stabilization of the unstable ship was studied and the models were tested. Because of the stabilizing function of the rudder on model C, the rudder was expected (and it was found) to stay deflected for larger intervals of time than the rudder in model A, and also to take sometimes larger deflections. That, of course, results in the expense of more energy than is required for the stable model under the same conditions.

The purpose of this chapter is to find a kind of relative measure for the deflection of the rudder and then investigate if and to what extent the introduction of a "Dead Zone" in the system can improve the situation, eliminating unnecessary deflections due to small amplitude excitations.

In order to accomplish this the stable model A and the stabilized model C are considered trying to keep a motion on a straight line under the effect of a sinusoidal excitation on the system due to say the presence of waves.

### A. MODELS FOR THE SINUSOIDAL EXCITATION

Because the two ships are considered moving on a straight line the linear equations can be used to study their behavior.

Assuming that the excitation has only three components,  $X_w$ -force,  $Y_w$ -force, and  $N_w$ -moment, the components of our interest remain again the  $Y_w$  and  $N_w$ , and equations (44) and (45) become: -

$$(As+B)v(s) + (Cs+D)r(s) + Y\delta(s) + Y_w(s) = 0 \quad (47)$$



$$(Es+F)v(s) + (Gs+H)r(s) + N\delta(s) + N_w(s) = 0. \quad (48)$$

Equations (47) and (48) can be again combined (Appendix C, Figure (C-1) and equations (C-8) and (C-9)) and give the block diagram shown in Figure 24.

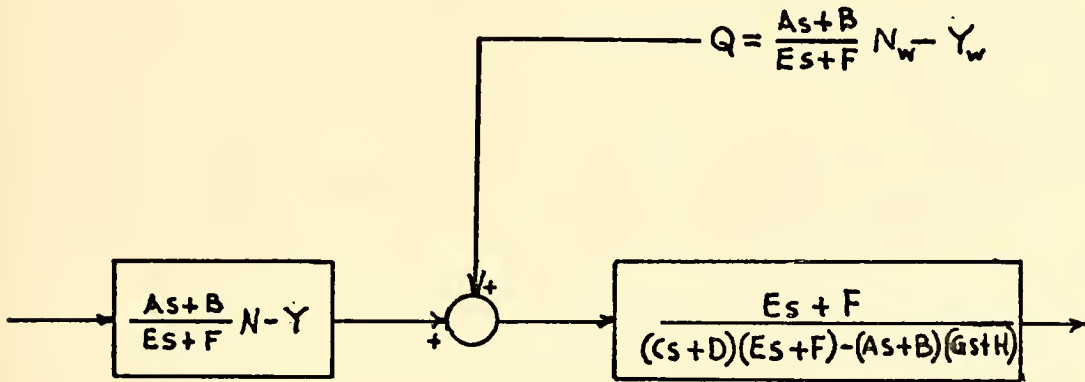


Figure 24. Block Diagram Representation of the Two Models A and C in the Presence of Waves.

Because of the existence of unstable blocks ( $E > 0$ ,  $F < 0$ ,  $A < 0$ ,  $B < 0$ ) the two branches before the summing point in Figure 24 are multiplied by  $Es+F/As+B$  and the branch right after the summing point by  $As+B/Es+F$ . The resulting block diagram is shown in Figure 25.

With this mathematical trick the block instabilities are eliminated without affecting the system's dynamics. Integrating  $r(t)$  and feeding back the ship's heading,  $\Psi$ , to compare it with an input course command, the block diagram of Figure 25 becomes as shown in Figure 26, where  $D(s)$ ,  $Q(s)$ , and  $G(s)$  represent the functions shown in the corresponding blocks in Figure 25.

A kind of "Figure of Merit" for the rudder's function is devised in this section. The square root of the area under



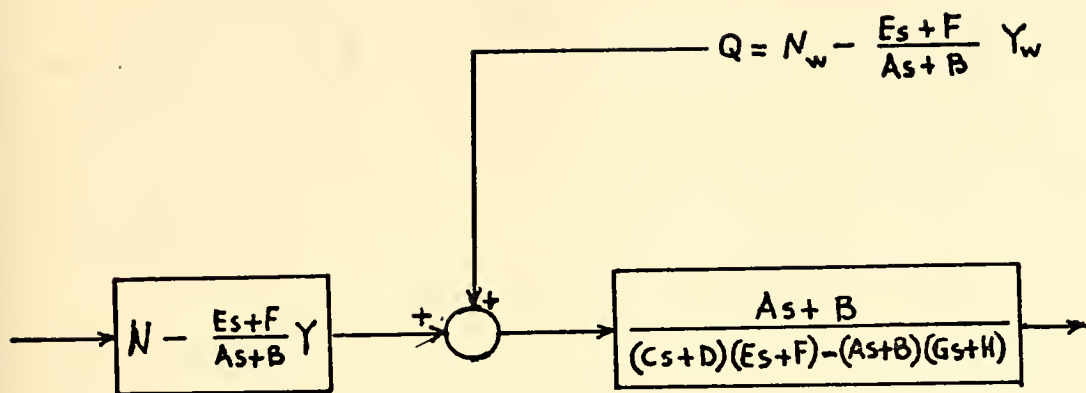


Figure 25. Block Diagram Representation of the Two Models A and C (Figure 24 transformed)

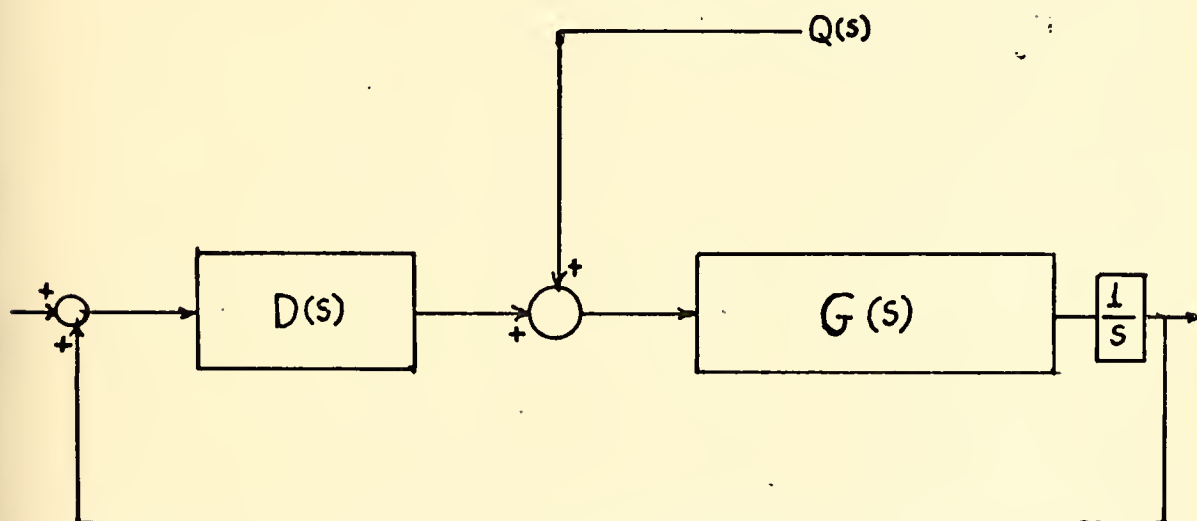


Figure 26. Block Diagram Representation of Models A and C with the Unity Feedback Loop.



the curve representing the deflection of the rudder, squared, vs. time is computed during each simulation, and that gives a quantitative measure of the rudder's function. The higher the deflection (positive or negative) and the longer the rudder remains at a certain position, the higher the "Figure of Merit" will be.

## B. SIMULATION

Substituting the numerical values of the parameters in  $G(s)$  we have:

$$\text{For model A } G_A(s) = \frac{39.1(s + 0.9134)}{s^2 + 3.4363s + 1.002}$$

$$\text{For model C } G_C(s) = \frac{40.775(s + 0.8094)}{s^2 + 2.624s - 0.7373}$$

Those two transfer functions can be modeled using the technique developed in Appendix D where now:

$$\text{For model A } K_A = 39.1$$

$$J_A = 0.9134$$

$$I_A = 3.4363$$

$$N_A = 1.002$$

$$\text{For model C } K_C = 40.775$$

$$J_C = 0.8094$$

$$I_C = 2.624$$

$$N_C = -0.73728$$

For the purposes of this study a pure sinusoid was assumed for  $Q$ , i.e.,  $Q = A_0 \sin(\omega t)$ .

The spectrum of sea wave frequencies encountered in practice (all sea states) is (Ref. 4)  $0.03 \leq f \leq 2$  (cycles/sec). Frequencies lower than 0.03 do not exist while frequencies higher than 2 do not have any effect on the ship.





For this study we choose one frequency within this range,  $f = 0.1$ . Then  $w$  nondimensionalized for  $L = 500$  and  $U = 25$  becomes:

$$w = 2\pi f = 2\pi \frac{f}{U/L} = 12.41.$$

A suitable value for  $A_0$  was found, after trials, to be  $A_0 = 0.113$ . With the model developed in this section the cases shown in Figure 27 and Figure 28, were simulated as follows:

1. Models A and Stabilized C Without Dead Zone OK

With Computer Program No. 6 the behavior of models A and stabilized C (rudder and hull) was studied. The results are shown in Figures 29, 30, 31, and 32.

It is evident that:

(a) After the transient has died out the two ships hold the same course.

(b) The error signals are almost the same for both ships.

(c) The rudder deflections of the stabilized ship are too large as compared to those of model A and are higher (maximum deflection 0.9 rad) than the assumed maximum deflection of 0.61 rad.

2. Models A and Stabilized C with Dead Zone OK

Computer Program No. 7 was used to simulate the two models with the Dead Zone introduced.

The results are shown in Figures 33, 34, 35, 36, and 37. In this case it is clear that:

(a) The path followed by the stabilized ship is close enough to that followed by the stable ship.



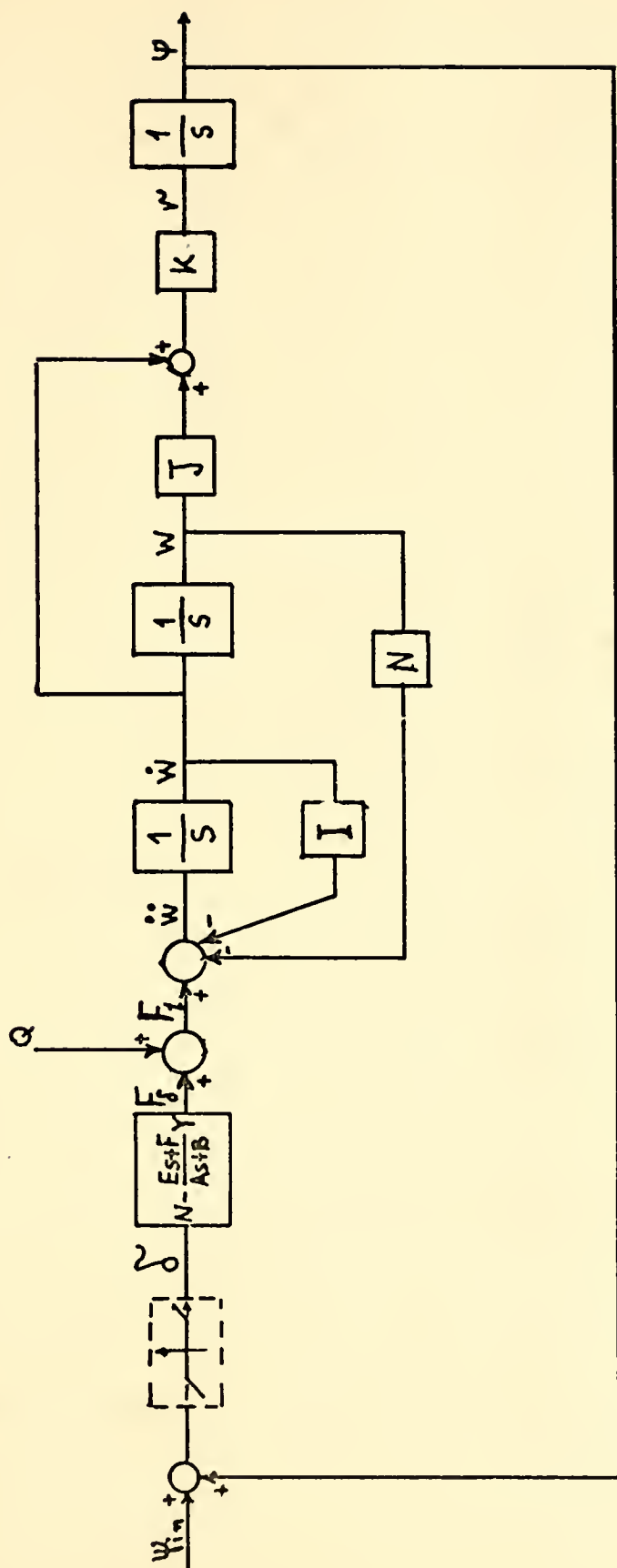


Figure 27. Block Diagram for Simulation of Models A and C in the Presence of Waves.



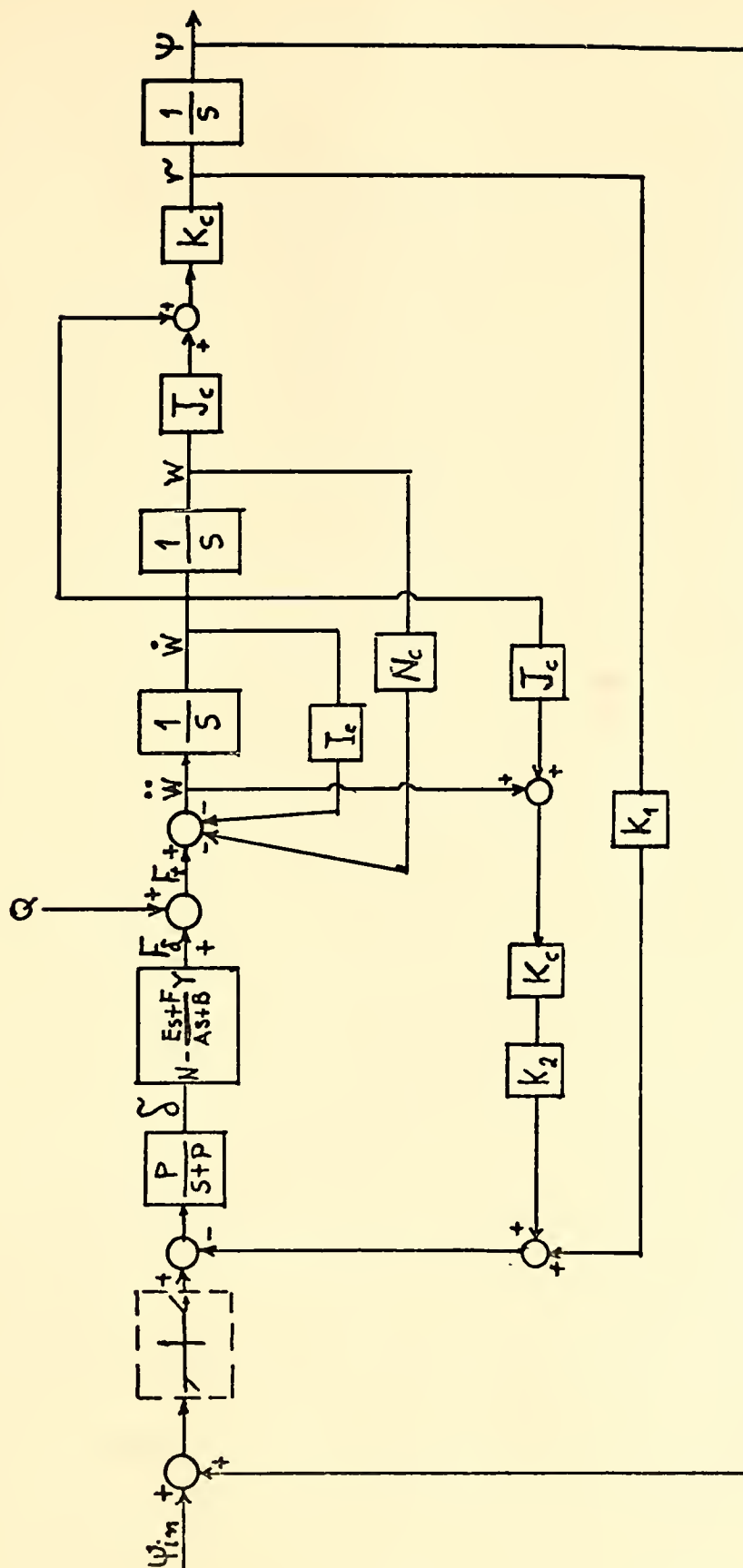


Figure 28. Block Diagram for Simulation of the Stabilized Model C in the Presence of Waves.



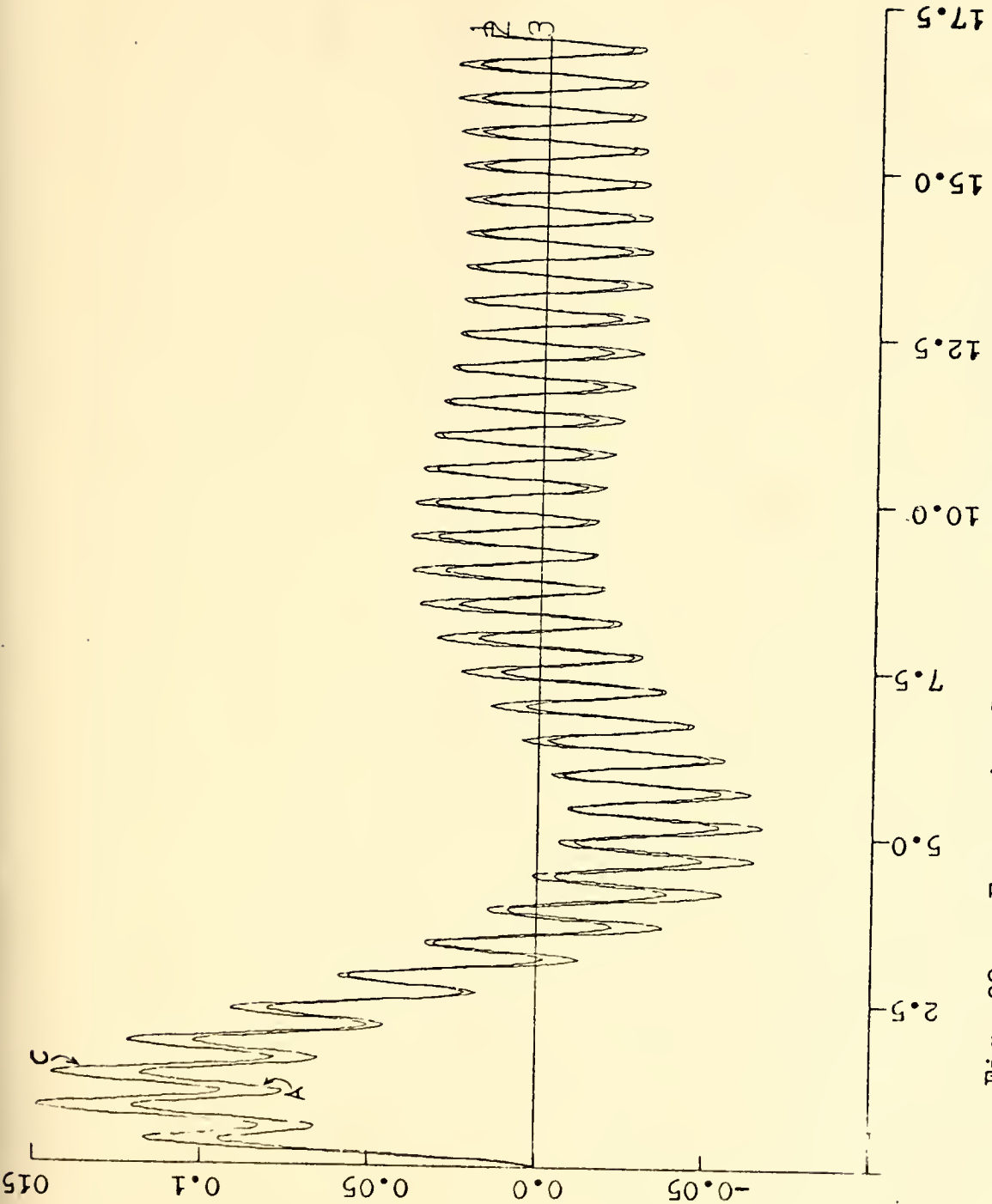


Fig. 29. Error signals vs time in the presence of sinusoidal waves.





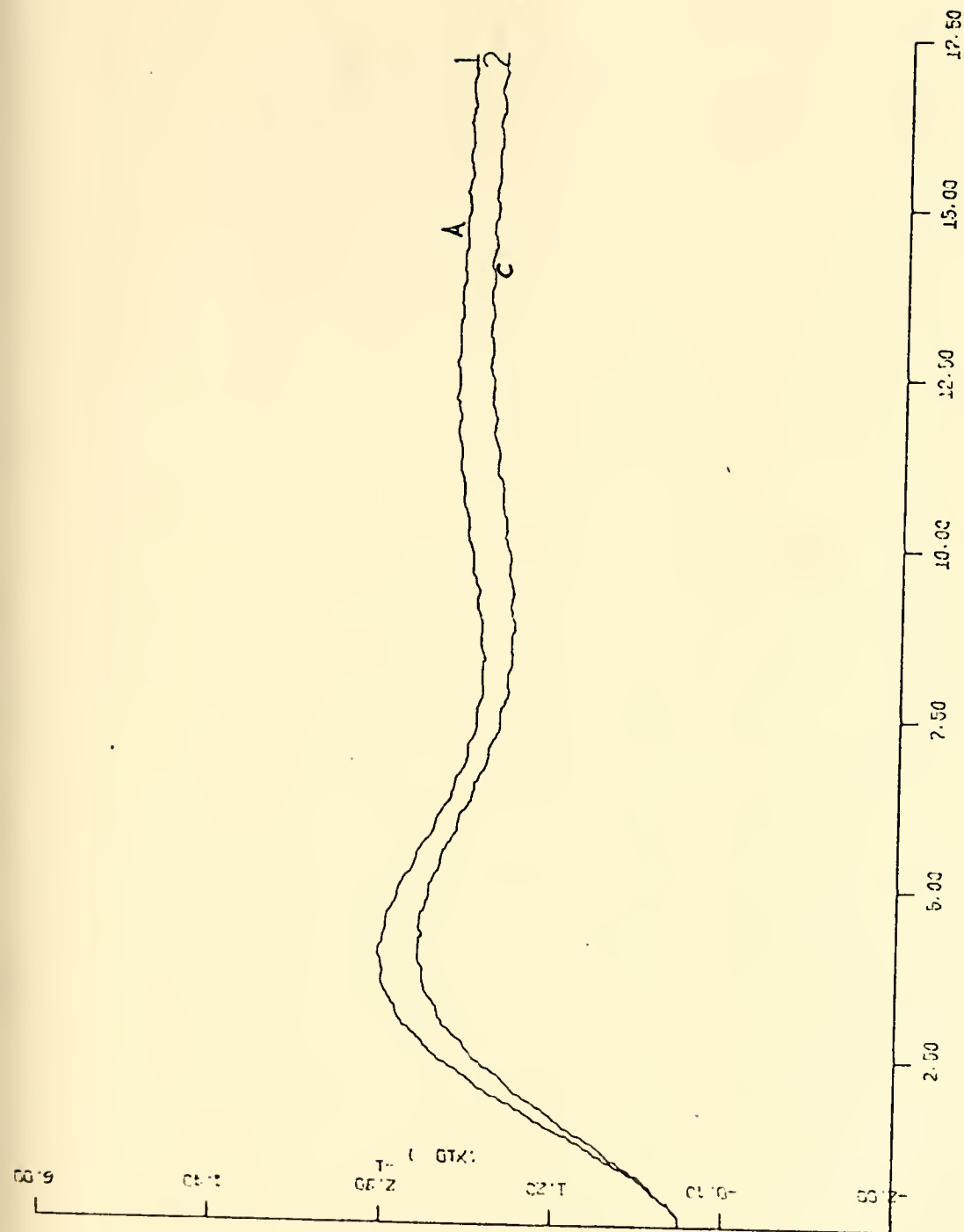


Fig. 30. Ship trajectories in the presence of sinusoidal waves.



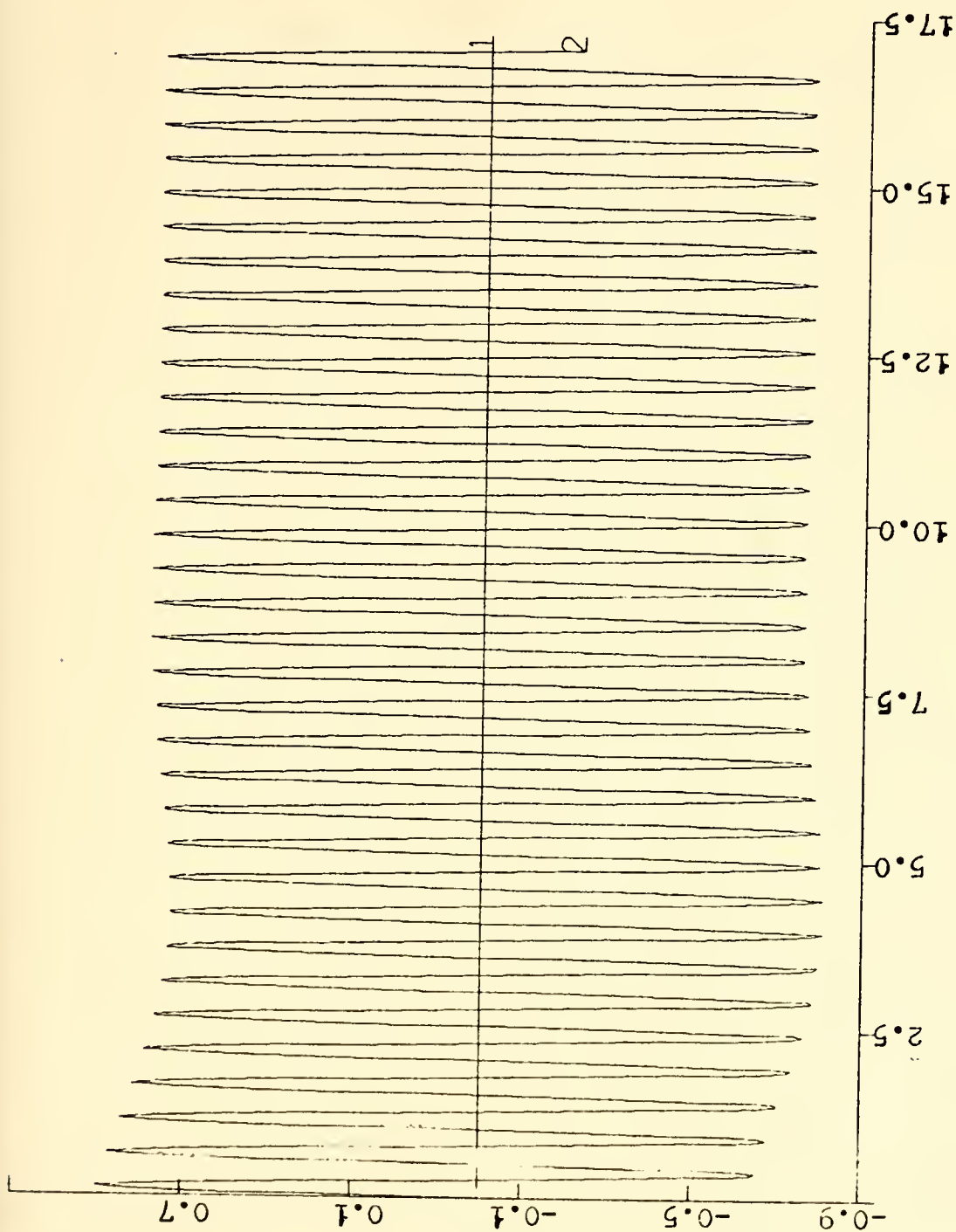


Fig. 31. Rudder deflections vs time of the stabilized model C in the presence of sinusoidal waves.



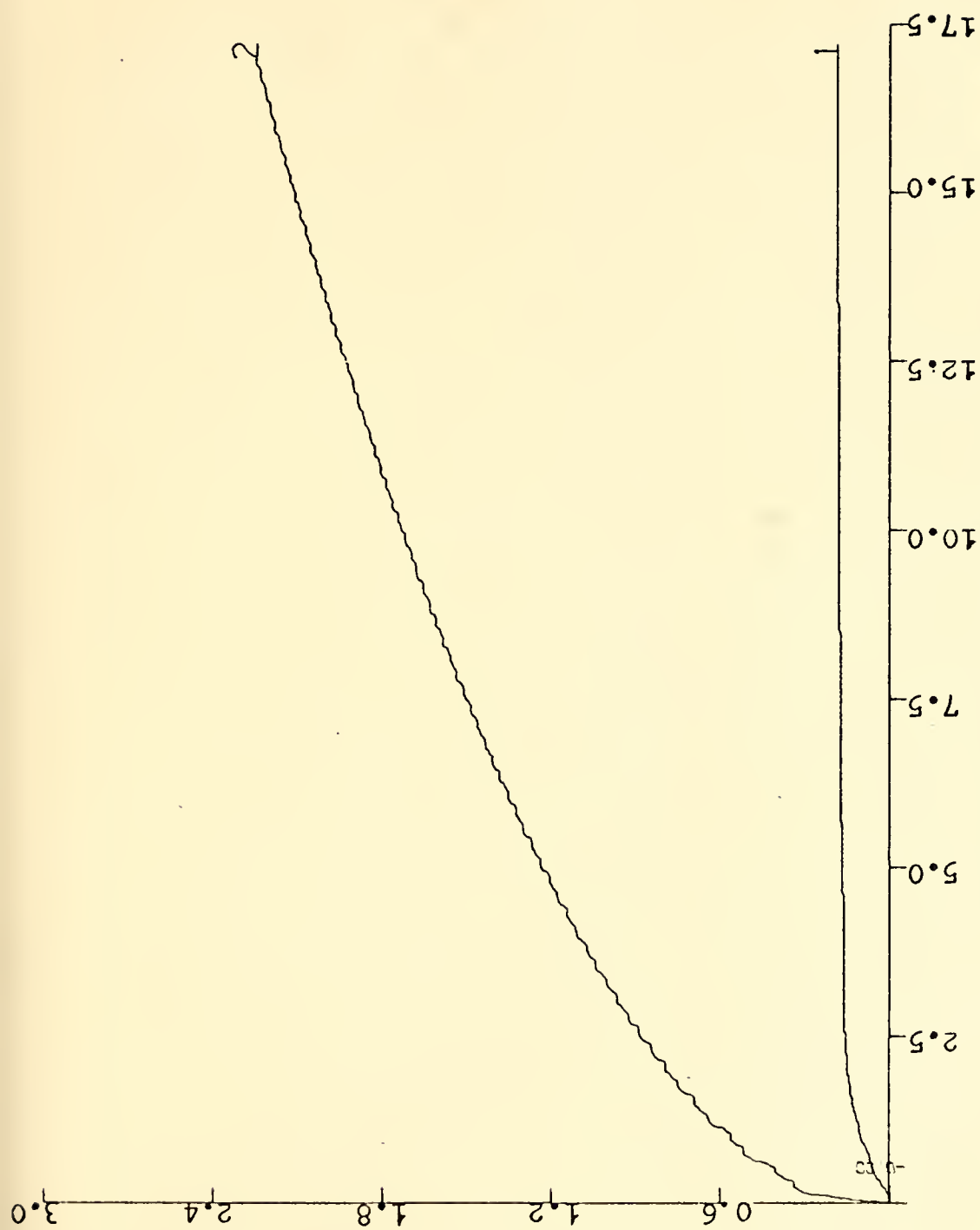


Fig. 32. Figure of merit vs time.



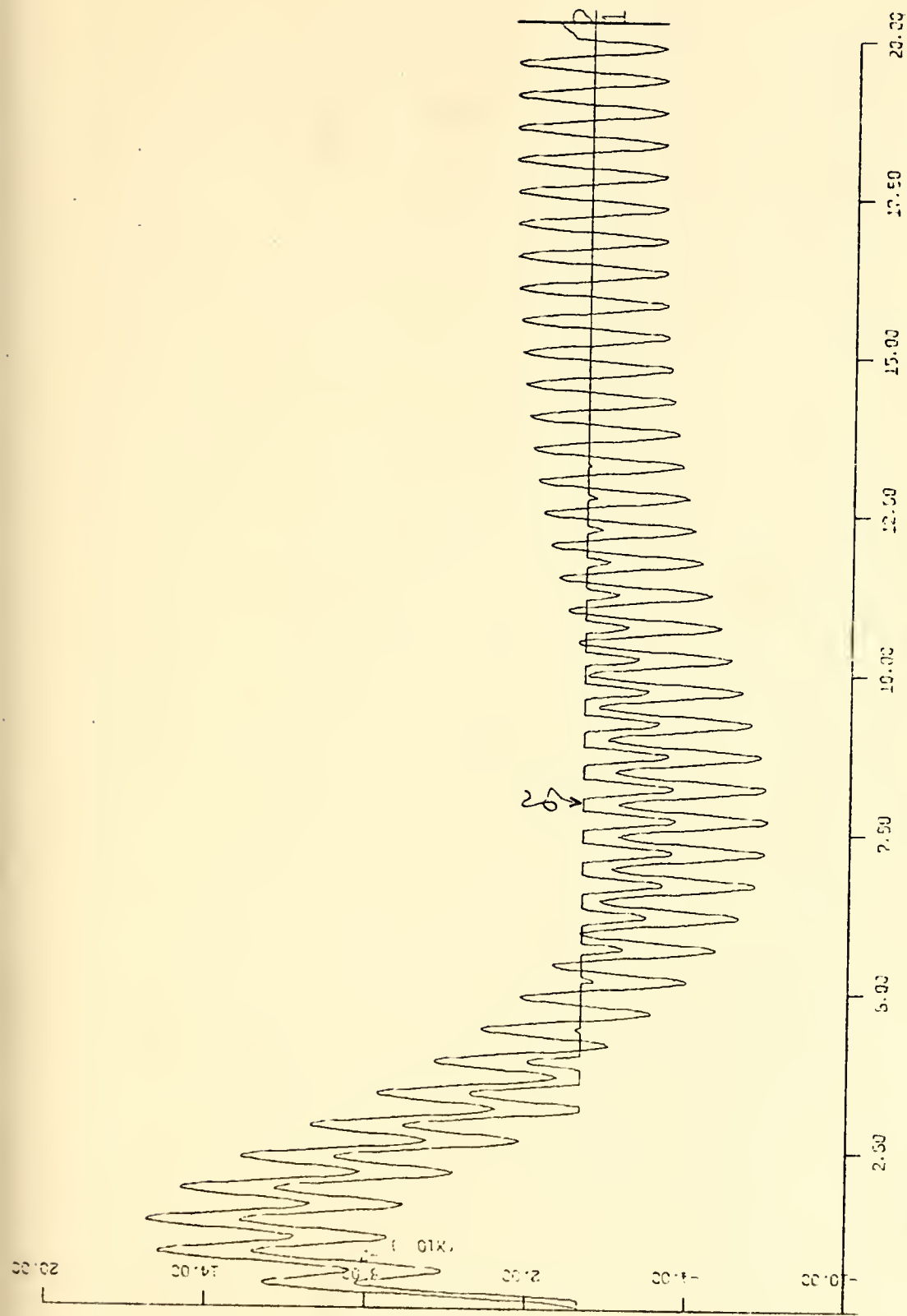


Fig. 33. Error signals vs time in the presence of sinusoidal waves (Model A with Dead Zone).





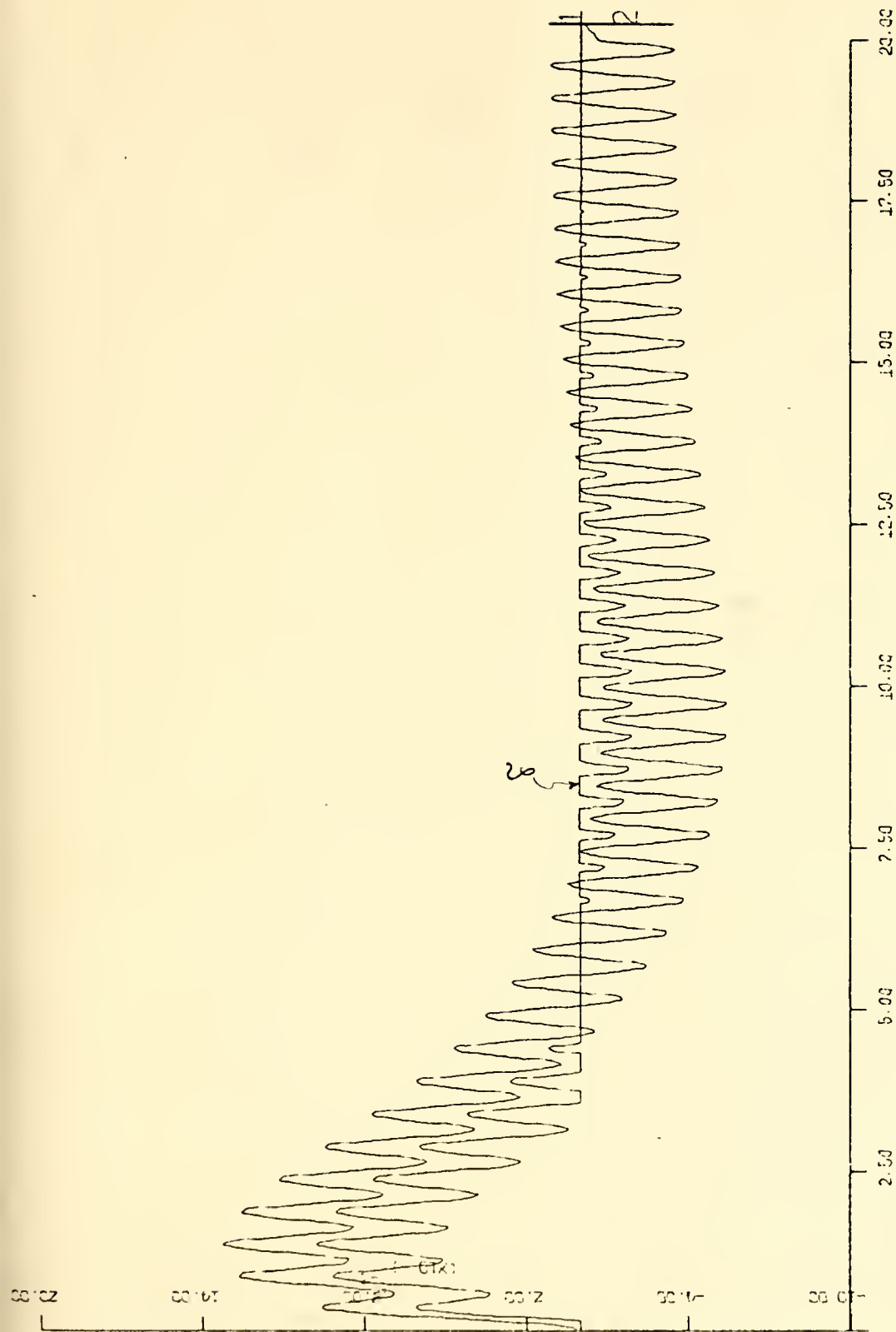


Fig. 34. Error signals vs time in the presence of sinusoidal waves (Stabilized model C with Dead Zone)



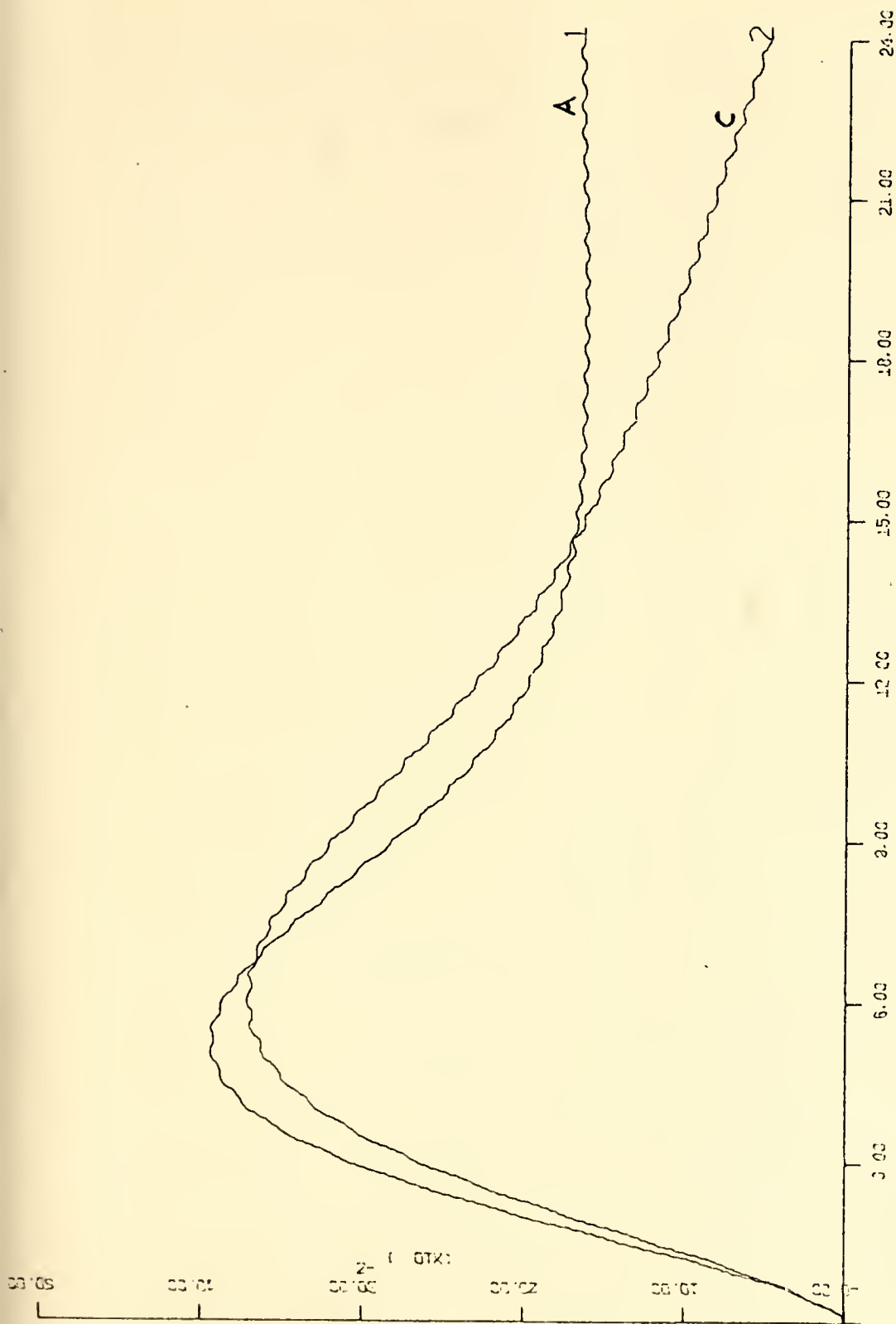


Fig. 35. Ship trajectories in the presence of sinusoidal waves  
(Models A and C stabilized with Dead Zone)







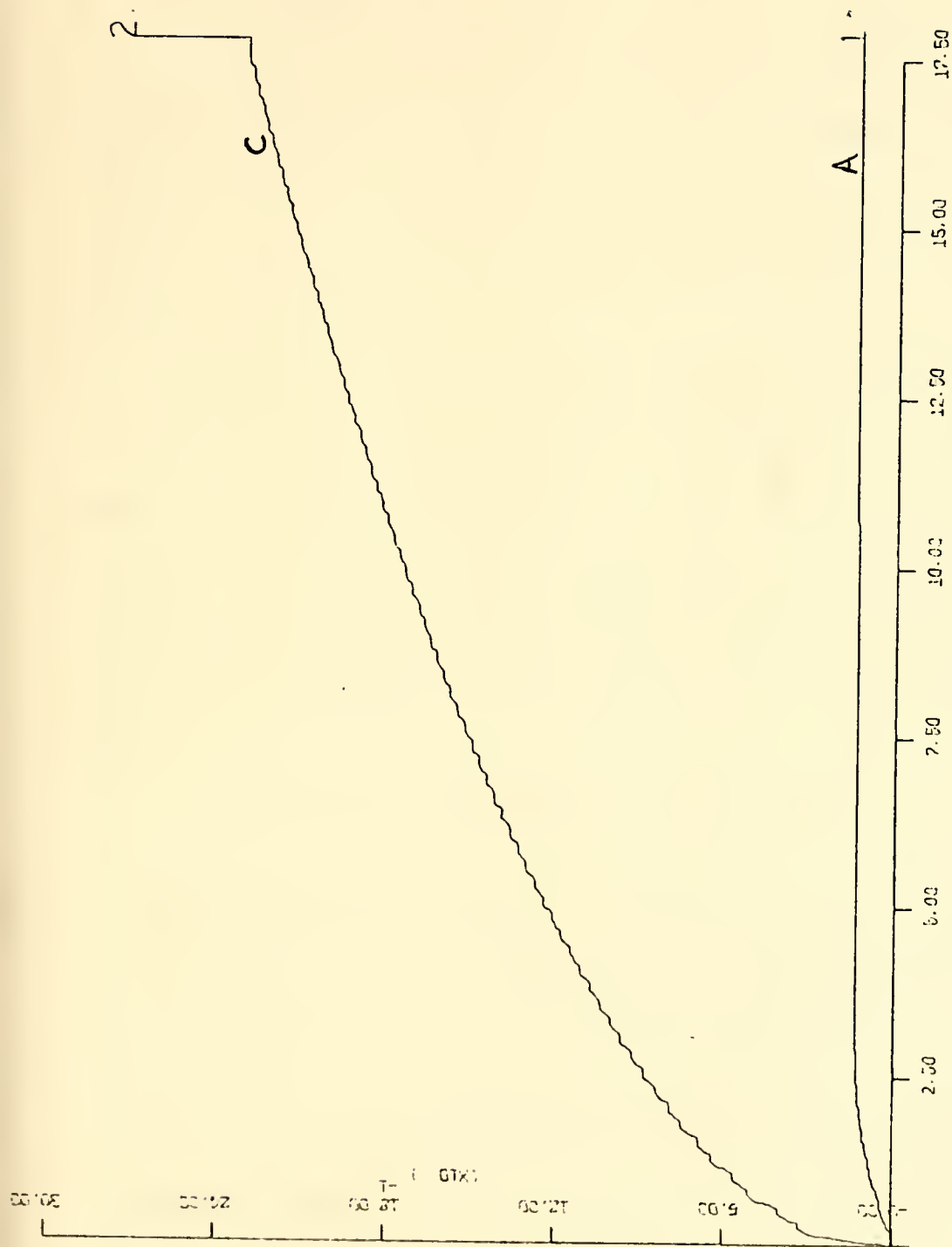


Fig. 37. Figure of merit for models A and C stabilized with Dead Zone.





(b) The error signals are almost the same for both ships.

(c) There was no significant improvement in the rudder's behavior of the stabilized ship.

From the results obtained in the last two simulations it can be seen that the stabilized system cannot work in the presence of waves, at least in the way the compensation was designed, due to the continuous motion of the rudder and the required high deflections (higher energy consumption and rudder design problems).

### C. SUPPRESSION OF THE RUDDER OSCILLATIONS

(NOT)

In this and the following sections, ways to suppress the rudder oscillations are studied.

As a first step to that direction the attenuation of the a.c components of the feedback signal with the introduction of a pole is considered. Using  $p/s+p$  the feedback gain becomes:

$$H(s) = \frac{p(K_1 + K_2 s)}{s+p} = (K_2 p) \frac{s + K_2/K_1}{s+p}.$$

Then the new characteristic equation of the system is

$$1 + P_c(s) H(s) = 1 + \frac{-1.3051(s+1.506)(-1.0232-0.21s)p}{(s+p)(s-0.256)(s+2.88)} = 0$$

or

$$1 + \frac{1.271p(s+0.3214)(s+3.114)}{(s-0.256)s(s+2.88)} = 0.$$

The root locus of this equation with parameter  $p$  is shown in Figure 38. Parameter  $p$  is selected so that the system remains stable, with behavior approaching that of the stable



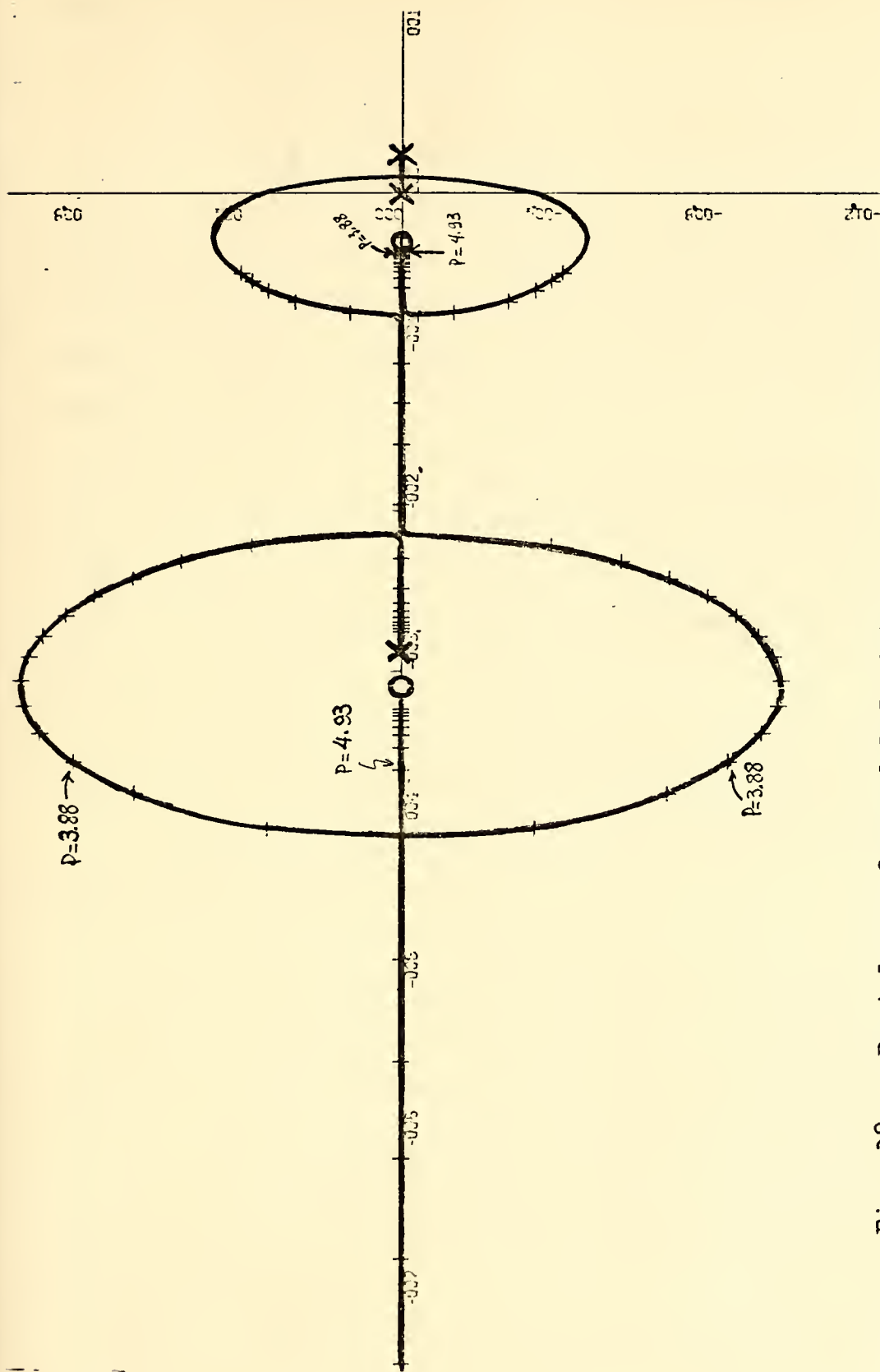


Fig. 38. Root locus for model C with a pole introduced in the stabilizing feedback loop.



ship and having reduced rudder motion. From Figure 38 the value  $p = 3.88$ , which gives roots:

$$\sigma_1 = - 0.36307$$

$$\sigma_2 = - 3.6 + j0.816$$

$$\sigma_3 = - 3.6 - j0.816$$

was selected and the system was simulated with Computer Program No. 6 modified to include the pole in the feedback loop. The results are shown in Figures 39, 40, 41, and 42 and can be stated as follows:

(1) The path of the stabilized ship approaches closely the path of the stable ship and is almost identical to that of the stabilized ship with velocity and acceleration feedback. This indicates that the behavior of the ship is dominated by the root  $\sigma_1 = - 0.36307$ .

(2) The error signal is identical to that of the stabilized ship with velocity and acceleration feedback.

(3) The amplitude of the rudder oscillation is reduced considerably (almost to 50%).

#### D. INTRODUCTION OF FILTERS IN THE STABILIZING LOOP

Another interesting result comes out from the root locus, Figure 38, and the response curves of the stabilized system. Making  $p = K_1/K_2 = 4.93$ , (and so the feedback gain becomes a pure number) the roots of the characteristic equation do not change appreciably and that assures the same behavior with only velocity feedback.

✓ Using  $p = 4.93$  the simulation was repeated, and the results are shown in Figures 43, 44, 45, and 46.



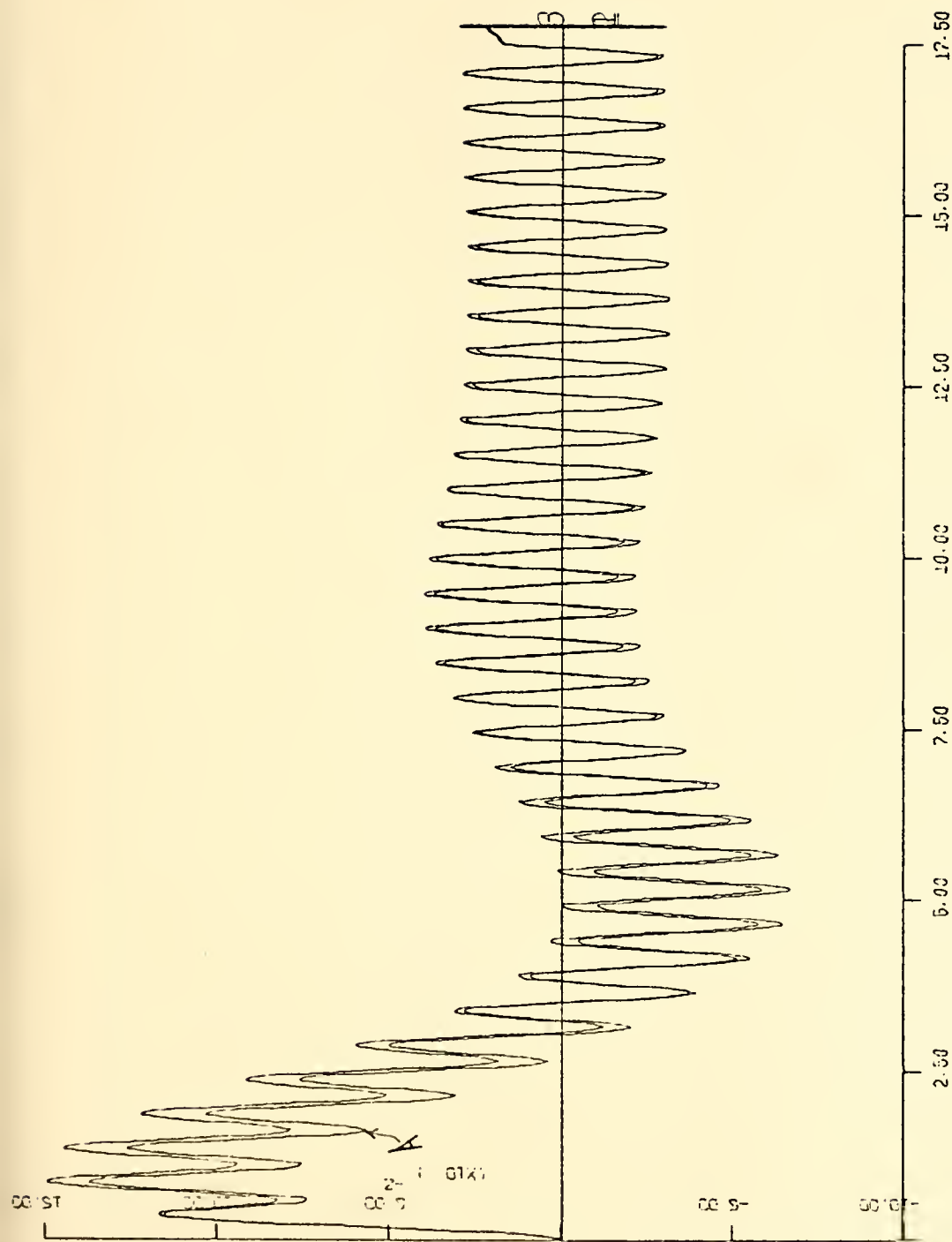


Fig. 39. Error signals vs time in the presence of sinusoidal waves (Models A and C stabilized with a pole in the stabilizing loop)





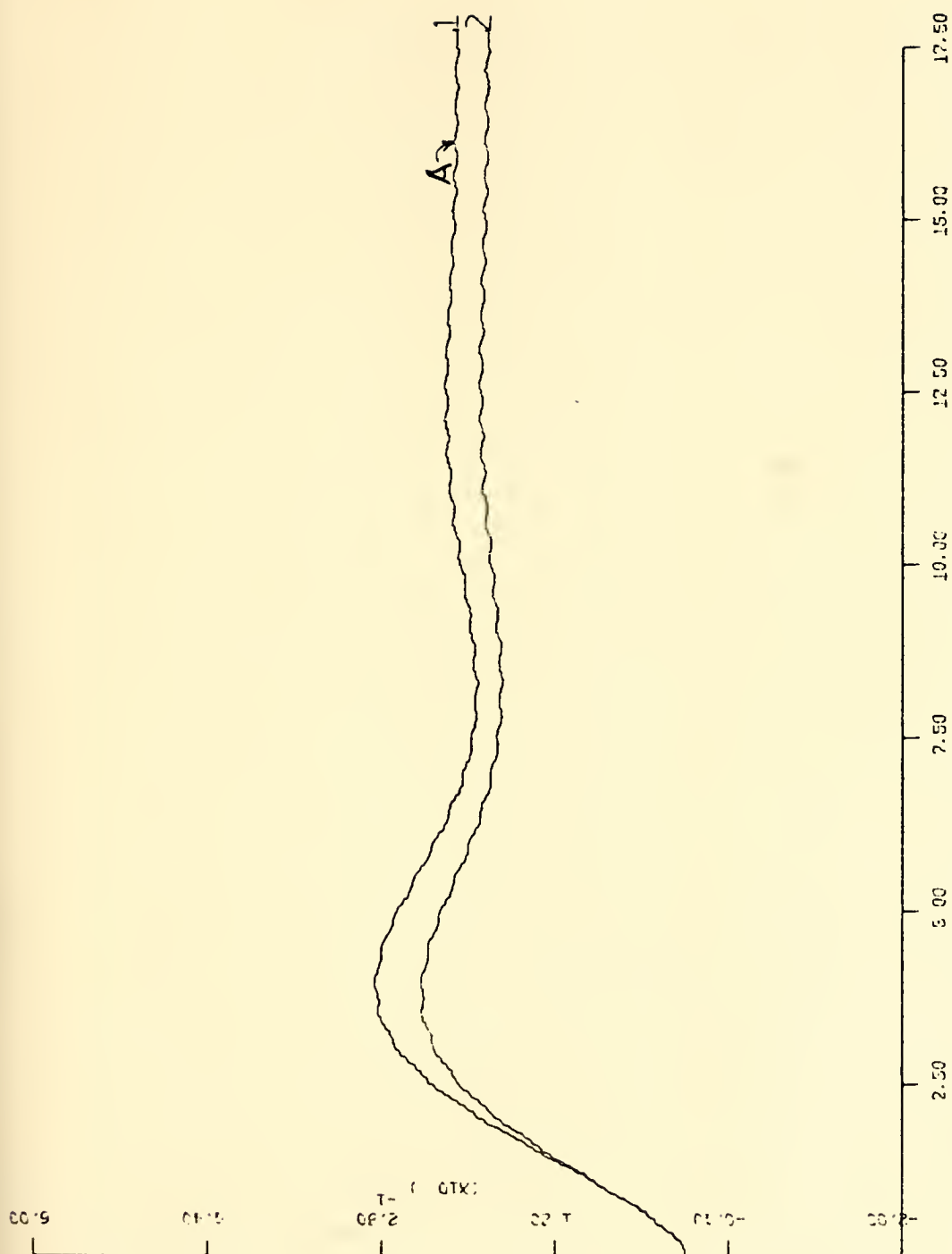


Fig. 40. Ship trajectories in the presence of sinusoidal waves  
(Models A and C stabilized with a pole in the stabilizing loop)



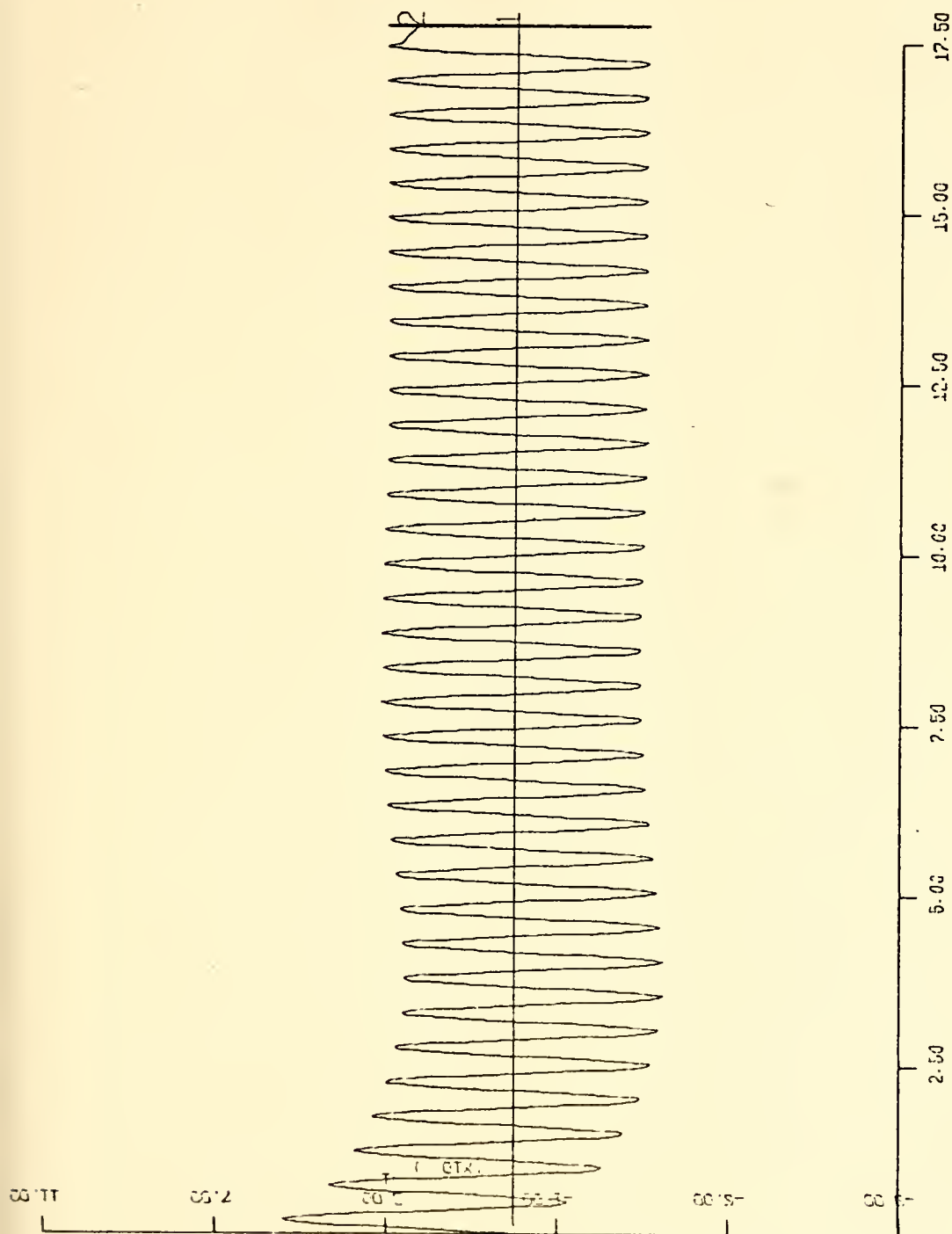


Fig. 41. Rudder deflections vs time of the stabilized model C in the presence of sinusoidal waves, with a pole in the stabilizing loop.



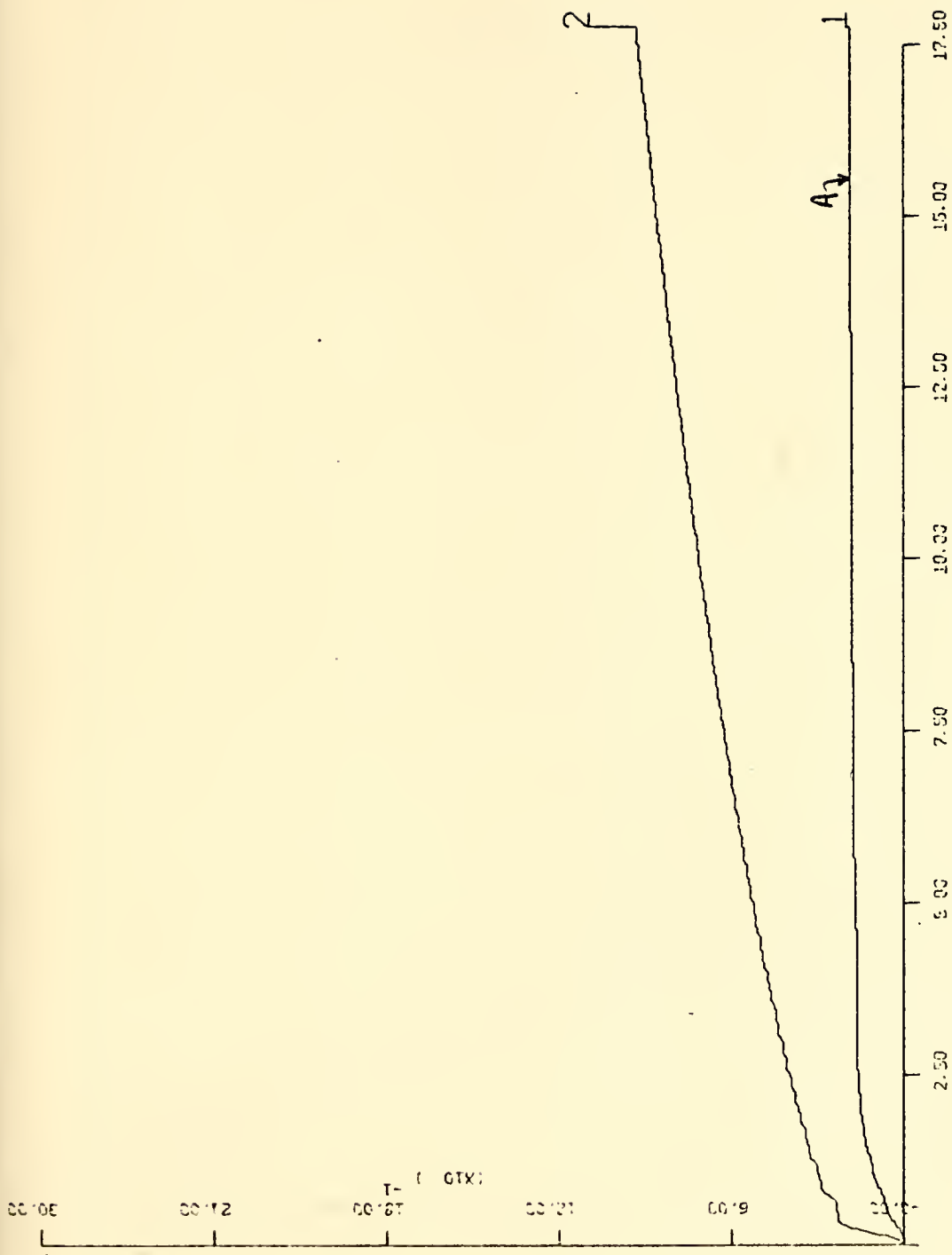


Fig. 42. Figure of merit for models A and C stabilized (with a pole in the stabilizing loop) in the presence of sinusoidal waves.





Fig. 43. Error signals vs time in the presence of sinusoidal waves (Model C stabilized with only velocity feedback)





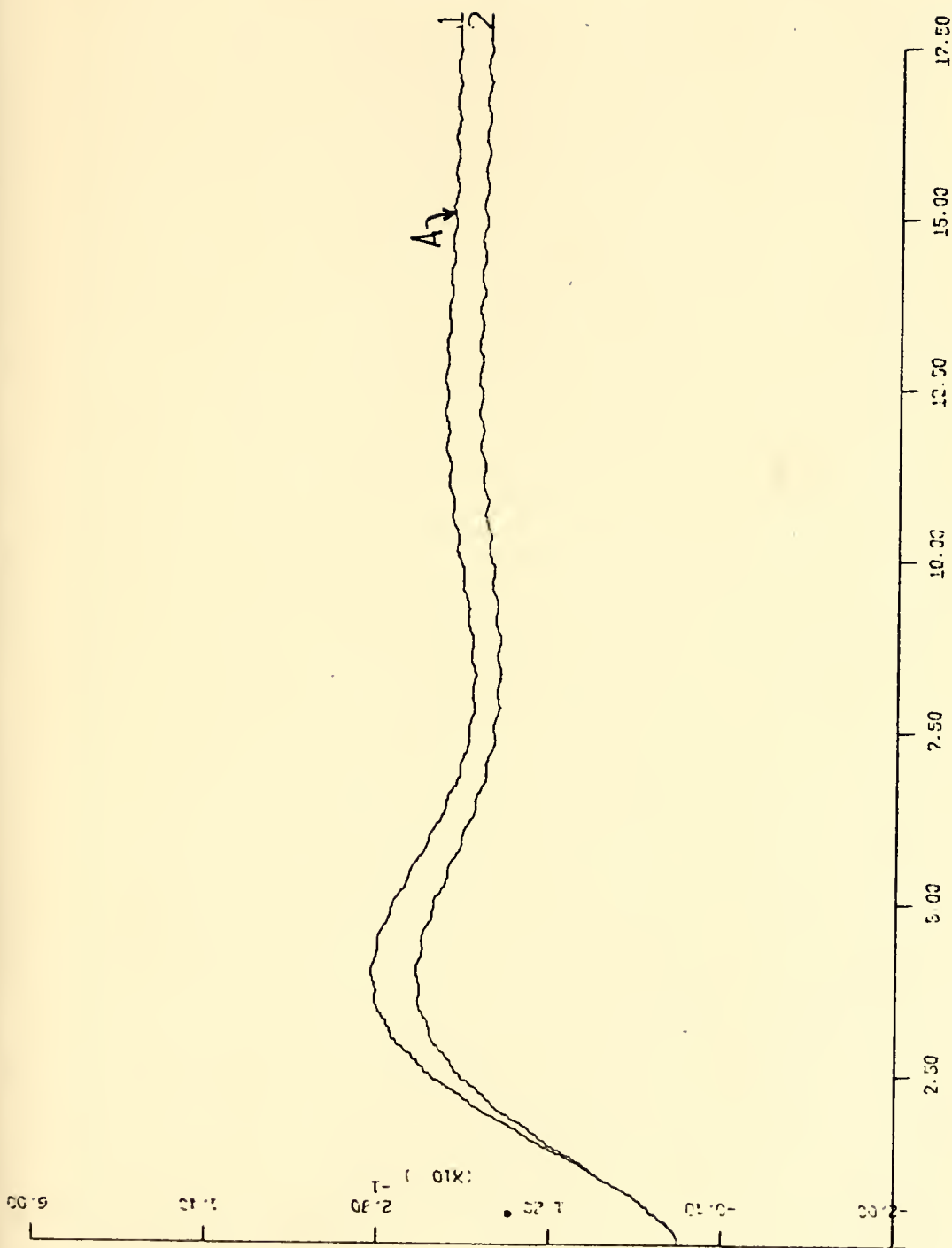


Fig. 44. Ship trajectories in the presence of sinusoidal waves (Models A and C stabilized with only velocity feedback).



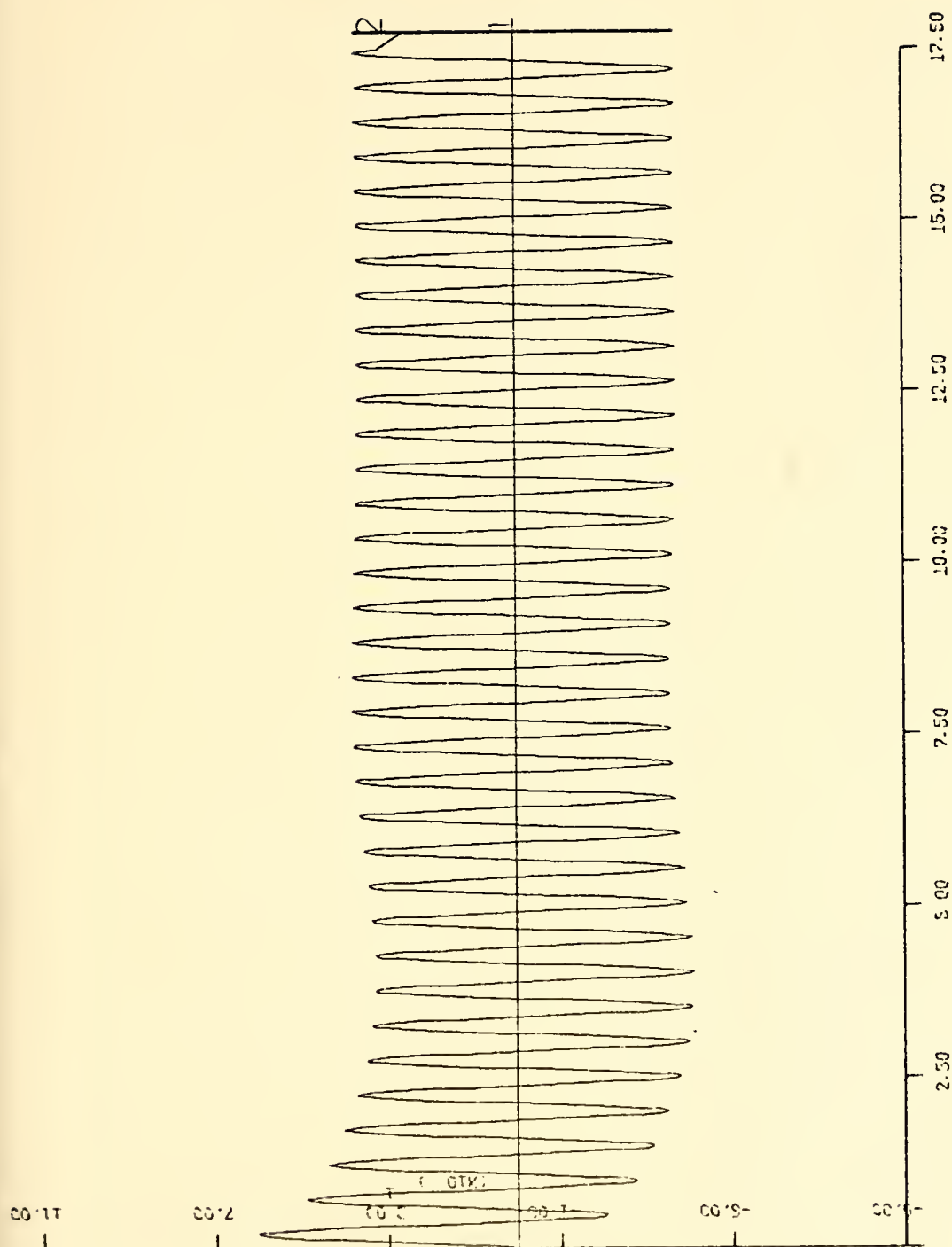


Fig. 45. Rudder deflections vs time in the presence of sinusoidal waves (Model C stabilized with only velocity feedback).



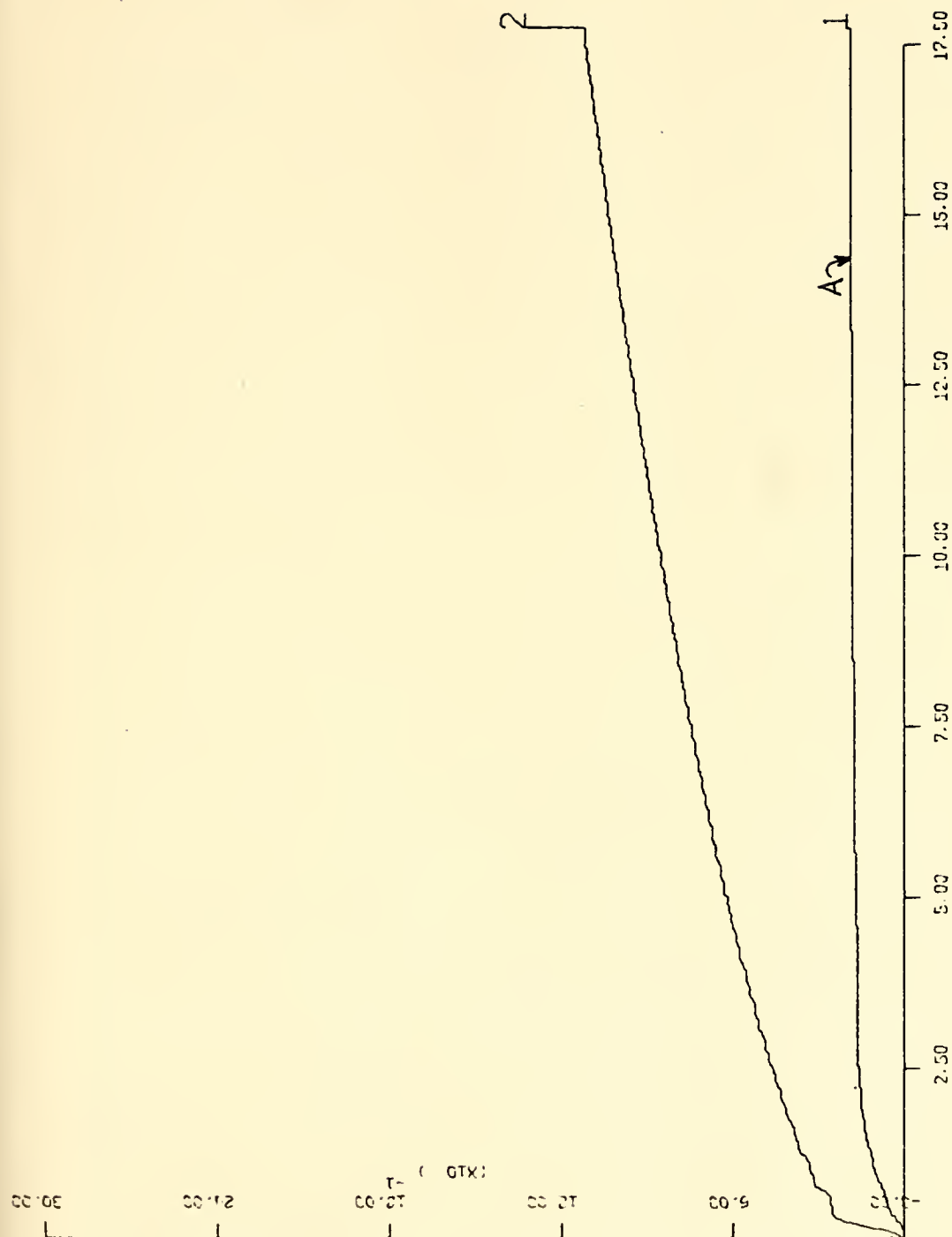


Fig. 46. Figure of merit (Models A and C stabilized with only velocity feedback).



The next step is to increase the attenuation of the a.c components of the feedback signal with the introduction of filters. The philosophy of this procedure can be stated as: The only component of  $r(t)$  needed for the stabilization of the system is the d.c. Introducing two branches, Figure 47, in the feedback loop in such a way so that the one passes only the a.c components and the other both a.c and d.c and then subtracting the two outcoming signals the a.c component is reduced. The ideal situation is to have the same gain and the same phase shift over the entire range of encountered frequencies in sea waves. Having the same gain in both paths is obtainable, but having the same phase shift over a certain range of frequencies is difficult and only approximations can be easily obtained.

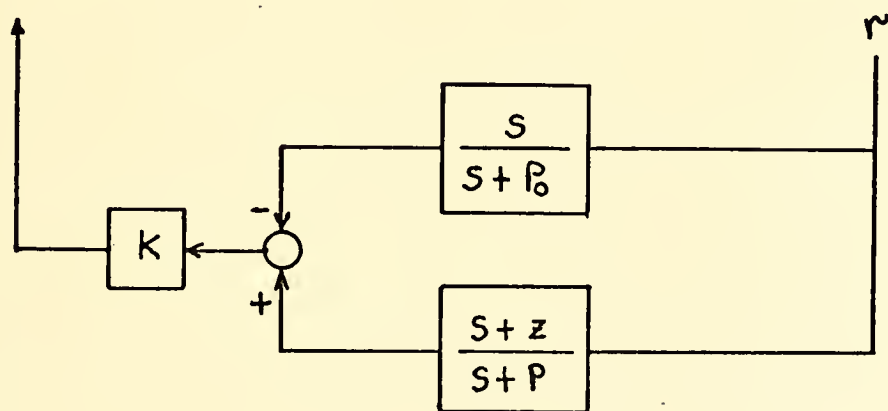


Figure 47. Block Diagram of the Stabilizing Loop.

The transfer functions for the two paths are  $s/s+p_0$  and  $s+z/s+p$ . Adjusting  $p_0$ ,  $p$  and  $z$  we tried to have the two filters matched in the vicinity of the chosen frequency in this thesis. The magnitude and phase curves for both filters and





for the selected parameters ( $p = 2.32$ ,  $z = 0.76$ ,  $p_o = 1.6$ ) are shown in Figure 48.

Parameter K, Figure 47, was introduced to the system in order to provide the necessary gain for the stabilization of the unstable ship.

The total feedback gain (Figure 47) is:

$$H(s) = (-K) \left( \frac{s + z}{s + p} - \frac{s}{s + p_o} \right) = (-K) \frac{(z + p_o - p)s + zp_o}{(s + p)(s + p_o)}$$

and the characteristic equation of the system becomes:

$$1 + \frac{1.3051K(s + 1.506)(0.03s + 1.2)}{(s + 2.88)(s + 1.6)(s + 2.32)(s - 0.256)} = 0$$

The root locus for this equation with varying parameter  $K' = 1.3051 K$  is shown in Figure 49. Selecting  $K' = 2.6$ , and so  $K = -1.992$ , the system was simulated using Computer Program No. 6, modified to include the new stabilizing loop. Results are shown in Figures 50, 51, and 52 and can be stated as:

(1) The stabilized ship behaves in a different way than the stable dueing the transient phase. That is the stabilized ship appears more oscillatory than the stable ship.

(2) In steady state the rudder behavior has been improved significantly. The maximum deflection has been reduced to 5% of that when the velocity and acceleration feedback were used for stabilization.

The simulation was repeated for a different value of the sinusoidal wave frequency in the design range. The results are identical to those presented for  $w = 12.41$  and are shown in Figures 53, 54, and 55.



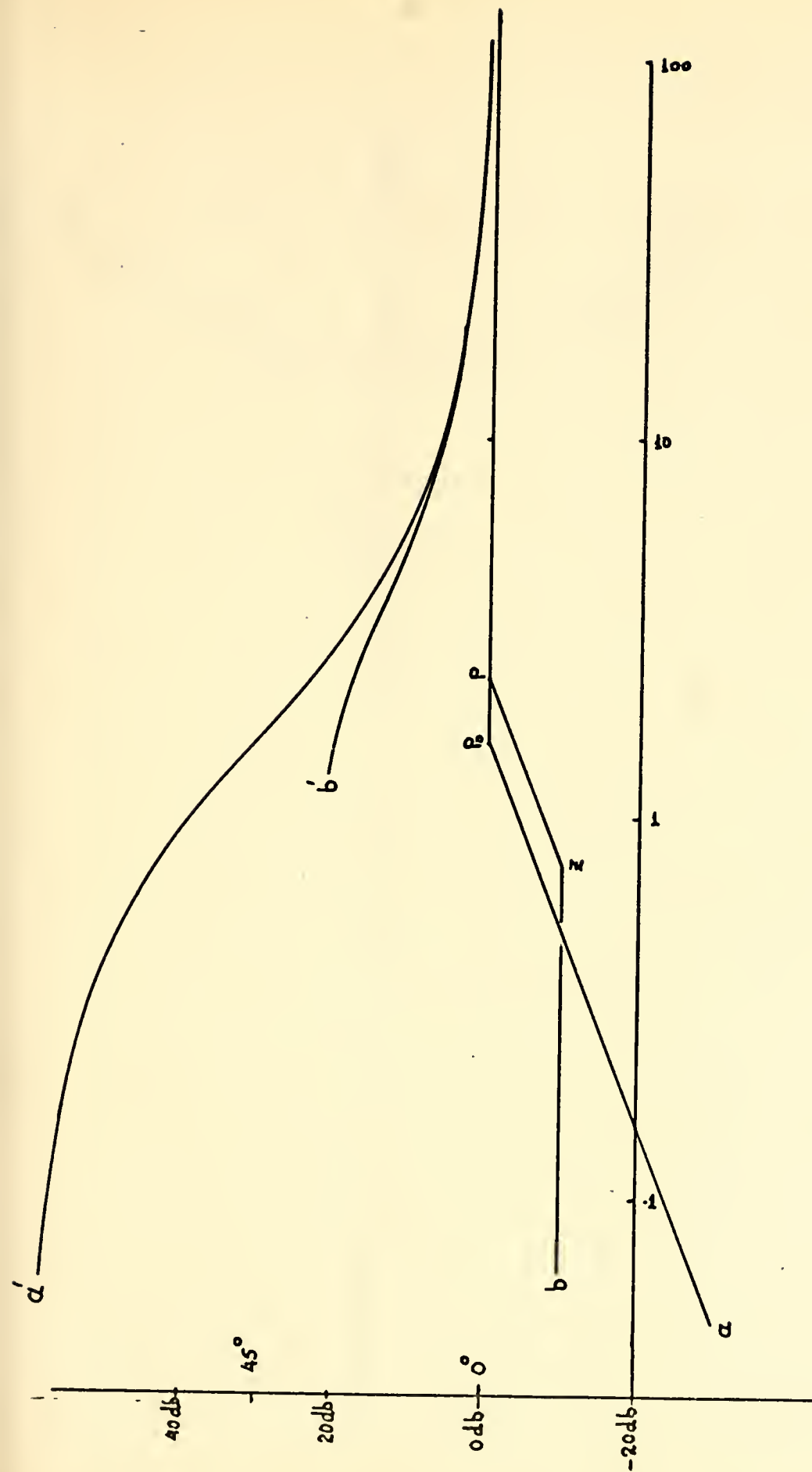


Figure 48. Gain and Phase vs. Frequency Curves for the Filters of the Stabilizing Loop.



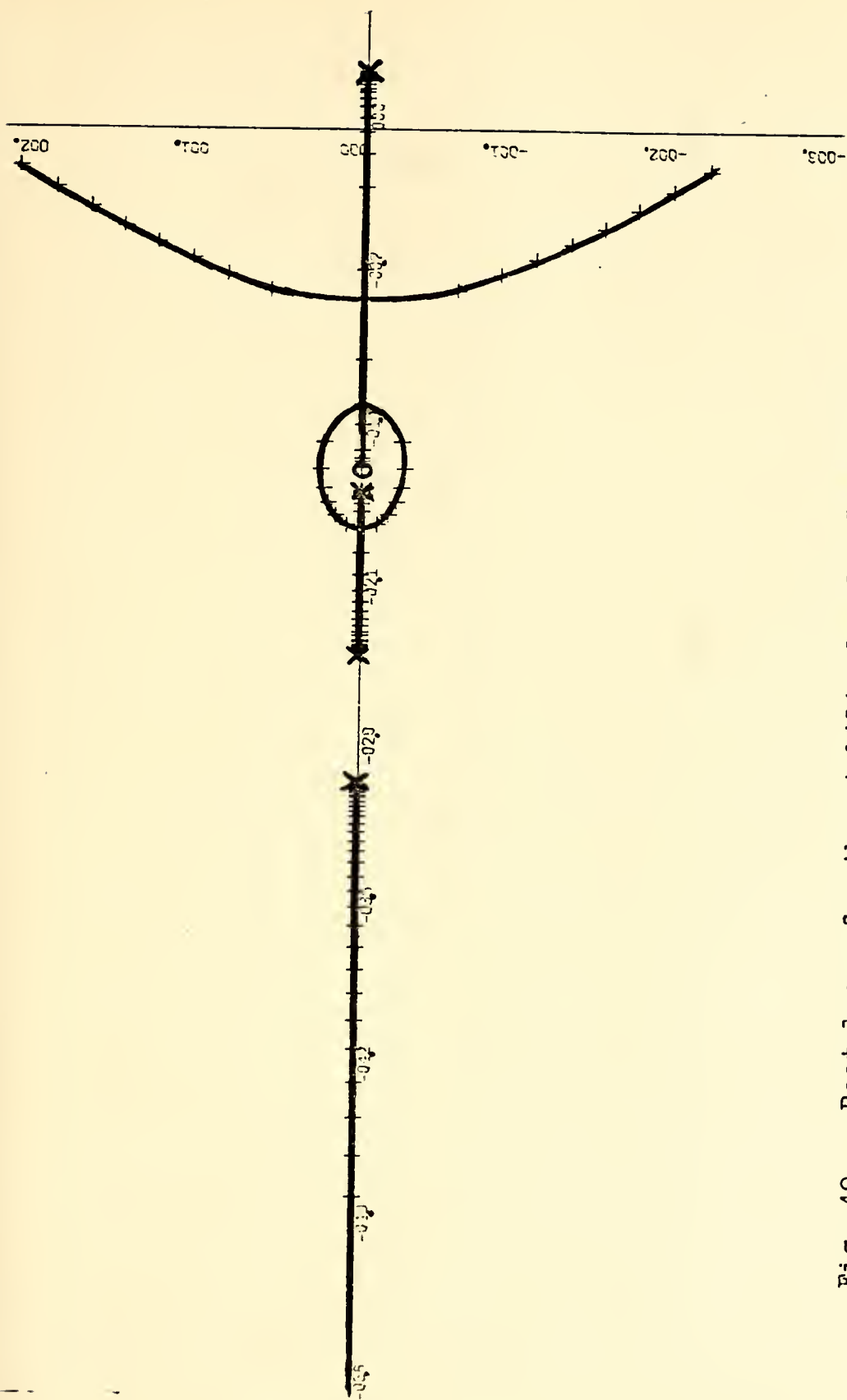


Fig. 49. Root locus for the stabilized model C with the filters in the stabilizing loop.



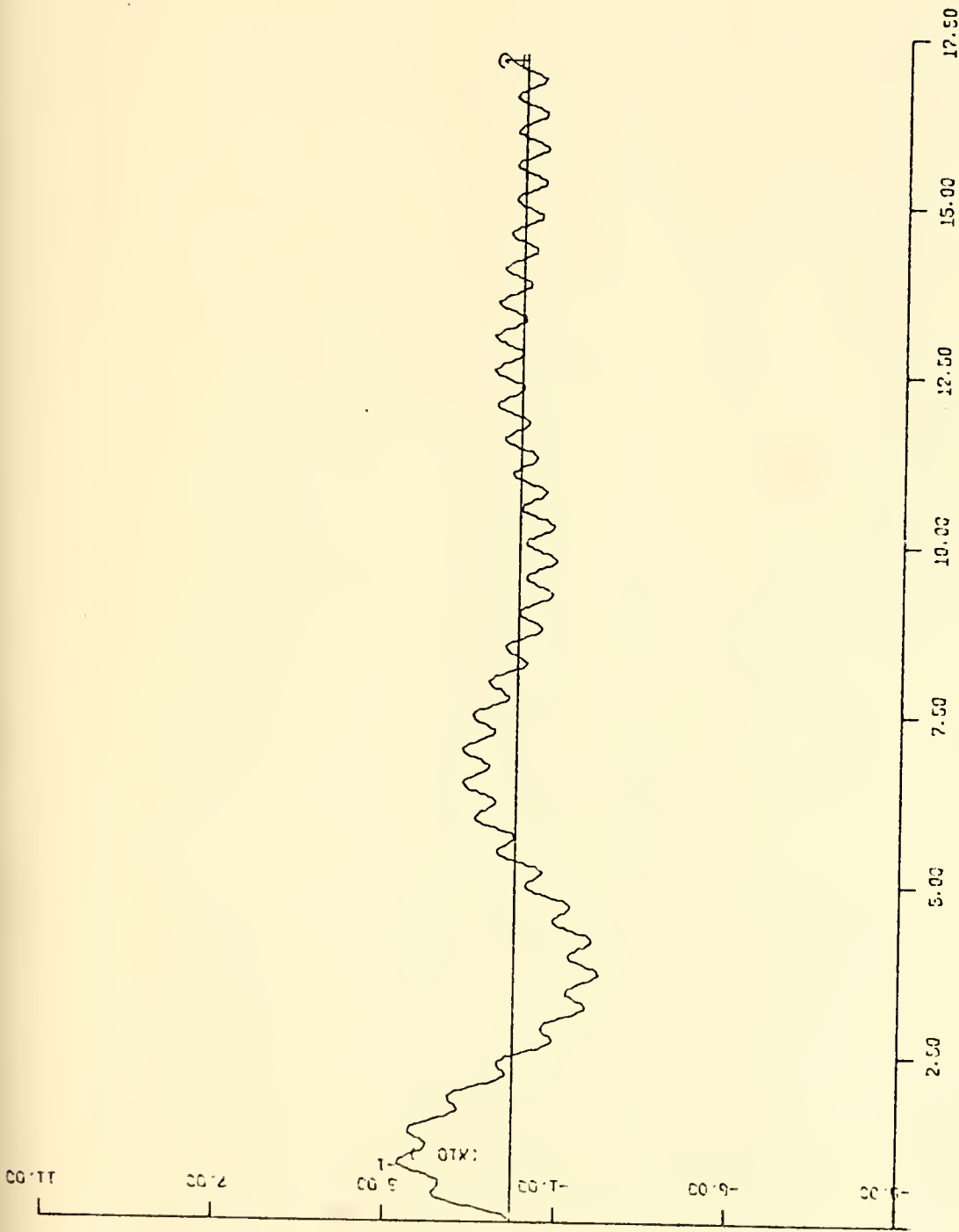


Fig. 50. Rudder deflections vs time in the presence of sinusoidal waves (Model C stabilized with the filters in the stabilizing loop) with  $w = 12.41$ .





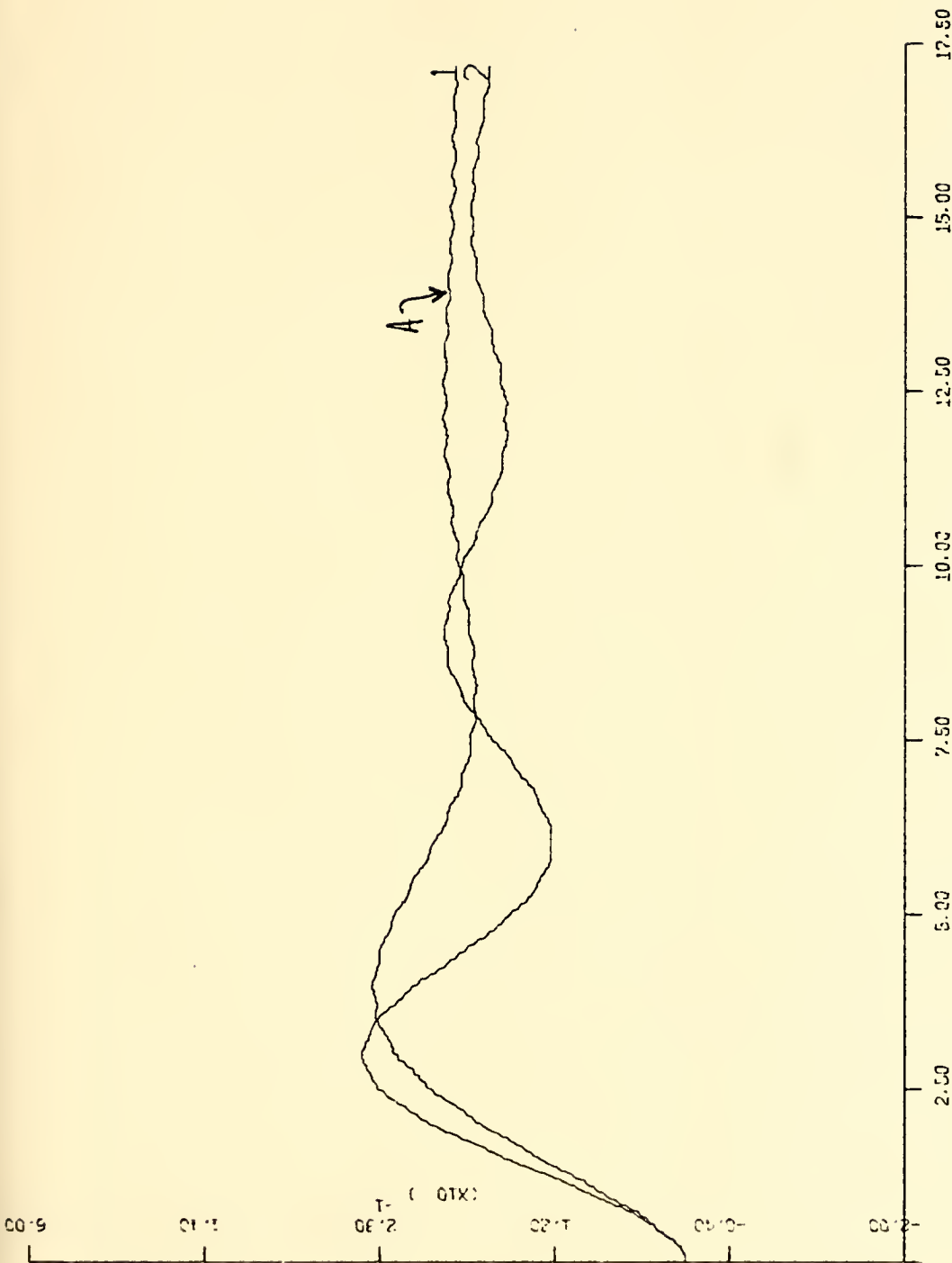


Fig. 51. Ship trajectories in the presence of sinusoidal waves  
 (Models A and C stabilized with the filters in the  
 stabilizing loop) with  $w = 12.41$ .



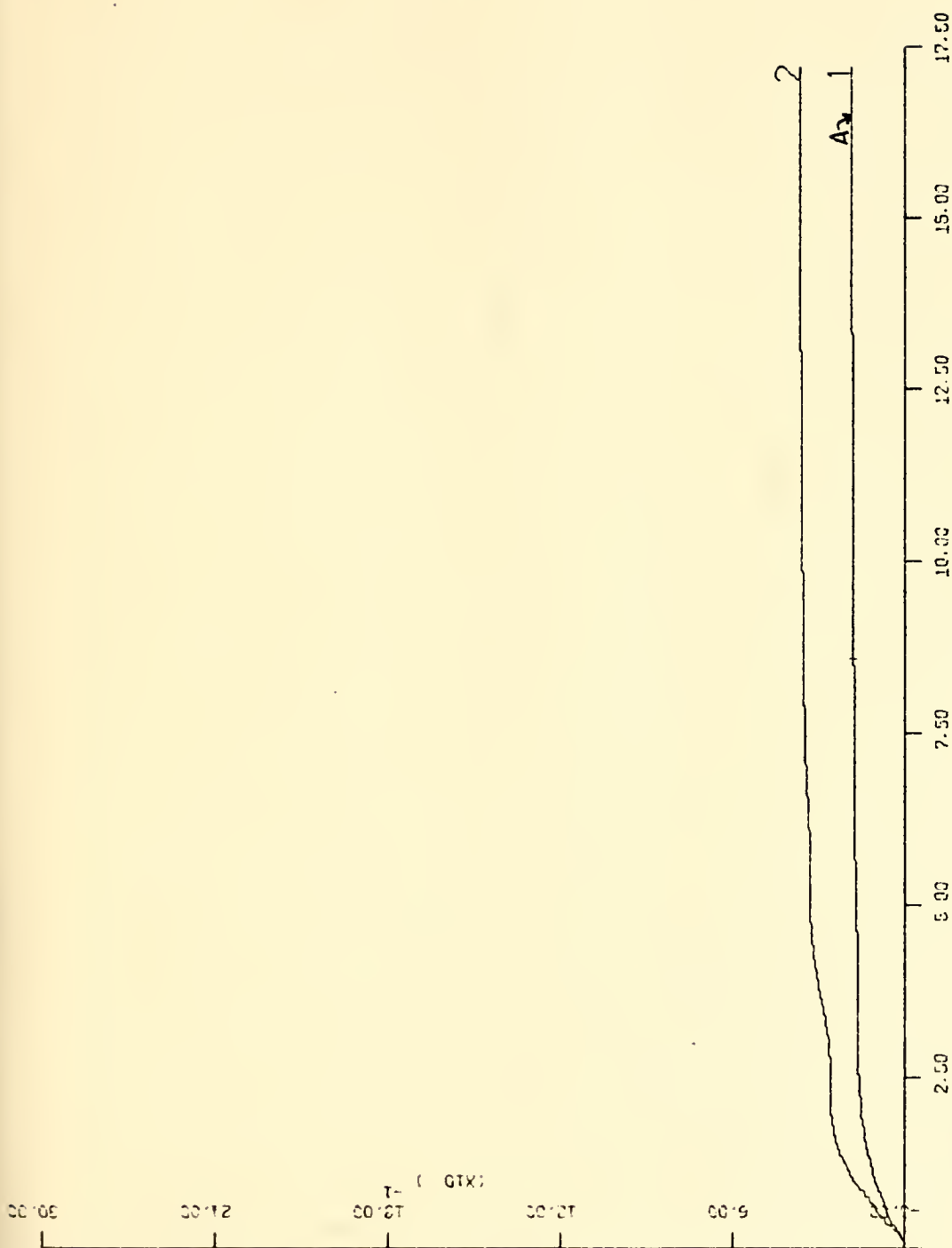


Fig. 52. Figure of merit. (Models A and C stabilized with the filters in the stabilizing loop in the presence of sinusoidal waves with  $w = 12.41$ )



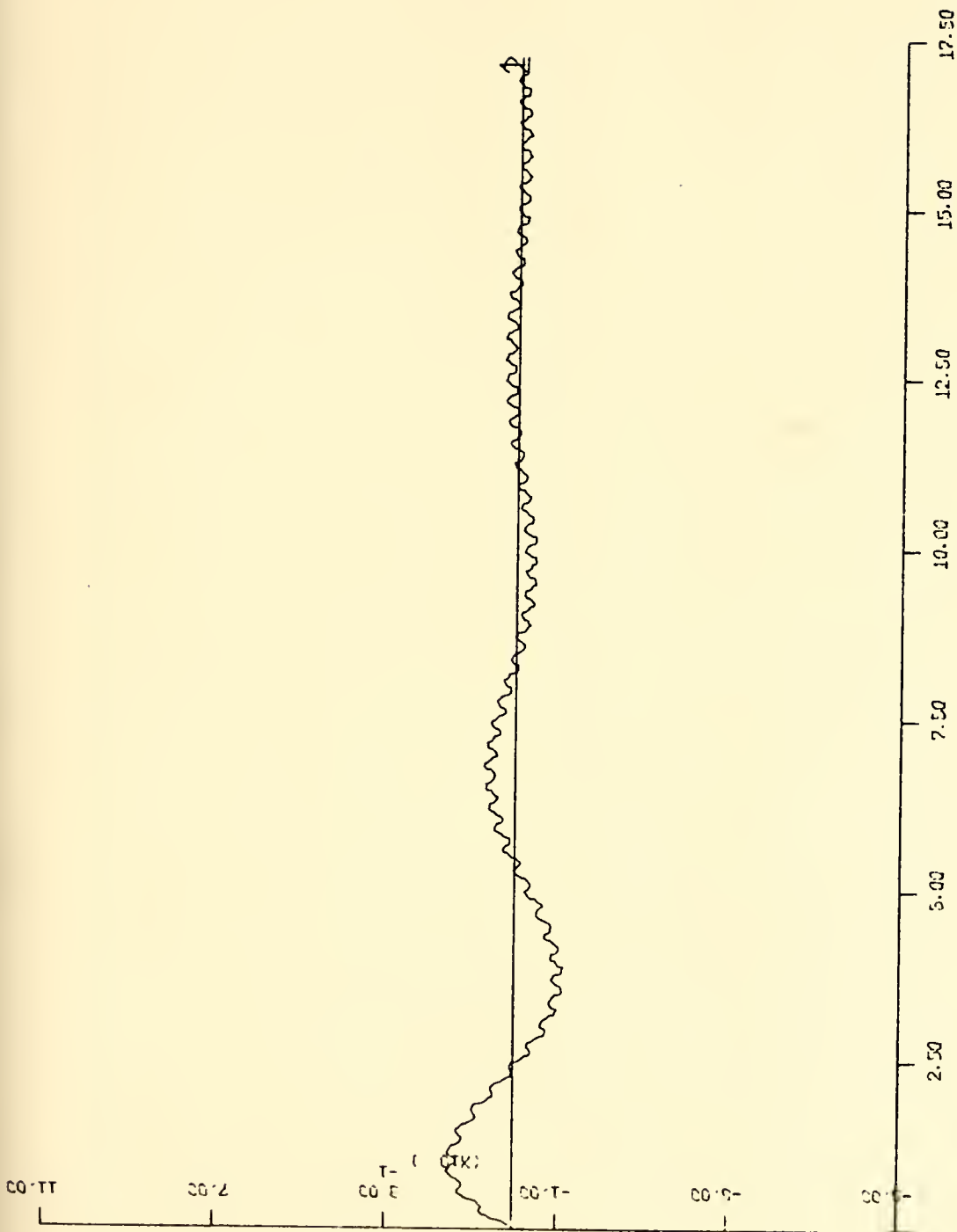


Fig. 53. Rudder deflections vs time in the presence of sinusoidal waves (Model C stabilized with the filters in the stabilizing loop) with  $w = 20$ .



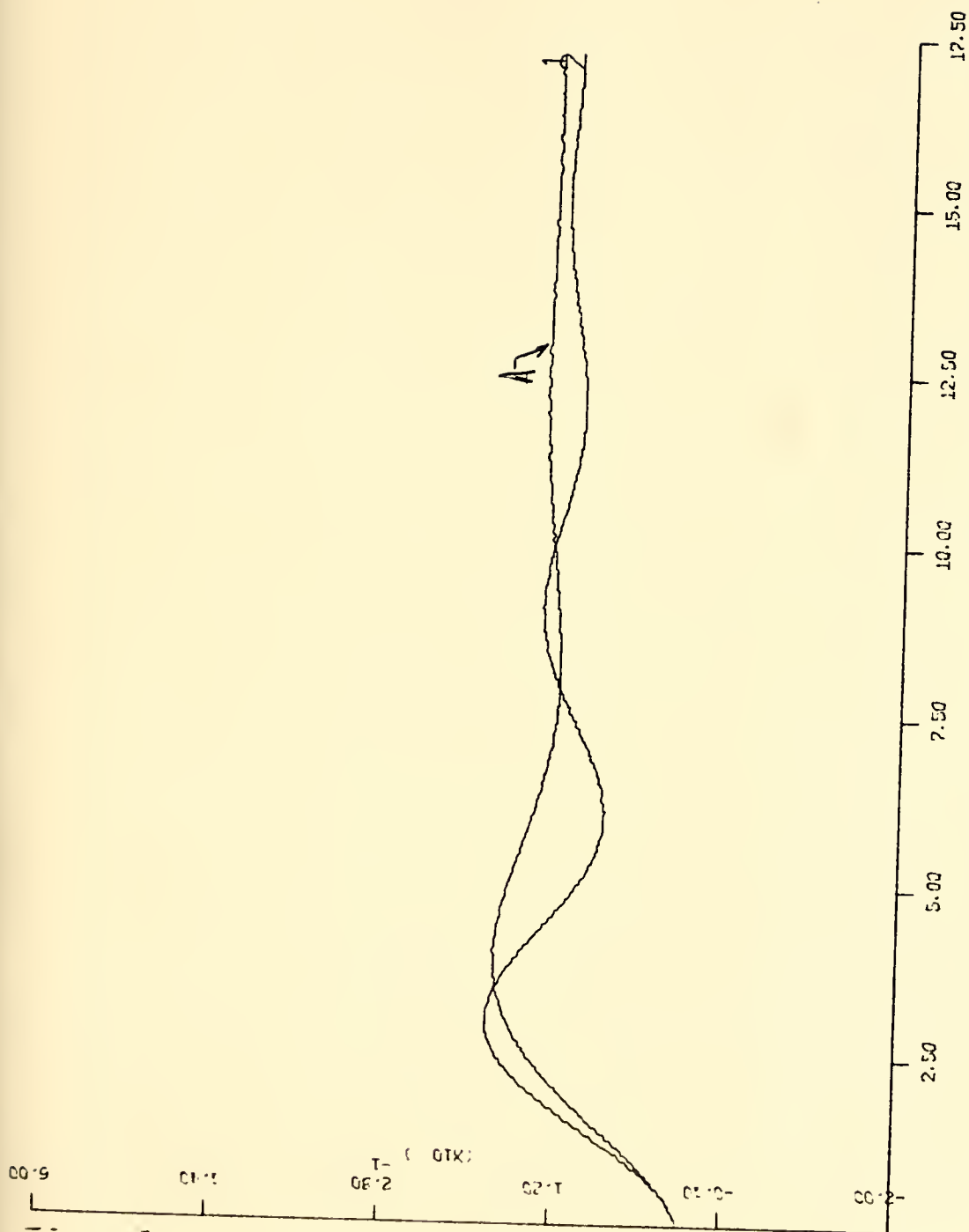


Fig. 54. Ship trajectories in the presence of sinusoidal waves (Models A and C stabilized with filters in the stabilizing loop) with  $w = 20$ .





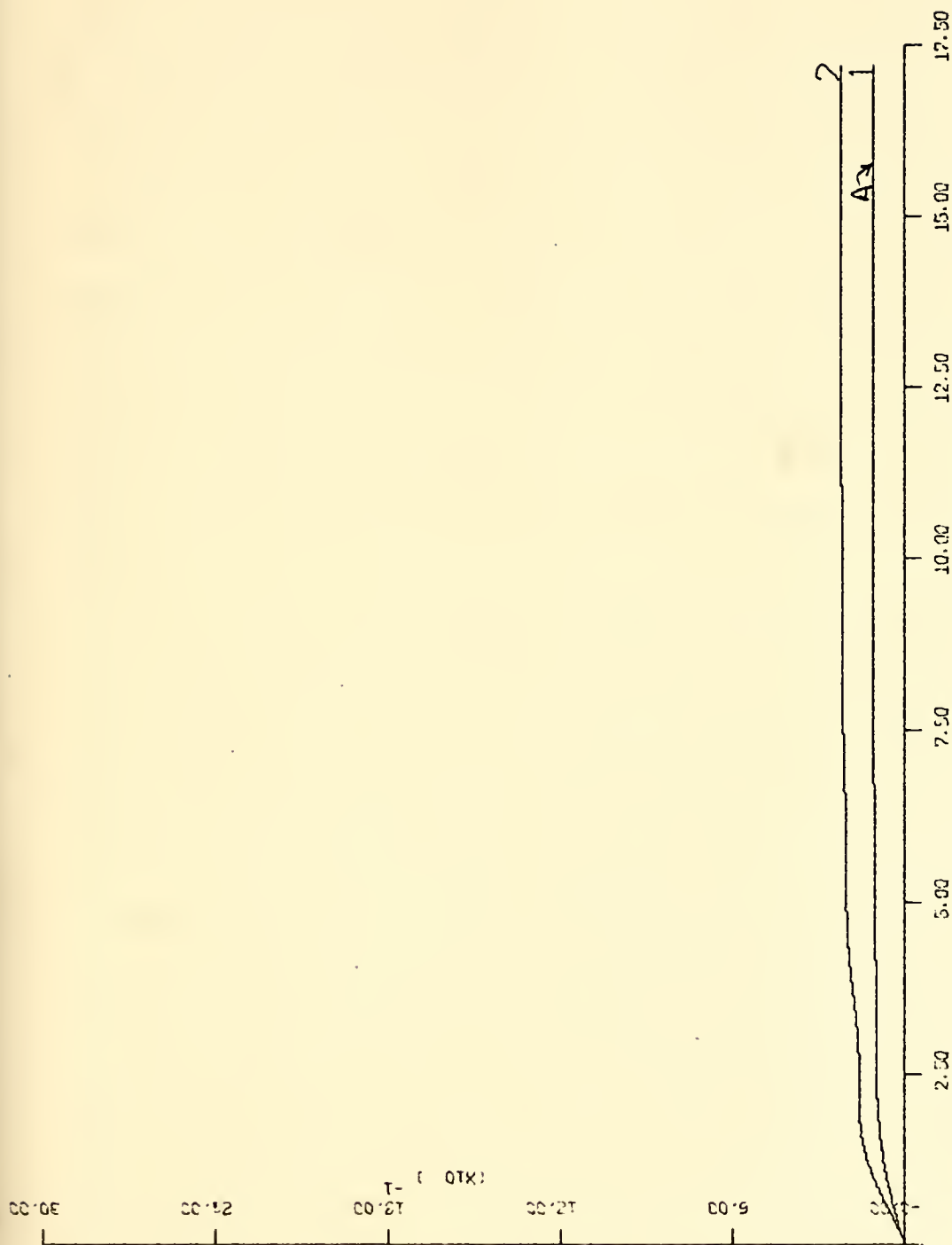


Fig. 55. Figure of merit. (Models A and C stabilized with the filters in the stabilizing loop, in the presence of sinusoidal waves with  $w = 20$ )



## E. USE OF DEAD ZONE 04

The Dead Zone used in chapter IV of this study is used again in the new stabilized model.

Using Computer Program No. 7 modified to include the new stabilizing loop, the two systems are again simulated. From the results presented in Figures 56, 57, and 58 it is seen that the oscillation of the rudder is reduced almost to zero.

In Figure 59 the complete block diagram for the final version of the stabilized model is shown. For simulation purposes instead of using the block  $s/s+p_0$  (which is realizable in real life) as shown in Figure 47, the pole  $1/s+p_0$  was introduced after  $\dot{r}$ . That pole introduces also the "storage function" required to take care of the existed implicit loop, so the block  $p/s+p$  (with  $p = 1000$ ) has been removed.

Using the nonlinear models, ships A and C (stabilized with the last designed compensation) were tested in the "Zig-Zag Maneuvers" test, with and without the Dead Zone present. The simulation was performed using Computer Program No. 4 modified to include the new compensation.

From the results, shown in Figures 60, 61, 62, 63, 64, 65, 66, and 67, it can be seen that

(1) there are no oscillations in the trajectory of the stabilized ship as were observed during the transient phase when the ship was tested in the presence of sinusoidal waves, and

(2) the overall behavior of the stabilized ship is similar to that of the stable.



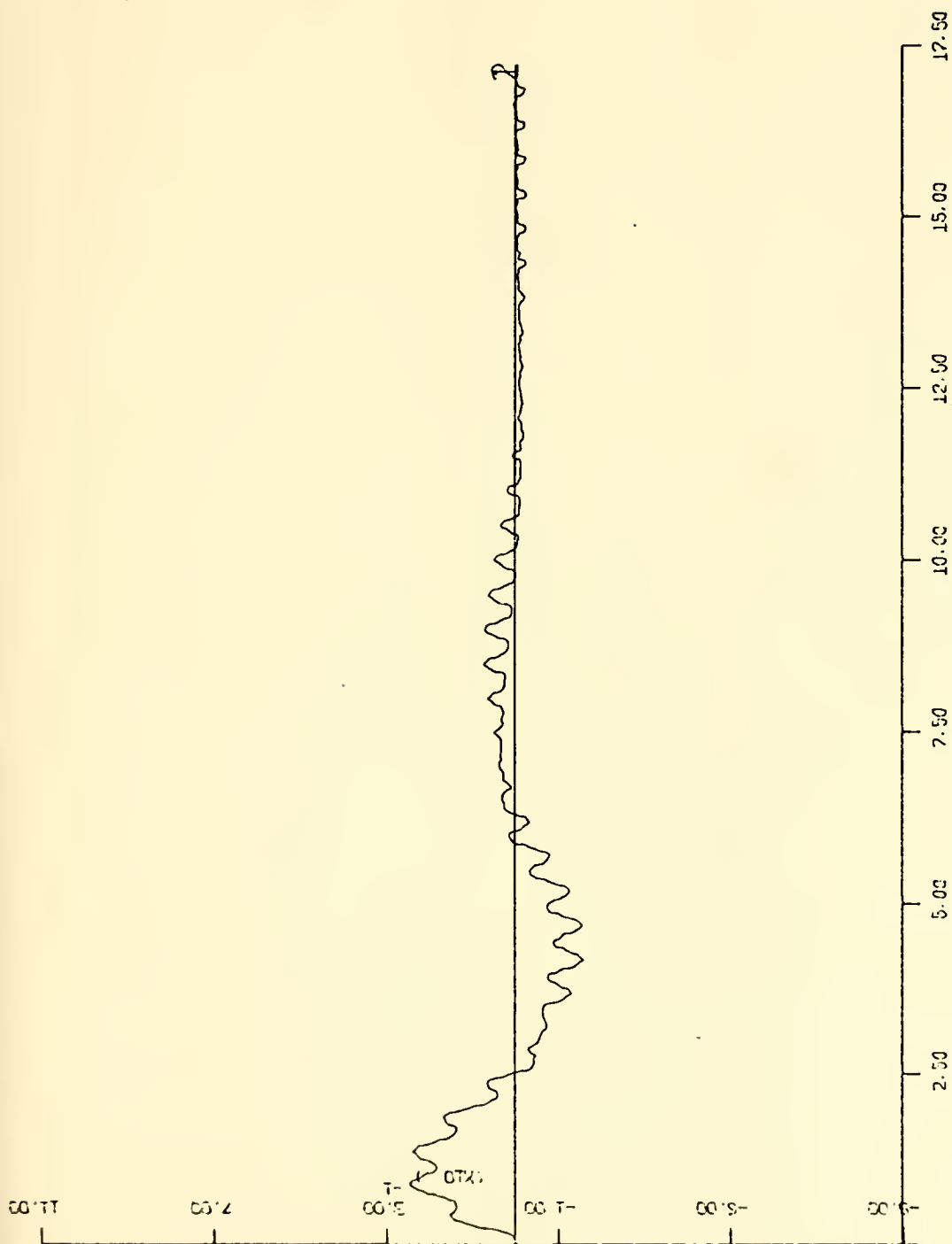


Fig. 56. Rudder deflections vs time in the presence of sinusoidal waves (Model C stabilized with the filters and the Dead Zone)



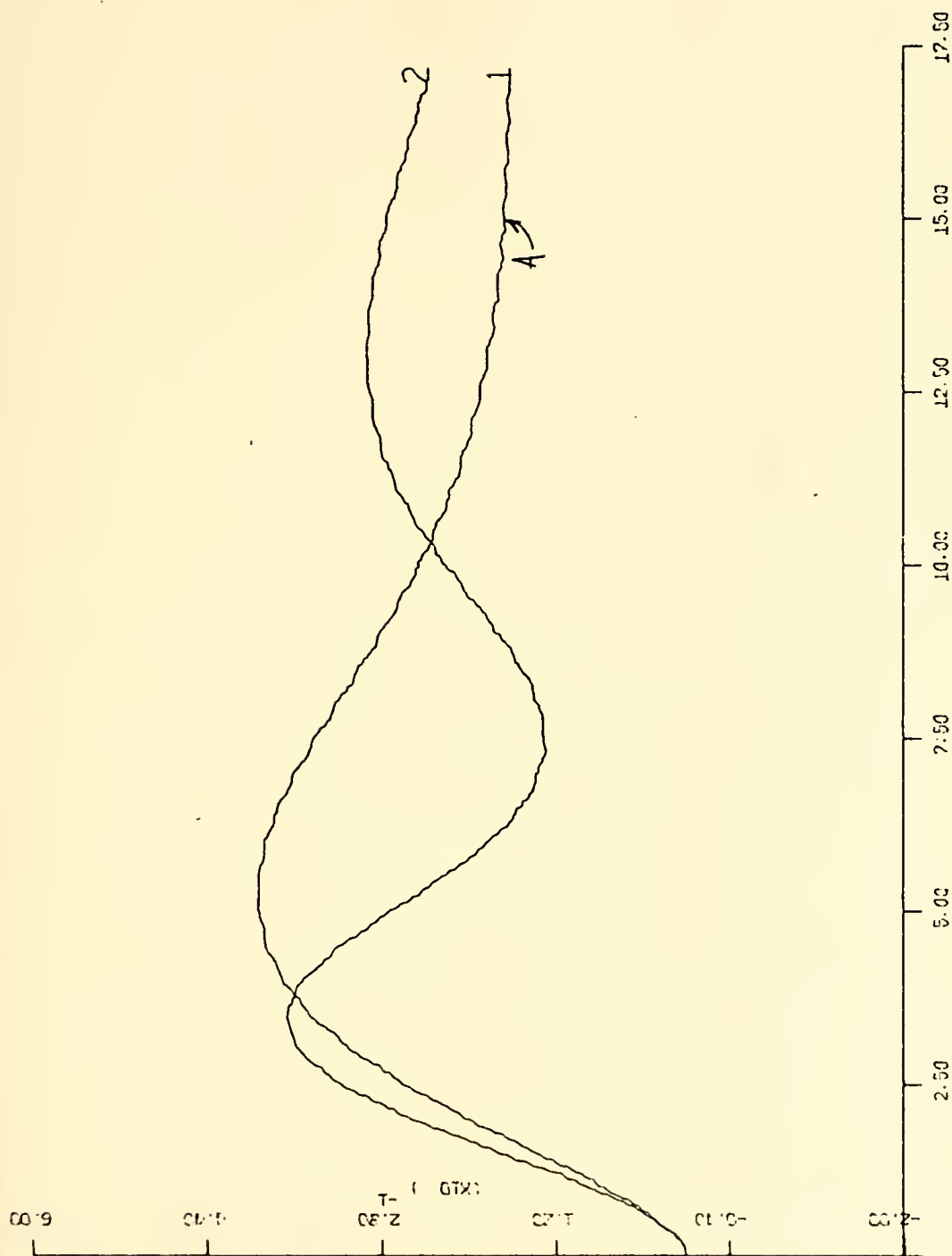


Fig. 57. Ship trajectories in the presence of sinusoidal waves  
(Models A and C stabilized with the filters and the  
Dead Zone)





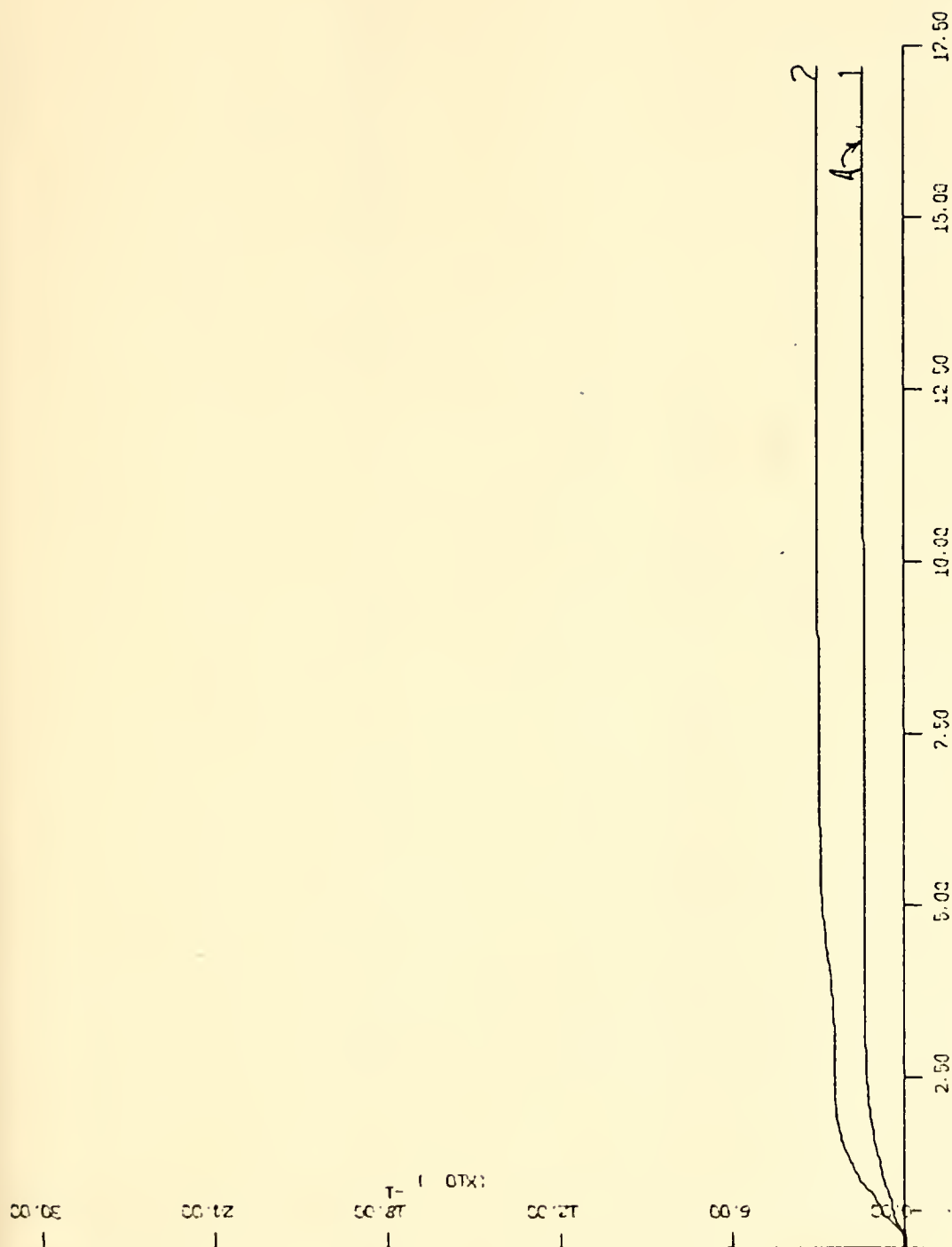


Fig. 58. Figure of merit. (Models A and C stabilized with the filters and the Dead Zone, in the presence of sinusoidal waves)



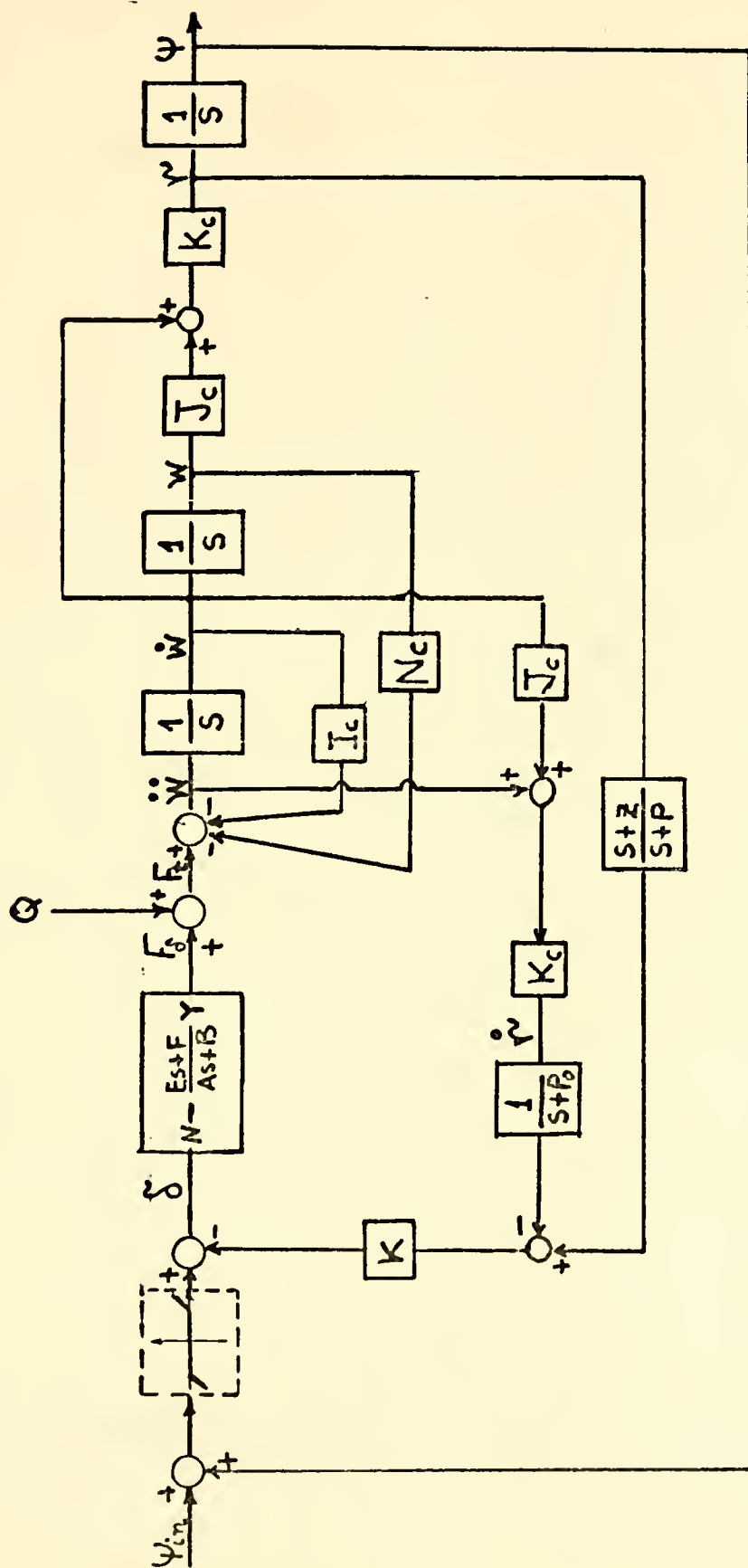


Figure 59. Block Diagram of the Stabilized Model C. (Final Version)



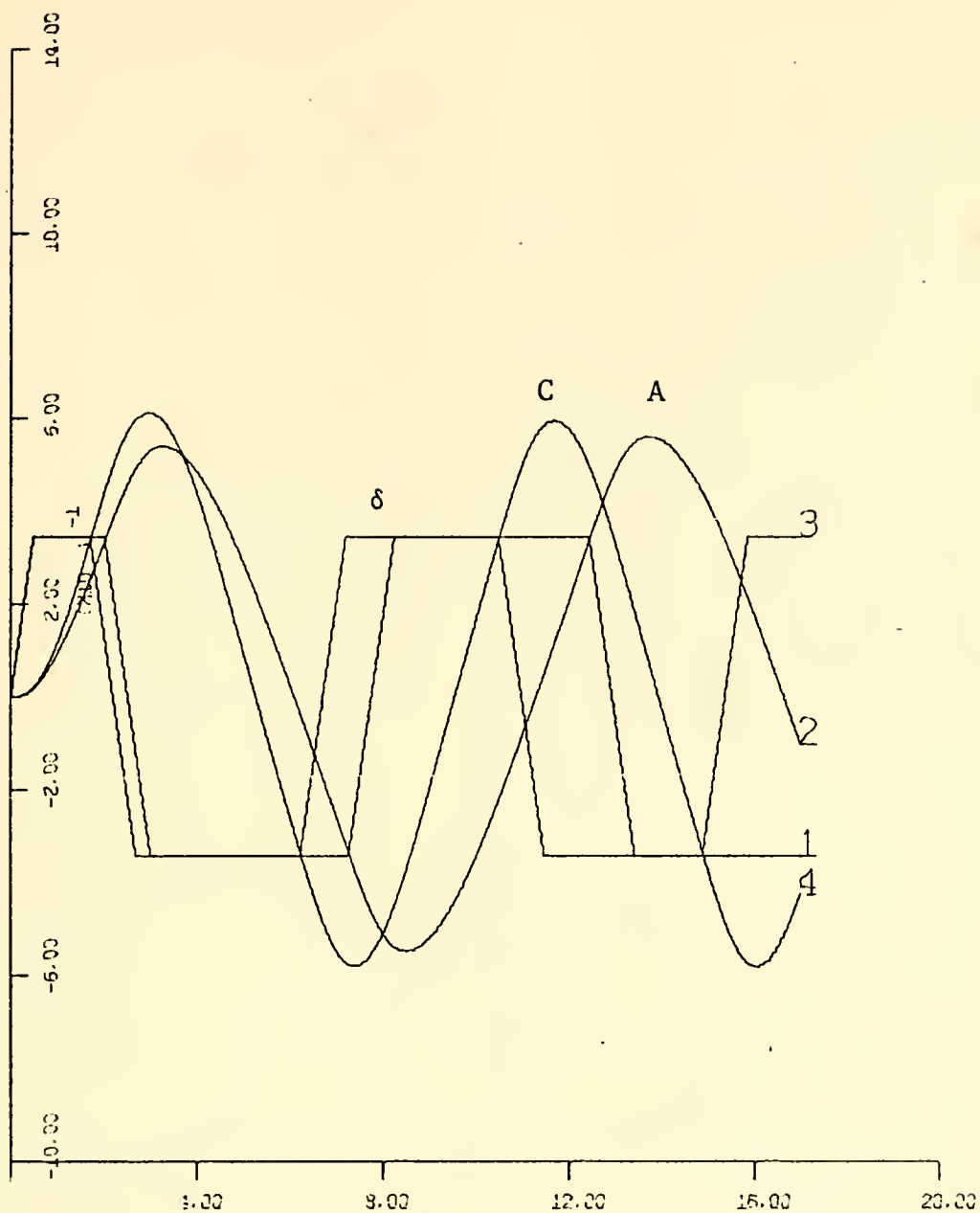


Figure 60. Input Commands and Ship Headings ( $\Psi$ ) vs. Time in the "Zig-Zag Maneuvers" Test. (Models A and C Stabilized, without the Dead Zone.)



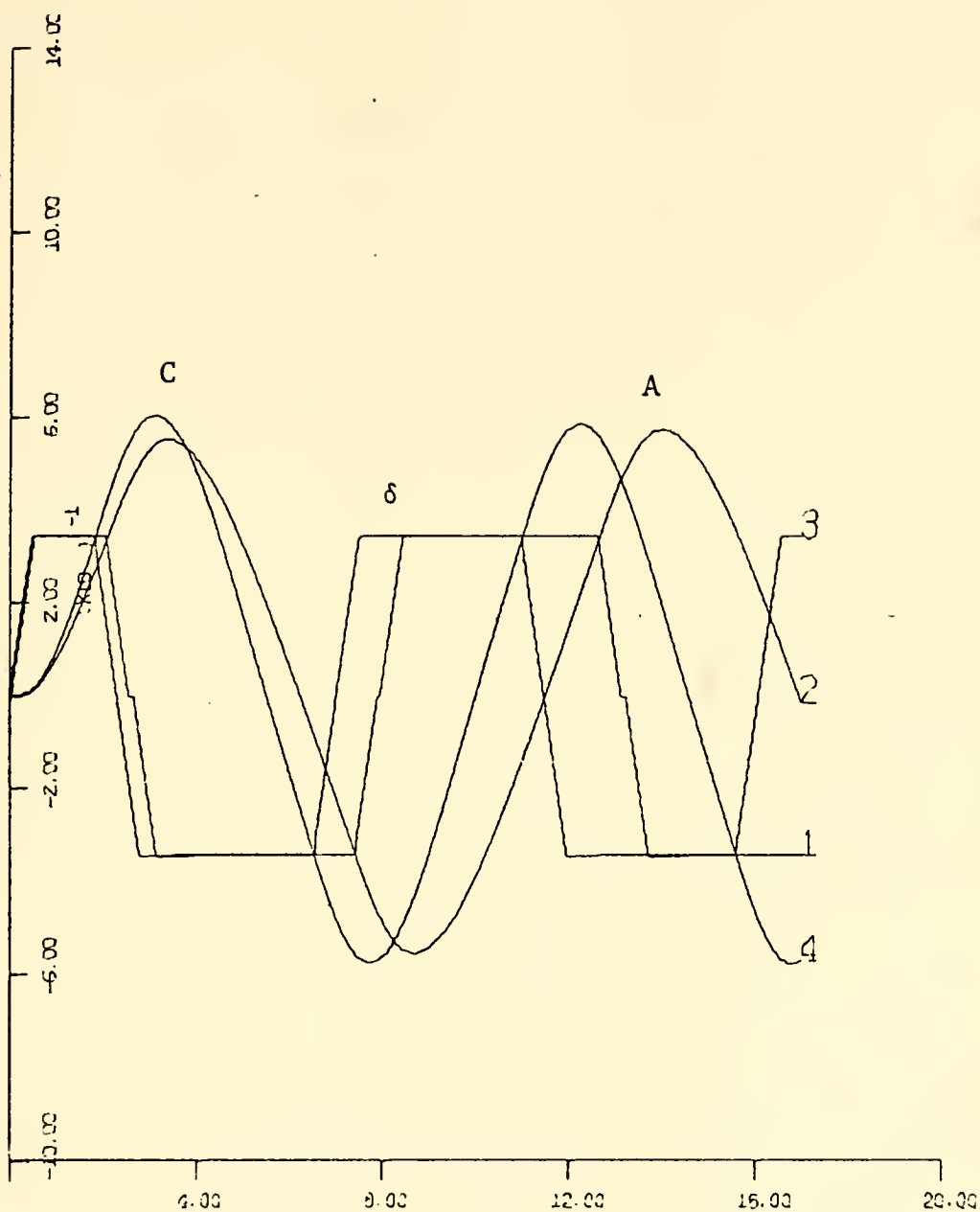


Figure 61. Input Commands and Ship Headings ( $\Psi$ ) vs. Time in the "Zig-Zag Manuevers" Test. (Models A and C Stabilized, with the Dead Zone.)





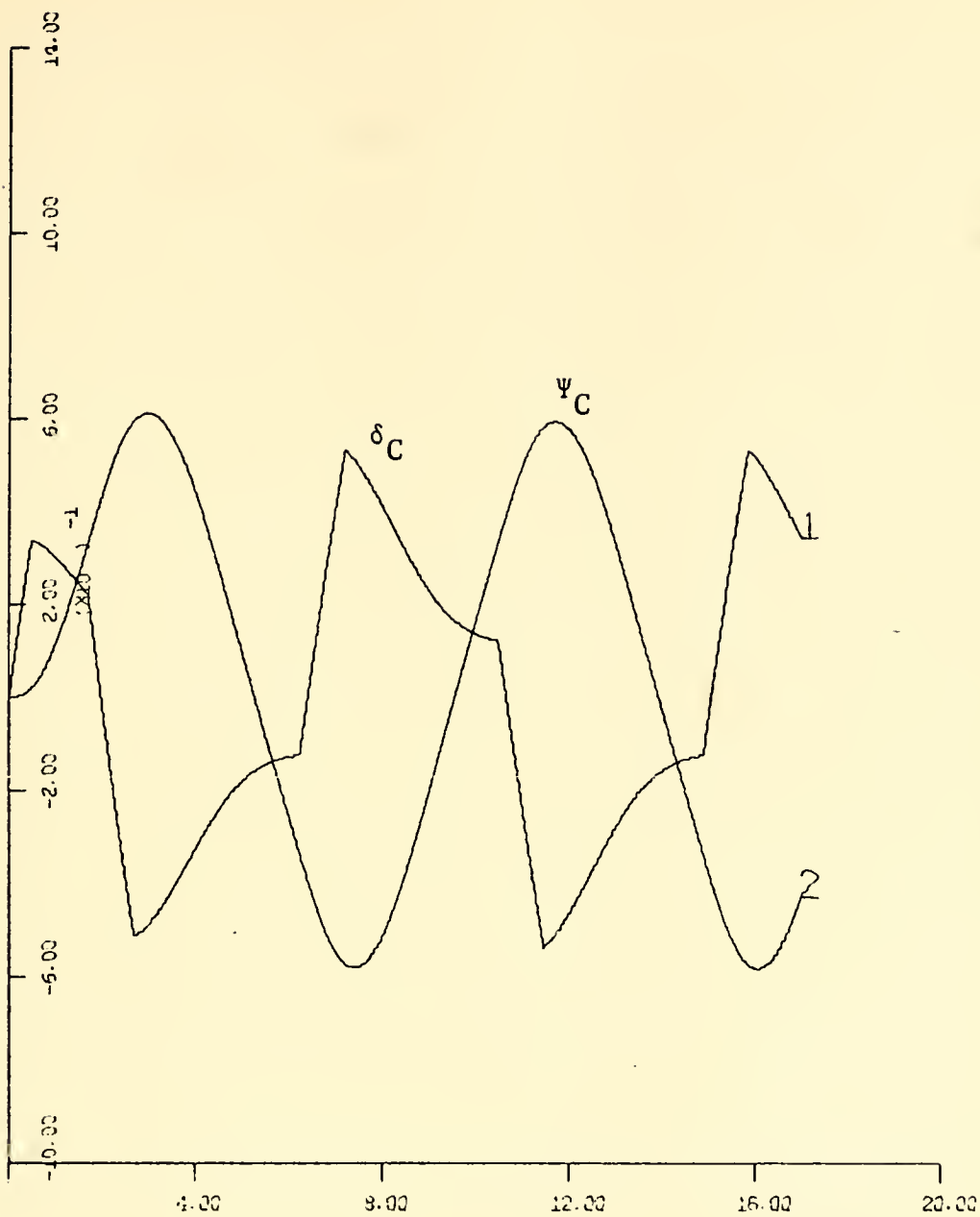


Figure 62. Rudder Deflection and Ship Headings ( $\Psi$ ) vs. Time in the "Zig-Zag Maneuvers" Test. (Model C Stabilized, without the Dead Zone.)



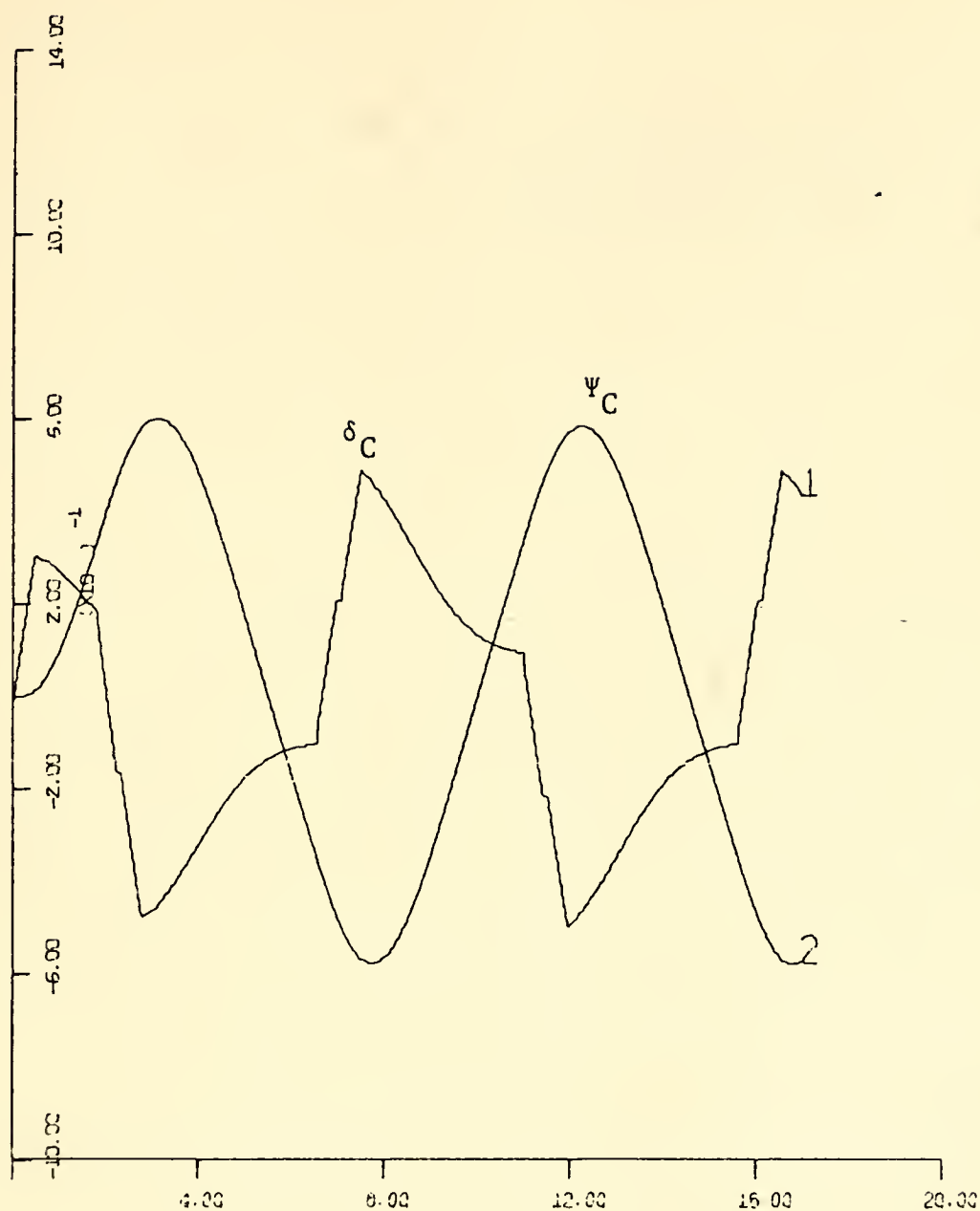


Figure 63. Rudder Deflections and Ship Headings ( $\Psi$ ) vs. Time in the "Zig-Zag Maneuvers" Test. (Model C Stabilized, with the Dead Zone.)



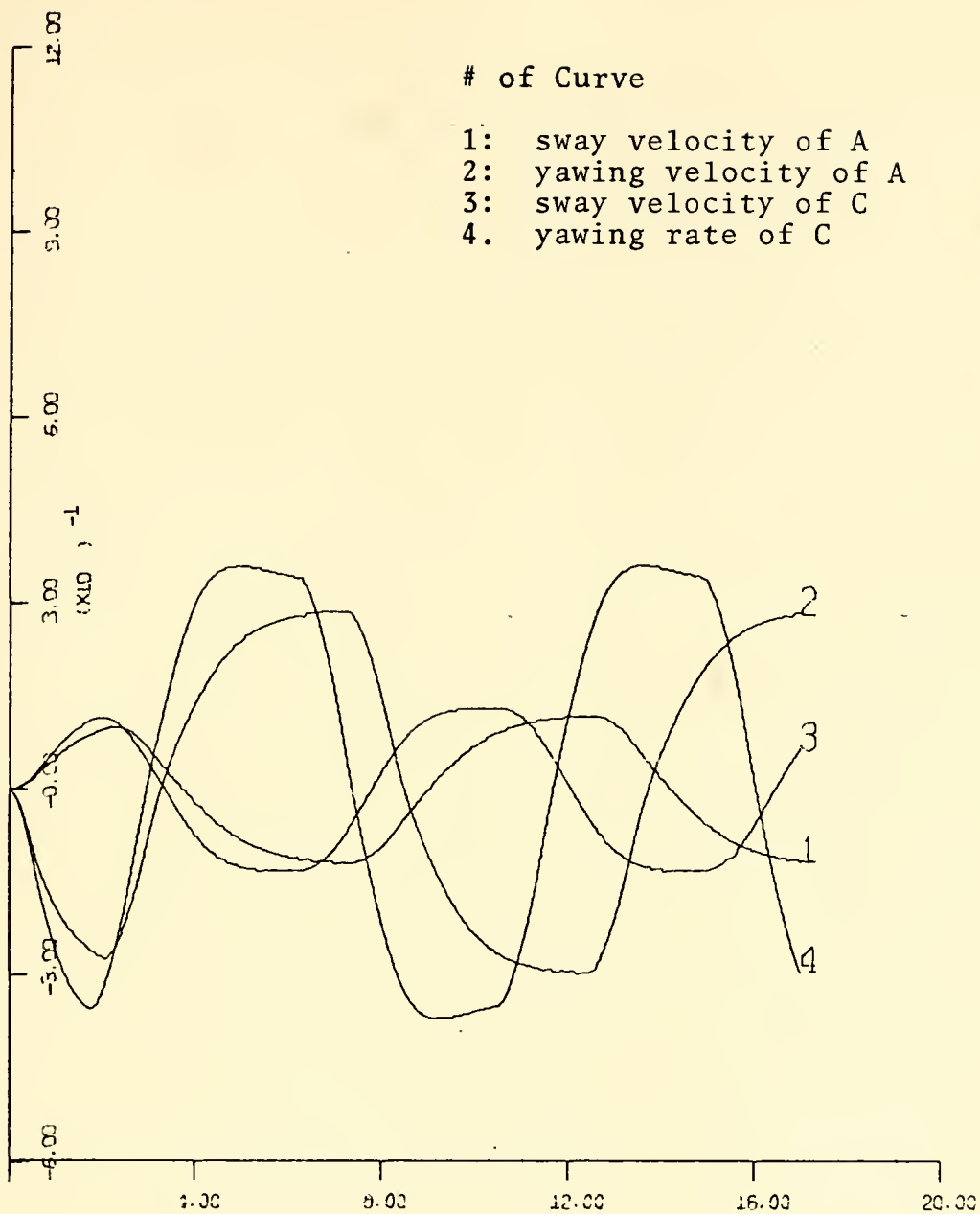


Figure 64. Yawing Rate and Sway Velocity vs. Time in the "Zig-Zag Maneuvers" Test. (Models A and C Stabilized, without the Dead Zone.)



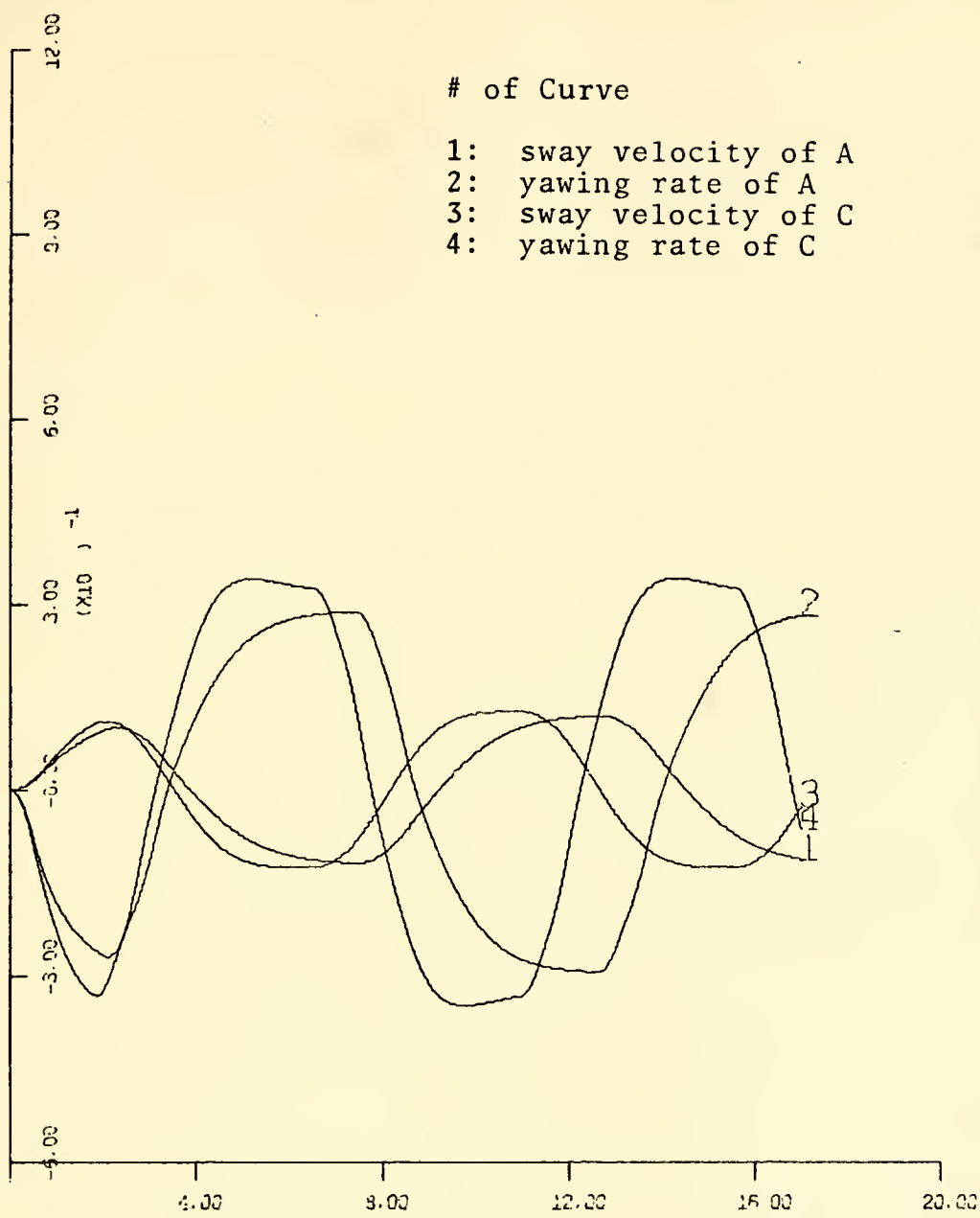


Figure 65. Yawing Rate and Sway Velocity vs. Time in the "Zig-Zag Maneuvers" Test. (Models A and C Stabilized, with the Dead Zone.)





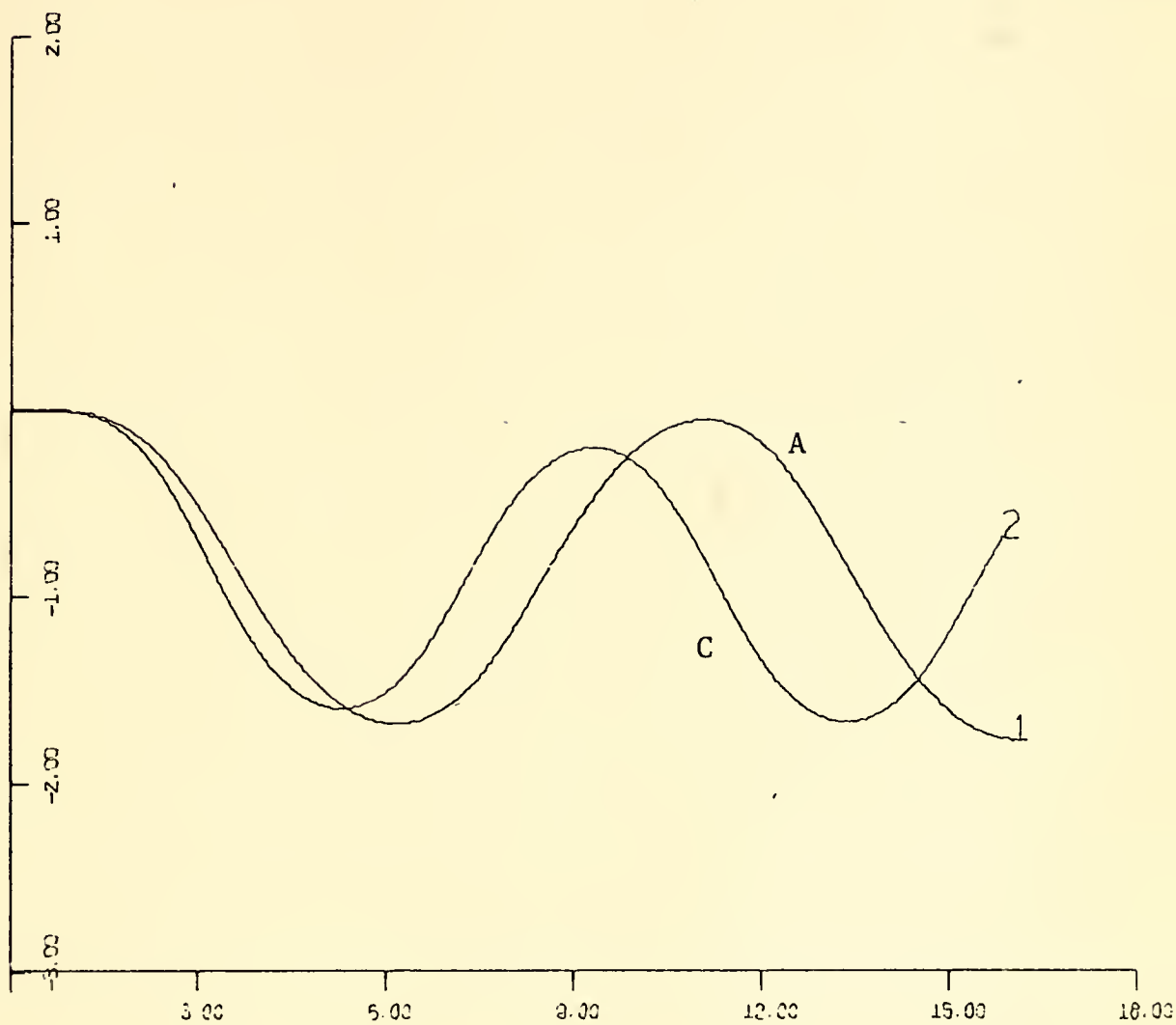


Figure 66. Ship Trajectories in the "Zig-Zag Maneuvers" Test. (Models A and C Stabilized, without Dead Zone.)



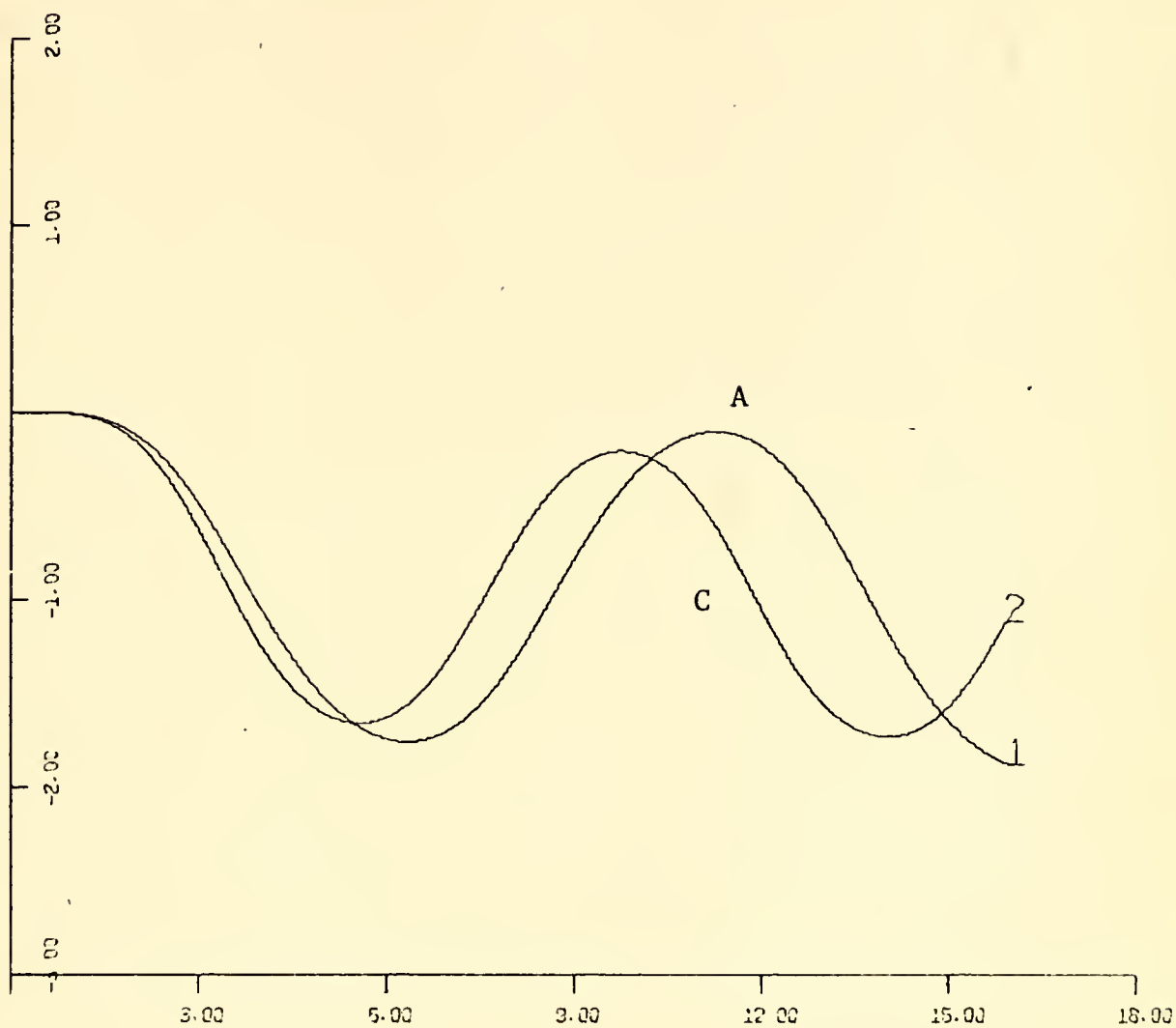


Figure 67. Ship Trajectories in the "Zig-Zag Maneuvers" Test. (Models A and C Stabilized, with the Dead Zone.)



## VI. CONCLUSIONS

Using velocity and acceleration feedback to activate the rudder, it was found possible to make the dynamically unstable ship behave in the same way the stable ship does. Then it was clearly shown that the fast turning capability of the unstable hull could still be achieved by disconnecting the automatic control and using manual operation.

Both ships exhibit rudder motions in the presence of waves, but those of the stable ship are minimized with the use of a Dead Zone. The stabilized ship shows extensive rudder motions and the use of a Dead Zone does not improve the situation.

The insertion of filters in the stabilizing loop highly reduces the rudder motions and makes possible the effective use of the Dead Zone in the stabilized ship. Then it was found that stabilized ship (with the filters and the Dead Zone) behaves in a similar way the stable does.

Digital Simulation Language (DSL/360) was found to be a very powerful tool in this study.



## VII. RECOMMENDATIONS

Topics for possible future studies may be considered the following:

(1) Rudder design requirements (in terms of expected fatigue and additional required power) for a stabilized dynamically unstable ship.

(2) Optimum design of the a.c suppression filters (in terms of better rudder and hull behavior).





## APPENDIX A



### MODELS FOR STABLE AND UNSTABLE SHIP

The original model adopted from a five foot Series 60 model (with block coefficient 0.7 and no propeller) as originally developed by the Davidson Laboratory.

#### PRINCIPAL CHARACTERISTICS OF PARENT MODEL

Length (L)-----	5.0 ft
Breadth (B)-----	0.714 ft
Draft (H)-----	0.267 ft
Block coefficient ( $C_B$ )-----	0.7
LCG from bow ( $x_G$ )-----	5.15 ft
Displacement (D)-----	41.64 lbs
Area of rudder ( $A_R$ )-----	0.021 sq ft
Rudder span-----	0.2 ft
Rudder chord-----	0.105 ft
Mass (m)-----	1.292 slugs
Mass coefficient ( $m'$ )-----	0.2
Longitudinal added mass ceff. ( $K_1 m'$ )-----	0.004
Lateral added mass coeff. ( $m_1'$ )-----	0.18
Rotational added mass coeff. ( $m_2'$ )-----	0.165
Radius of gyration in air-----	0.25L
C.G. of lateral added mass from midship ( $\bar{x}/L$ )-----	0.024
Drag coeff. at zero drift angle-----	0.019



# HYDRODYNAMIC DERIVATIVES FOR THE LINEAR ROTATIONS

In Reference 1 the parent model was modified to the desired models. The hydrodynamic derivatives for the two models A and C are listed below.

	<u>Model A</u>	<u>Model C</u>
$Y'_V$	-0.3544	-0.31306
$N'_V$	-0.0938	-0.1266
$Y'_R$	0.0774	0.0446
$N'_R$	-0.0635	-0.0435
$Y'_{\dot{V}}$	-0.188	-0.1868
$N'_{\dot{V}}$	0.004	0.0024
$Y'_{\dot{R}}$	0.004	0.0024
$N'_{\dot{R}}$	-0.0132	-0.0121
$I'_Z$	0.0125	0.0125
$m'$	0.2	0.2
$x'_G$	-0.015	-0.015
$N'$	-0.03293	-0.03293
$Y'$	0.06585	0.06585

The roots of the characteristic equations were computed and are listed below:

<u>Model A</u>	<u>Model C</u>
-0.32167	+0.2561
-3.114564	-2.880



## APPENDIX B

### HYDRODYNAMIC DERIVATIVES FOR THE NONLINEAR EQUATIONS

The hydrodynamic derivatives for the nonlinear equations used in Reference 1 were taken from Reference 2 and were the same for both models, A and C. They are listed below in two columns, column 1 and column 2, for the Y-force and N-moment equations respectively.

<u>Column 1</u>	<u>Column 2</u>
$Y'_{vvv} = - 12.9$	$N'_{vvv} = - 2.31$
$Y'_{vrr} = - 2.36$	$N'_{vrr} = - 0.612$
$Y'_v = 0.0$	$N'_v = 0.0$
$Y'_{vu} = 0.0$	$N'_{vu} = 0.0$
$Y'_{vuu} = 0.0$	$N'_{vuu} = 0.0$
$Y'_{rrr} = - 0.2766$	$N'_{rrr} = - 0.606$
$Y'_{rvv} = - 0.2$	$N'_{rvv} = - 2.84$
$Y'_r = 0.0$	$N'_r = 0.0$
$Y'_{ru} = 0.0$	$N'_{ru} = 0.0$
$Y'_{ruu} = 0.0$	$N'_{ruu} = 0.0$
$Y' = 0.0$	$N' = 0.0$
$Y'_{vv} = 0.0$	$N'_{vv} = 0.0$
$Y'_{rr} = 0.0$	$N'_{rr} = 0.0$
$Y'_u = 0.0$	$N'_u = 0.0$
$Y'_{uu} = 0.0$	$N'_{uu} = 0.0$
$Y'_{vr} = 0.0$	$N'_{vr} = 0.0$
$Y'_o = 0.00016$	$N'_o = - 0.0003$



	<u>Column 1</u>
$Y'_{ou}$	= 0.0

$Y'_{ouu}$	= 0.0
------------	-------

	<u>Column 2</u>
$N'_{ou}$	= 0.0

$N'_{ouu}$	= 0.0
------------	-------





## APPENDIX C

### EVALUATION OF THE FEEDBACK GAINS

The differential equations (24) and (25) can be written in the following form:

$$\dot{A}v + Bv + Cr + Dr + Y = 0 \quad (C-1)$$

$$\dot{E}v + Fv + Gr + Hr + N = 0 \quad (C-2)$$

where the coefficients were computed and are listed below, for both models A and C.

	<u>Model A</u>	<u>Model C</u>
$A = Y'_v - m'$	- 0.388	- 0.3868
$B = Y'_v$	- 0.3544	- 0.31306
$C = Y'_r - m'x'_G$	0.007	0.0054
$D = Y'_r - m'$	- 0.1226	- 0.1554
$E = N'_v - m'x'_G$	0.007	0.0054
$F = N'_v$	- 0.0938	- 0.1266
$G = N'_r - I'_z$	- 0.0257	- 0.0246
$H = N'_r - m'x'_G$	- 0.0605	- 0.0405
$N = N'$	- 0.03293	- 0.03293
$Y = Y'$	0.06585	0.06585

Taking the Laplace Transforms of equations (C-1) and (C-2), and rearranging terms we have:

$$(As+B)v(s) + (Cs+D)r(s) + Y\delta(s) = 0 \quad (C-3)$$

$$(Es+F)v(s) + (Gs+H)r(s) + N\delta(s) = 0 \quad (C-4)$$

Eliminating one of the variables in equations (C-3) and (C-4) an equation including the other variable and the forcing



function is obtained, and the new equation can give the transfer function of the system.

Solving equation (C-4) for  $v(s)$ :

$$-v(s) = \frac{Gs+H}{Es+F} r(s) + \frac{N}{Es+F} \delta(s) \quad (C-5)$$

Solving equation (C-3) for  $sr(s)$ :

$$sr(s) = \frac{1}{C} [(As+B)(-v(s)) - Dr(s) - Y\delta(s)]. \quad (C-6)$$

Substituting equation (C-5) into equation (C-6) we get

$$sr(s) = \frac{1}{C} \frac{(As+B)(Gs+H) - D(Es+F)}{Es+F} r(s) + \frac{As+B}{Es+F} N - Y\delta(s). \quad (C-7)$$

A block diagram corresponding to equation (C-7) is shown in figure (C-1). From that block diagram we have:

$$\frac{r(s)}{F_{\delta}(s)} = \frac{\frac{1}{Cs}}{1 + \frac{1}{Cs} \frac{D(Es+F) - (As+B)(Gs+H)}{Es+F}} \quad (C-8)$$

or

$$\frac{r(s)}{F_{\delta}(s)} = \frac{Es+F}{(Cs+D)(Es+F) - (As+B)(Gs+H)} \quad (C-9)$$

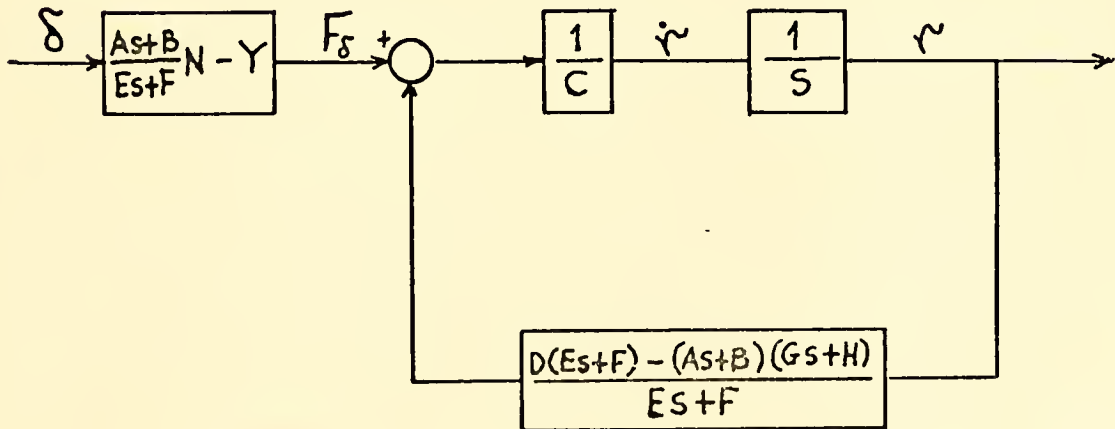


Figure (C-1).



From the block diagram in Figure (C-1) we also have

$$F_{\delta}(s) = \left[ \frac{(As+B)N}{Es+F} - Y \right] \delta(s) . \quad (C-10)$$

Substituting (C-10) into equation (C-9) we obtain the transfer function for both models, stable A and unstable C:

$$P_i(s) = \frac{r(s)}{\delta(s)} = \frac{(As+B)N - (Es+F)Y}{(Cs+D)(Es+F) - (As+B)(Gs+H)}; (i=A,C) \quad (C-11)$$

Substituting the numerical values for the parameters for both models A and C we obtain:

$$P_C(s) = \frac{-1.3051(s+1.506)}{(s-0.256)(s+2.88)} \quad (C-12)$$

$$P_A(s) = \frac{-1.2412(s+1.449)}{(s+0.32167)(s+3.114564)} . \quad (C-13)$$

As it was expected one root in equation (C-12) is in the right half plane. Also the minus sign in both equations (C-12) and (C-13) was expected because according to the sign convention with which the equations of motion were developed a positive rudder deflection results in a negative output.

To take care of the instability of model C and to make the roots of the stabilized system to coincide with the roots of the stable model A we apply a feedback compensation with gain  $Q(s) = K_1 + K_2s$ . The block diagram of the new system is shown in Figure (C-2), where an integration block is added after  $r(t)$  to give the heading angle.

From Figure (C-2) we have:



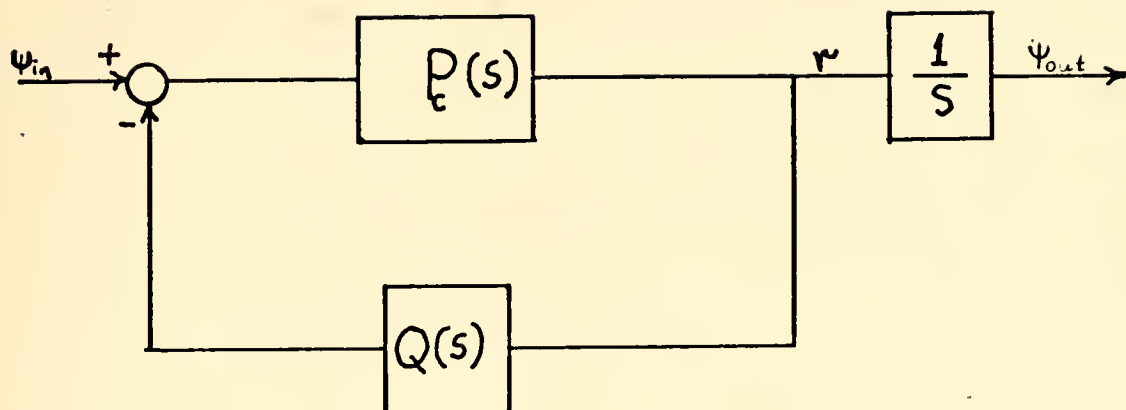


Figure (C-2).

$$\psi_{in} \frac{r(s)}{(s)} = \frac{P_C(s)}{1 + P_C(s)Q(s)} = \frac{\frac{-1.3051(s+1.506)}{(s-0.256)(s+2.88)}}{1 + (K_1 + K_2 s) \frac{-1.3051(s+1.506)}{(s-0.256)(s+2.88)}}$$

or

$$\psi_{in} \frac{r(s)}{(s)} = \frac{1.305(s+1.506)}{(1.3051K_2 - 1)s^2 + (1.3051K_1 + 1.965K_2 - 2.624)s + (1.965K_1 + 0.7373)}$$

The characteristic equation then of the stabilized ship becomes:

$$(1.3051K_2 - 1)s^2 + (1.3051K_1 + 1.965K_2 - 2.624)s + (1.965K_1 + 0.7373) = 0$$

or

$$R_C(s) = s^2 + \frac{1.3051K_1 + 1.965K_2 - 2.624}{1.3051K_2 - 1} s + \frac{1.965K_1 + 0.7373}{1.3051K_2 - 1} = 0.$$

-- The characteristic equation of model A is the denominator of equation (C-13) which becomes:





$$R_A(s) = s^2 + 3.4363s + 1.002.$$

In order the roots of the two characteristic equations to be the same, the two polynomials  $R_C(s)$  and  $R_A(s)$  must be identically equal, which is obtained when the coefficients of the terms of same power are equal. So:

$$\frac{1.3051K_1 + 1.965K_2 - 2.624}{1.3051K_2 - 1} = 3.4363 \quad (C-14)$$

$$\frac{1.965K_1 + 0.7373}{1.3051K_2 - 1} = 1.002. \quad (C-15)$$

Solving the two simultaneous linear equations (C-14) and (C-15) the values of the two parameters  $K_1$  and  $K_2$  are obtained:

$$K_1 = - 1.0232$$

$$K_2 = - 0.207472.$$



meme

me

meme

me

meme

me

me



Taking the inverse Laplace transform in equations (D-2) and (D-3) we obtain:

$$r(t) = K \dot{W}(t) + JW(t) \quad (D-4)$$

$$S(t) = \ddot{W}(t) + I\dot{W}(t) + NW(t). \quad (D-5)$$

Differentiating both sides of equation (D-4) and rearranging equation (D-5) we obtain

$$\dot{r}(t) = K \ddot{W}(t) + J\dot{W}(t)$$

$$\ddot{W}(t) = S(t) - I\dot{W}(t) - NW(t).$$

The last two differential equations can be represented with the block diagram shown in Figure D-1.



## APPENDIX E

### ZIG-ZAG MANEUVERS

An important definitive maneuver for both commercial and naval ships is the Zig-Zag maneuver. The results of this maneuver are indicative of the ability of a ship's rudder to control the ship.

The typical procedure for conducting the Zig-Zag maneuver is as follows (Ref. 2):

(1) Deflect the rudder, at a maximum rate, to a preselected position, say  $20^\circ$ , and hold until a change of heading angle of  $20^\circ$  is reached.

(2) At this point, deflect the rudder at maximum rate to an opposite angle of  $20^\circ$  and hold until the execute change of heading angle on the opposite side is reached.

(3) Deflect the rudder at maximum rate to an angle of  $20^\circ$  in the first direction. This cycle can be repeated through the third, fourth or more executes.

Figure E-1 shows the relation between the rudder deflection ( $\delta$ ) and the ship's heading ( $\Psi$ ).

The rudder displacement can be modeled for the simulation using the RAMP function as follows:

$$\delta(t) = d_r [\text{RAMP}(t-t_1) - \text{RAMP}(t-t_2) - \text{RAMP}(t-t_3) + \text{RAMP}(t-t_4) + \text{RAMP}(t-t_5)]$$

for one cycle until  $t \leq t_6$ , where:





$d_r$  = rudder displacement rate (degrees/sec)

$t_1$  = time delay of rudder

$t_2$  = time at  $\delta = \delta_{\max}$

$t_3$  = time at  $\delta = -\psi$

$t_4$  = time at  $\delta = -\delta_{\max}$

$t_5$  = time at  $\delta = \psi$ .

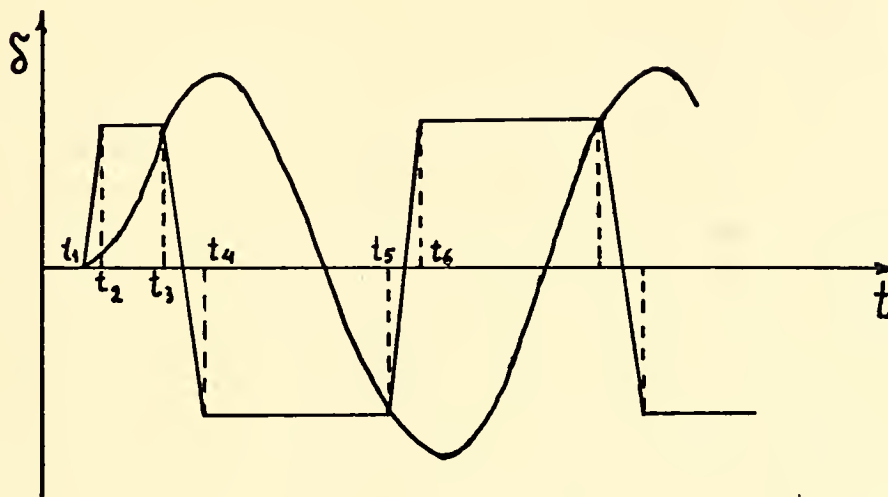


Figure E-1. Relations Between Rudder Deflection and Ship's Heading in Standard Zig-Zag Maneuver.







```

YA=INTGRL(0.0,YADOT)
PSINC=PSINA
EC=PSINC+PSIOC-K1*RC-K2*RDOTC
RDOTC=KC*(JC*WDC+WDDC)
DELTAC=REALPL(0.0,0.001,EC)
WDDC=DELTAC-IC*WDC-NC*WC
WDC=INTGRL(0.0,WDDC)
WC=INTGRL(0.0,WDC)
RC=KC*(WDC+JC*WC)
PSIOC=INTGRL(0.0,RC)
VC1=LEDLA(0.0,P1C,P2C,RC)
VC2=REALPL(0.0,P2C,DELTAC)
VC=- (G1C*VC1+G2C*VC2)
XCDDT=COS(PSIOC)-VC* SIN(PSIOC)
YCDDT=SIN(PSIOC)+VC* COS(PSIOC)
XC=INTGRL(0.0,XCDDT)
YC=INTGRL(0.0,YCDDT)

```

SAMPLE

```

CALL DRWG(1,1,TIME,PSIOA)
CALL DRWG(1,2,TIME,PSIOC)
CALL DRWG(1,3,TIME,PSINAA)
CALL DRWG(2,1,TIME,DELTAA)
CALL DRWG(2,2,TIME,DELTAC)
CALL DRWG(3,1,XA,YA)
CALL DRWG(3,2,XC,YC)

```

TERMINAL

```
CALL ENDRW(NPLOT)
```

END  
STOP

```
//PLOT,SYSIN,DD *
PSIOA , 4.0 PSIOC
```

0.0	DELTAA	4.0	DELTAC	-0.08	0.016	6.0	6.0
0.0	VS	XA	AND	YC	VS	XC	6.0
0.0	YA	VS	XA	AND	YC	VS	6.0

5  
5  
5



```

*** ** *
COMPUTER PROGRAM NO 2
** *
MODELS A AND C - STABILIZED IN THE 'TURNING MANEUVERS' TEST. THE LINEAR MODELS ARE USED.
** *
THIS PROGRAM IS REFERRED TO FIGS. 4,5
** *
//HOZOS JOB (1159,0728,EA32),'HOZOS',TIME=12
//EXEC DSL
//DSL.INPUT DD *
INTER NPLDT
CONST NPLOT=3
CCNST KA=-1.2412,JA=1.449,IA=3.4363,NA=1.002
CCNST KC=-1.3051,JC=1.506,IC=2.624,NC=-0.73728
CCNST K1=-1.0232,K2=-0.207472,Y=0.06585
CCNST AA=-0.388,BB=-0.3544,CA=0.007,DA=-0.1266
CCNST AC=-0.3868,BC=-0.31306,CC=0.0054,DC=-0.1554
CCNTRL FINTIM=24.0,DELT=0.0001,DELS=0.02
CPRINTI O.1,DELTA,DELTAC,PSIOA,PSIOC,XA,YA,XC,YC
INITIAL
DRATE=40./57.3
G1A=DA/BA
G2A=Y/bA
P1A=CA/DA
P2A=AA/BA
G1C=DC/BC
G2C=Y/cC
P1C=CC/DC
P2C=AC/BC
DERIVATIVE
PSINA=(RAMP(1.0)-RAMP(1.5))-RAMP(5.0)+RAMP(6.0)+...
RAMP(11.0)-RAMP(11.5))*DRATE
PSINAA=-PSINA
EA=PSINA
DELTA=REALPL(0.0,0.001,EA)
WEDA=DELTA-1A*WDA-NA*WA
WUA=INTGRL(0.0,WDDA)
WA=INTGRL(0.0,WDA)
RA=KA*(WDA+JA*WA)
PSIOA=INTGRL(0.0,RA)
VA1=LEDLA(0.0,P1A,P2A,KA)
VA2=REALPL(0.0,P2A,DELTA)
VA=-((G1A*VA1+G2A*VA2)
XADOT=COS(P1AUA)-VA*SIN(P1OAU)
YADOT=SIN(P1OAU)+VA*COS(P1AUA)

```





```

XA=INTGRL(0.0,XADOT)
YA=INTGRL(0.0,YADOT)
PSINC=PSINA
EC=PSINC-K1*RC-K2*RODTC
RODTC=KC*(JC*WDC+WDDC)
DELTAC=REALPL(0.0,0.001,EC)
WDDC=DELTAC-IC*WDC-NC*WC
WDC=INTGRL(0.0,WDDC)
WC=INTGRL(0.0,WDC)
RC=KC*(WDC+JC*WC)
PSIUC=INTGRL(0.0,RC)
VC1=LEDLA(0.0,PLC,P2C,RC)
VC2=REALPL(0.0,P2C,DELTAC)
VC=-(G1C*VC1+G2C*VC2)
XCDDT=COS(PSIUC)-VC*Sin(PSIUC)
YCDDT=Sin(PSIUC)+VC*Cos(PSIUC)
XC=INTGRL(0.0,XCDDT)
YC=INTGRL(0.0,YCDDT)

```

SAMPLE

```

CALL DRWG(1,1,TIME,PSIOA)
CALL DRWG(1,2,TIME,PSIOC)
CALL DRWG(1,3,TIME,PSINAA)
CALL DRWG(2,1,TIME,DELTAA)
CALL DRWG(2,2,TIME,DELTAC)
CALL DRWG(3,1,XA,YA)
CALL DRWG(3,2,XC,YC)

```

TERMINAL

CALL ENDRW(NPLOT)

END

STOP

//PLOT-SYSIN DD \*

```

PSIOA , 4.0 PSIUC , -2.0 PSINAA 0.6
0.0 DELTAA , 4.0 DELTAC -0.5 XC 0.2
YA VS XA AND YC VS XC 1.6
0.0 3.0

```

```

6.0 6.0 5.0
6.0 6.0 5.0
6.0 6.0 5.0

```

5 5 5







```

XAXA=INTGRL(XAXO,XAXDTA)
YAXA=INTGRL(YAXO,YAXDTA)
CC=DRATE*(RAMP(TC1)-RAMP(TC2)-RAMP(TC3)+RAMP(TC4)+RAMP(TC5))
DC=CC
VC=INTGRL(VO,VDTTC)
RC=INTGRL(RO,RDTTC)
PSIC=INTGRL(PSIO,RC)
F2C=YO+YVC*VC+1./6.*YVRR*RC**3+1./6.*YVVV*VC**3+1./2.*YVRR*VC*RC**2+(YRC-MASS)*...
F3C=NO+NVC*VC+1./6.*YVRR*RC**3+1./6.*YVVV*VC**3+1./2.*YVRR*VC*RC**2+(NRC-MASS*XC)*...
NMVDTTC=(IZ-NRDTTC)*F2C-(MASS*XC-YRDTTC)*F3C
NMRDTTC=(MASS-YVDTTC)*F3C-(MASS*XC-NVDTTC)*F2C
VDTTC=NMRDTTC/DETC
RDTTC=NMRDTTC/DETC
XAXDTTC=U*COS(PSIC)-VC*SIN(PSIC)
YAXDTTC=U*SIN(PSIC)+VC*COS(PSIC)
XAXC=INTGRL(XAXO,XAXDTTC)
YAXC=INTGRL(YAXO,YAXDTTC)
PSIAA=-PSIA
PSICC=-PSIC

```

DYNAMIC

```

IF(I.NE.0) GO TO 1
IF(ABS(DMAX-DA).GT.0.010) GO TO 1
TA2=TIME
I=I+1
1 IF(I.NE.1) GO TO 2
IF(ABS(DA+PSIA).GT.0.010) GO TO 2
TA3=TIME
I=I+1
2 IF(I.NE.2) GO TO 3
IF(ABS(DMAX+DA).GT.0.010) GO TO 3
TA4=TIME
I=I+1
3 IF(I.NE.3) GO TO 31
IF(ABS(DA+PSIA).GT.0.010) GO TO 31
TA5=TIME
I=I+1
31 IF(I.NE.4) GO TO 4
IF(ABS(DA).GT.0.002) GO TO 4
TA1=TIME
I=0
TA2=1000.
TA3=1000.
TA4=1000.
TA5=1000.
4 IF(J.NE.0) GO TO 5
IF(ABS(DMAX-CC).GT.0.010) GO TO 5

```



```

TC2=TIME
J=J+1
IF(J.NE.1) GO TO 6
IF(ABS(CC+PSIC).GT.0.010) GO TO 6
TC3=TIME
J=J+1
IF(J.NE.2) GO TO 7
IF(ABS(DMAX+CC).GT.0.010) GO TO 7
TC4=TIME
J=J+1
IF(J.NE.3) GO TO 71
IF(ABS(CC+PSIC).GT.0.010) GO TO 71
TC5=TIME
J=J+1
IF(J.NE.4) GO TO 8
IF(ABS(CC).GT.0.010) GO TO 8
TC1=TIME
J=0
TC2=1000.
TC3=1000.
TC4=1000.
TC5=1000.
CGNTINUE

```

8 SAMPLE

```

CALL DRWG(1,1,TIME,DA)
CALL DRWG(1,2,TIME,PSIAA)
CALL DRWG(1,3,TIME,CC)
CALL DRWG(1,4,TIME,PSICC)
CALL DRWG(2,1,TIME,VA)
CALL DRWG(2,2,TIME,RA)
CALL DRWG(2,3,TIME,VC)
CALL DRWG(2,4,TIME,RC)
CALL DRWG(3,1,XAXA,YAXA)
CALL DRWG(3,2,XAXC,YAXC)

```

TERMINAL  
CALL ENDRW(NPLOT)

END  
STOP

```

//PLCT.SYSIN DD *
DA , PSIAA , CC , PSICC
0.0 4.0 -1.0
VA , RA , VC , RC
0.0 4.0 -0.6
YA VS XA , YC VS XC
0.0 3.0 -3.0

```

```

5.0 6.0
5.0 6.0
5.0 6.0

```

5 5 5





```

***
**      COMPUTER PROGRAM NO 4
**
**      MODELS A AND C-STABILIZED IN ZIG ZAG MANE-
**      UVERS. THE NON LINEAR MODELS ARE USED.
**
**      //HOZQS JOB (1159,0728,EA32),'HOZOS',TIME=12
**      //EXEC DSL
**      //DSL INPUT DD #
**      INTEGER INPLOT, I, J
**      CONST NPLCT=4
**      CONST TA1=0., TA2=1000., TA3=1000., TA4=1000., TA5=1000.,...
**      CONST TC1=0., TC2=1000., TC3=1000., TC4=1000., TC5=1000.
**      CONST YVA=-.3544, NVA=-.0538, YKA=.0774, NRA=-.0635, ...
**      CONST YVDTA=-.188, NVDTA=.004, NRDTA=-.0132, YRDTA=.004
**      CONST YVC=-.31306, NVC=-.1266, YRC=.0446, NRC=-.0435, ...
**      CONST YVDTC=-.1858, NVDTC=.0024, NRDTC=-.0121, YRDTC=0.0024
**      CONST YVV=-.12.9, YRR=-.2766, YRV=-.2, NVV=-2.31, ...
**      CONST NVRR=-.612, NRR=-.606, NRVV=-2.84, YVRR=-2.36
**      CONST IZ=.0125, MASS=.2, XG=-.015, YC=.0016, NO=-.0003, ...
**      CONST ND=-.03293, YD=.06585, U0=1., V0=0., RO=0., XAX0=0., YAX0=0.
**      CONTRL FINIM=17.0, DELT=0.0001, DELS=0.01
**      PRINT 0.1, DA, CC, PSIAA, PSICC, XAXA, YAXA, XAXC, YAXC, DCDOT, DC
**      INITIAL
**      I=0
**      J=0
**      U=1.
**      PSIO=0.0
**      DMAX=20./57.3
**      DRATE=40./57.3
**      DETA=(MASS-YVDTA)*{(IZ-NRDTA)}-{(MASS*XG-NVDTA)}*(MASS*XG-YRDTA)
**      DETC=(MASS-YVDTC)*{(IZ-NRDTC)}-{(MASS*XG-NVDTC)}*(MASS*XG-YRDTC)
**
**      DERIVATIVE
**      DA=CRATE*(RAMP(TA1)-RAMP(TA2)-RAMP(TA3)+RAMP(TA4)+RAMP(TA5))
**      VA=INTGRL(V0,VDTA)
**      RA=INTGRL(R0,RDTA)
**      PSIA=INTGRL(PSIO,RA)
**      F2A=Y0+YVA*VA+1./6.*YVRR*RA+1./6.*YVVV*VA**3+1./2.*YVRR*VA*RA**2+(YRA-MASS)*...
**      F3A=NO+NVA*VA+1./6.*YRRR*RA+1./6.*NVVV*VA**3+.5*YRVV*RA**2+YD*DA
**      NMVDTA=(IZ-NRDTA)*F2A-(MASS*XG-NVDTA)*F3A
**      NMVDTA=(MASS-YVDTA)*F3A-(MASS*XG-NVDTA)*F2A
**      NMVDTA=NMVDTA/DETA
**      RCGTA=NMVDTA/DETA
**      XAXDTA=U*COS(PSIA)-VA*SIN(PSIA)
**      YAXDTA=U*SIN(PSIA)+VA*COS(PSIA)

```



```

XAXA=INTGRL(XAXO,XAXDTA)
YAXA=INTGRL(YAXO,YAXDTA)
CC=DRATE*(RAMP(TC1)-RAMP(TC2)-RAMP(TC3)+RAMP(TC4)+RAMP(TC5))
RDOTCC=REALPL(0.0,0.001,RDOTC)
DC=CC-K1*RC-K2*RDOTCC
VC=INTGRL(VO,VDOTC)
RC=INTGRL(RO,RDOTC)
PSIC=INTGRL(PSIO,RC)
F2C=YO+YVC*VC+1./6.*YVVR*VC**3+1./2.*YVRR*VC*RC**2+(YRC-MASS)*...
      RC+1./6.*YVRR*RC**3+.5*YRVV*RC*VC**2+YD*DC
F3C=NO+NVC*VC+1./6.*NVR*RC**3+.5*NVR*VC*RC**2+(NRC-MASS*XG)...
      *RC+1./6.*NVR*RC**3+NRVV*RC*VC**2*.5+ND*DC
NMVDTC=(IZ-NRDOTC)*F2C-(MASS*XG-YVDTC)*F3C
NMRDTC=(MASS-YVDTC)*F3C-(MASS*XG-NVDTC)*F2C
VDCDTC=NMDTC/DETC
RDOTC=NMRDTC/DETC
XAXDTC=U*COS(PSIC)-VC*SIN(PSIC)
YAXDTC=U*SIN(PSIC)+VC*COS(PSIC)
XAXC=INTGRL(XAXO,XAXDTC)
YAXC=INTGRL(YAXO,YAXDTC)
PSIAA=-PSIA
PSICC=-PSIC
DYNAMIC
IF(I.NE.0) GO TO 1
IF(ABS(CMAX-DA).GT.0.010) GO TO 1
TA2=TIME
I=I+1
1 IF(I.NE.1) GO TO 2
IF(ABS(DA+PSIA).GT.0.010) GO TO 2
TA3=TIME
I=I+1
2 IF(I.NE.2) GO TO 3
IF(ABS(CMAX+DA).GT.0.010) GO TO 3
TA4=TIME
I=I+1
3 IF(I.NE.3) GO TO 31
IF(ABS(DA+PSIA).GT.0.010) GO TO 31
TA5=TIME
I=I+1
31 IF(I.NE.4) GO TO 4
IF(ABS(DA).GT.0.002) GO TO 4
TA1=TIME
I=0
TA2=1000.
TA3=1000.
TA4=1000.
TA5=1000.
4 IF(J.NE.0) GO TO 5

```



```

IF (ABS(DMAX-CC).GT.0.010) GO TO 5
TC2=TIME
J=J+1
5 IF (J.NE.1) GO TO 6
IF (ABS(CC+PSIC).GT.0.010) GO TO 6
TC3=TIME
J=J+1
6 IF (J.NE.2) GO TO 7
IF (ABS(DMAX+CC).GT.0.010) GO TO 7
TC4=TIME
J=J+1
7 IF (J.NE.3) GO TO 71
IF (ABS(CC+PSIC).GT.0.010) GO TO 71
TC5=TIME
J=J+1
71 IF (J.NE.4) GO TO 8
IF (ABS(CC).GT.0.010) GO TO 8
TC1=TIME
J=0
TC2=1000.
TC3=1000.
TC4=1000.
TC5=1000.
CONTINUE

```

8 SAMPLE

```

CALL DRWG(1,1,TIME,DA)
CALL DRWG(1,2,TIME,PSIAA)
CALL DRWG(1,3,TIME,CC)
CALL DRWG(1,4,TIME,PSICC)
CALL DRWG(2,1,TIME,VA)
CALL DRWG(2,2,TIME,VC)
CALL DRWG(2,3,TIME,RC)
CALL DRWG(2,4,TIME,RA)
CALL DRWG(3,1,XAXA,YAXA)
CALL DRWG(3,2,XAXC,YAXC)
CALL DRWG(4,1,TIME,DC)
CALL DRWG(4,2,TIME,PSICC)

```

TERMINAL

```
CALL ENDRW(NPLOT)
```

END

STOP

```
//PLCT,SYSIN DD *
```

```
DA , PSIAA , CC , PSICC
```

```
0.0 4.0 , VC , RC 0.4
```

```
0.0 VA , RA , VC , RC 0.3
```

```
0.0 YA VS XA , YC VS XC 1.0
```

```
0.0 3.0 , YC VS XC -3.0
```

5

6.0

5.0

0.4

-1.0

4.0

4.0

3.0

-3.0

-0.6

VS

5

6.0

5.0

0.3

-0.6

4.0

4.0

3.0

-3.0

-0.6

VS

5

6.0

5.0

1.0

-3.0

4.0

4.0

3.0

-3.0

-0.6

VS









```

VDDTA=NMVDTA/DETA
RDOTA=NMRTDTA/DETA
XAXDTA=U*COS(PSIA)-VA*SIN(PSIA)
YAXDTA=U*SIN(PSIA)+VA*COS(PSIA)
XAXA=INTGRL(XAXO,XAXDTA)
YAXA=INTGRL(YAXO,YAXDTA)
DACOT=DERIV(O.O,DA)
VC=INTGRL(VO,VDDTC)
RC=INTGRL(RO,RDOTC)
PSIC=INTGRL(PSIO,RC)
F2C=YC+YVC*VC+1./6.*YVRRR*RC**3+1./2.*YVRRR*VC*RC**2+(YRC-MASS)*...
RC+1./6.*YVRRR*RC**3+1./2.*YVRRR*VC*RC**2+YD*DC
F3C=NC+NVC*VC+1./6.*YVRRR*RC**3+1./2.*YVRRR*VC*RC**2+(NRC-MASS*XG)...
*RC+1./6.*YVRRR*RC**3+1./2.*YVRRR*VC*RC**2+YD*DC
NMVDTC=(IZ-NRDTC)*F2C-(MASS*XG-YRDTC)*F3C
NMRTDC=(MASS-YVDTC)*F3C-(MASS*XG-NVDTC)*F2C
VDDTC=NMVDTC/DETC
RDOTC=NMRTDC/DETC
XAXDTC=U*COS(PSIC)-VC*SIN(PSIC)
YAXDTC=U*SIN(PSIC)+VC*COS(PSIC)
XAXC=INTGRL(XAXO,XAXDTC)
YAXC=INTGRL(YAXO,YAXDTC)
PSIAA=-PSIA
PSICC=-PSIC
DCCOT=DERIV(O.O,DC)
DYNAMIC
IF(TIME.LE.1.0) GO TO 12
IF(I.NE.O) GO TO 2
YA=0.00016
YC=0.00016
NA=-0.0003
NC=-0.0003
I=I+1
IF(I.NE.1) GO TO 3
IF(ABS(DMAX-DA).GT.0.001) GO TO 3
TA2=TIME
I=I+1
IF(I.NE.2) GO TO 4
IF(ABS(PSIS+PSIA).GT.0.002) GO TO 4
TA3=TIME
I=I+1
IF(I.NE.3) GO TO 5
IF(ABS(DA).GT.0.002) GO TO 6
YA=0.0
NA=0.0
I=I+1
IF(I.NE.4) GO TO 6
DA=6.283+PSIA

```



```

6      GC TO 7
7      DA=DRATE*((RAMP(TA1))-RAMP(TA2))-RAMP(TA3)+RAMP(TA4))
      IF(J.NE.0) GO TO 8
      IF(ABS(DMAX-CC).GT.0.002) GO TO 8
      TC2=TIME
      J=J+1
8      IF(J.NE.1) GO TO 9
      IF(ABS(PSIS+PSIC).GT.0.002) GO TO 9
      TC3=TIME
      J=J+1
9      IF(J.NE.2) GO TO 10
      IF(ABS(CC).GT.0.002) GO TO 11
      YC=0.0
      NC=0.0
      K1=-1.0232
      K2=-0.207472
      J=J+1
10     IF(J.NE.3) GO TO 11
      CC=6.283+PSIC
      GO TO 12
11     CC=DRATE*((RAMP(TC1))-RAMP(TC2))-RAMP(TC3)+RAMP(TC4))
12     CCCONTINUE
      SAMPLE
      CALL DRWG(1,1,TIME,DA)
      CALL DRWG(1,2,TIME,CC)
      CALL DRWG(1,3,TIME,PSIA)
      CALL DRWG(1,4,TIME,PSIC)
      CALL DRWG(2,1,XAXA,YAXA)
      CALL DRWG(2,2,XAXC,YAXC)
      TERMINAL
      CALL ENDRW(NPLOT)
      END
      STOP
      //PLCT-SYSIN DD *
      DA, CC, PSIA, PSIC
      0.0 6.0 AND YC VS XC
      -1.0 2.5
      1.5 6.0
      2.5 9.0
      6.0 6.0
      5.0 5.0

```







```

WDDA=FTA-IA*WDA-NA*WA
WDA=INTGRL(0.0,WDDA)
WA=INAGRL(0.0,WDA)
RA=KA*(WDA+JA*WA)
PSIOA=INTGRL(0.0,RA)
VA1=LEDLAG(0.0,P1A,P2A,RA)
VA2=REALPL(0.0,P2A,DELTA)
VA=-(G1A*VA1+G2A*VA2)
XADOT=CCS(PSIOA)-VA* SIN(PSIOA)
YADOT=SIN(PSIOA)+VA* COS(PSIOA)
XA=INTGRL(0.0,XADOT)
YA=INTGRL(0.0,YADOT)
PSINC=PSINA
PERC1=PSINC+PSIOC
ERC1=ERC1
DELTAC=ERC-K1*RC-K2*RDOTC
FIC=LEDLAG(0.0,P3C,P2C,DELTAC)
FDC=N*DELTAC-Y*G3C*FIC
FTCC=Q+FDC
FTC=REALPL(0.0,0.001,FTCC)
WDDC=FTC-IC*WDC-NC*WC
RDOTC=KC*(JC*WDC+WDDC)
WDC=INTGRL(0.0,WDDC)
WC=INTGRL(0.0,WDC)
WRC=KC*(WDC+JC*WC)
PSICC=INTGRL(0.0,RC)
VC1=LEDLAG(0.0,P1C,P2C,RC)
VC2=REALPL(0.0,P2C,DELTAC)
VC=-(G1C*VC1+G2C*VC2)
XCDDT=CCS(PSIOC)-VC* SIN(PSIOC)
YCDDT=SIN(PSIOC)+VC* COS(PSIOC)
XC=INTGRL(0.0,XCDDT)
YC=INTGRL(0.0,YCDDT)
DASQ=DELTAA*2
FMA2=INT(FMA2)
FMSQ=SQRT(FMA2)
DCSQ=DELTAC*2
FMC2=INTGRL(0.0,DCSQ)
FMC=SQRT(FMC2)

SAMPLE
CALL DRWG(1,1,TIME,PSINA)
CALL DRWG(1,2,TIME,DELTAC)
CALL DRWG(2,1,TIME,DELTA)
CALL DRWG(2,2,TIME,ERC)
CALL DRWG(2,3,TIME,PSINA)
CALL DRWG(3,1,XA,YA)
CALL DRWG(3,2,XC,YC)
CALL DRWG(4,1,TIME,FMA)

```









\*\*\*\*\*  
\*\*\*\*\*

COMPUTER PROGRAM NO 7

MODELS A AND C - STABILIZED IN A STRAIGHT  
LINE MOTION IN THE PRESENCE OF WAVES. DEAD  
ZONE HAS BEEN INTRODUCED.

THIS PROGRAM IS REFERRED TO FIGS. 33, 34

```
//HOZOS JOB (1159,0728,EA32),'HOZOS',TIME=12
```

```

// EXEC DSL
//DSL INPUT DD *
//INTGER NPLUT
CUNST NPLUT=5
PPARAM A0=0.113
PPARAM W=12.41
CCUNST KA=35.1,JA=0.9134,IA=3.4363,NA=1.002
CCUNST KC=40.775,JC=0.8094,IC=2.624,NC=-0.73728
CCUNST AA=-0.368,BA=-0.3544,CA=0.007,DA=-0.1266
CCUNST EA=0.007,FA=-0.0938,EC=0.0054,FC=-0.1266
CCUNST K1=-1.0232,K2=-0.207472,Y=0.06585,N=-0.3293
CCUNST AC=-0.3838,BC=-0.31306,CC=0.0054,DC=-0.1554
CCUNTRL FINTIN=24.0,DELT=0.00001,DELS=0.02
PRINTIAL 0.1,ERA,DELTA,FMA,FMC,XA,YA

```

$$P_1 = -2.157.3$$
$$p_2 = 2.157.3$$
$$GIA=DA/BA$$
$$G2A=Y/BA$$
$$G_3A = FA/BA$$
$$PIA=CA/DA$$
$$P2A = AA / BA$$
$$P_{3A} = E_A / F_A$$
$$GIC = DC / BC$$
$$G2C=Y/BC$$
$$GC = FC / BC$$

PIC=CE/DC

$$P2C = AC / BC$$

P3C=EC/FC

DERIVATIVE

 $\text{PSINA} = 0.0$ 

# THE NEW TIME

$$Q = A \cdot \Delta S \cdot \ln \left( \frac{T_H}{T_C} \right)$$

ERA=PSI NA+PSIUA

DELIA=DEADSP1,P2,ERA)

FIA=LEULAG(U.O.,P3A,P2A,DELIAA)  
EDV=NI\*DELIAA-Y\*P3A\*EIA

FDA=N\*DELIAA-Y\*G3A\*FLA



```

FTA=Q+FDA
WDDA=FTA-IA*WDA-NA*WA
WDA=INTGRL(0.0,WDDA)
WA=INTGRL(0.0,WDA)
RA=KA*(WDA+JA*WA)
PSIOA=INTGRL(0.0,RA)
VA1=LEDLAG(0.0,P1A,P2A,RA)
VA2=REALPL(0.0,P2A,DELTA)
VA=-(G1A*VA1+G2A*VA2)
XADOT=COS(PSIOA)-VA*SIN(PSIOA)
YADOT=SIN(PSIOA)+VA*COS(PSIOA)
XA=INTGRL(0.0,XADOT)
YA=INTGRL(0.0,YADOT)
PSINC=PSINA
ERCI=PSINC+PSIOC
ERC=DEADSP(P1,P2,ERC1)
DELTAC=ERC-K1*RC-K2*RDOOTC
FIC=LEDLAG(0.0,P3C,P2C,DELTAC)
FDC=N*DELTAC-Y*G3C*FIC
FTCC=Q+FDC
FTC=REALPL(0.0,0.001,FTCC)
WDDC=FTC-IC*WDC-NC*WC
RDOOTC=KC*(JC*WDC+WDDC)
WDC=INTGRL(0.0,WDDC)
WC=INTGRL(0.0,WDC)
RC=KC*(WDC+JC*WC)
PSIOC=INTGRL(0.0,RC)
VC1=LEDLAG(0.0,P1C,P2C,RC)
VC2=REALPL(0.0,P2C,DELTAC)
VC=-(G1C*VC1+G2C*VC2)
XCDDOT=COS(PSIOC)-VC*SIN(PSIOC)
YCDDOT=SIN(PSIOC)+VC*COS(PSIOC)
XC=INTGRL(0.0,XCDDOT)
YC=INTGRL(0.0,YCDDOT)
DASQ=DELTAA*#2
FMA2=INTGRL(0.0,DASQ)
FMA=SQRT(FMA2)
DCSQ=DELTAC*#2
FMC2=INTGRL(0.0,DCSQ)
FMC=SQRT(FMC2)

```

SAMPLE

```

CALL DRWG(1,1,TIME,ERA)
CALL DRWG(1,2,TIME,DELTA)
CALL DRWG(2,1,TIME,DELTA)
CALL DRWG(3,1,TIME,FMA)
CALL DRWG(3,2,TIME,FMC)
CALL DRWG(4,1,XA,YA)
CALL DRWG(4,2,XC,YC)

```



```

CALL DRWG(5,1,TIME,ERC)
CALL DRWG(5,2,TIME,ERC1)
TERMINAL
CALL ENDRW(NPLOT)
END
STOP
//PLOT.SYSIN DD *
ERA , DELTAA
0.0 DELTAC 2.5
0.0 FMA , FMC 2.5
0.0 YA VS XA AND
0.0 YC VS XC
ERC , ERC1 3.0
0.0 2.5

```

5 5 5 5 5

5.0 8.0 0.06 8.0 5.0  
5.0 8.0 0.4 7.0 5.0  
5.0 8.0 0.6 8.0 5.0  
5.0 8.0 0.1 8.0 5.0  
5.0 8.0 0.06 8.0 5.0





## LIST OF REFERENCES

1. Park, D. S., Dynamical Stability and Maneuverability of Dynamically Unstable Ships, M.S. Thesis, Naval Postgraduate School, Monterey, California, 1973.
2. Principles of Naval Architecture, SNAME, 1968.
3. Abkowitz, M. A., Stability and Motion Control of Ocean Vehicles, Massachusetts Institute of Technology, 1969.
4. The Anti-Roll Stabilization of Ships by Means of Activated Tanks, Technical Report No. 15, Stanford University, December 1950, by Joseph H. Chadwick.



# INITIAL DISTRIBUTION LIST

	No. Copies
1. Defense Documentation Center Cameron Station Alexandria, Virginia 22314	2
2. Library, Code 0212 Naval Postgraduate School Monterey, California 93940	2
3. Department Chairman Department of Electrical Engineering Naval Postgraduate School Monterey, California 93940	1
4. Dr. G. J. Thaler, Code 52Tr Department of Electrical Engineering Naval Postgraduate School Monterey, California 93940	5
5. Professor M. L. Wilcox, Code 52Wx Department of Electrical Engineering Naval Postgraduate School Monterey, California 93940	1
6. Professor A. Gerba, Jr., Code 52Gz Department of Electrical Engineering Naval Postgraduate School Monterey, California 93940	1
7. Mr. Walter Blumberg NSRDC Annapolis, Maryland 21402	1
8. Hellenic Navy Command STRATOPEDON PAPAGOU-HOLARGOS Athens, GREECE	1
9. LCDR Andreas Hozos Hellenic Navy Command STRATOPEDON PAPAGOU-HOLARGOS Athens, GREECE	2
10. LCDR Dae-Song Park BUSHIPS Headquarters of Navy Daebang-dong Seoul, KOREA	1



Thesis

H8285 Hozos  
c.1

Maneuvering character-  
istics of automatically  
controlled ships with  
directionally unstable  
hulls.

156144

12 MAY 75

3 PL 803

19 MAY 87

23261

27180

33307

Thesis

H8285 Hozos  
c.1

Maneuvering character-  
istics of automatically  
controlled ships with  
directionally unstable  
hulls.

156144

thesH8285

Maneuvering characteristics of automatic



3 2768 001 01545 6

DUDLEY KNOX LIBRARY